Energetic costs of AhR activation in rainbow trout (Oncorhynchus mykiss) hepatocytes

Rance Nault

Thesis submitted to the
Faculty of Graduate and Postdoctoral Studies
University of Ottawa
In partial fulfillment of the requirements for the
M.Sc. degree in the
Chemical and Environmental Toxicology Program
Ottawa-Carleton Institute of Biology

Thèse soumise à
L'École des Études Supérieures et Postdoctorales
Université d'Ottawa
En vue de l'obtention d'une Maîtrise dans le
Programme de
Toxicologie Chimiques et Environnemental
L'Institut de Biologie Ottawa-Carleton

Abstract

Aquatic organisms in response to toxic insults from environmental pollutants activate defence systems including the aryl hydrocarbon receptor (AhR) in an attempt to metabolize and excrete these toxicants and their metabolites. These detoxification mechanisms however may come with certain energetic costs. I hypothesize that the activation of the AhR by β-Naphthoflavone (β-NF), a model AhR agonist, results in increased energetic costs requiring metabolic reorganization in rainbow trout hepatocytes. While the results obtained suggest that there are no significant energetic costs of AhR activation, analysis of enzyme activities suggests possible metabolic reorganization. This study also showed significant changes in cellular processes in hepatocytes over the incubation periods which previously were not reported. Furthermore, for the first time in fish hepatocytes, *metabolic flux analysis* (MFA) was used to examine intra-cellular metabolism, the applicability of which is discussed.

Résumé

Les organismes aquatiques sont capables, en présence de polluants environnementaux, d'activer des systèmes de défense tels que le récepteur d'hydrocarbure aromatique (AhR) afin de métaboliser et d'excréter ces agents toxiques et leurs métabolites. Cependant, l'activation de ces mécanismes de détoxification peuvent présenter un certain coût énergétique. J'émets donc l'hypothèse que l'activation du AhR par β-naphthoflavone (β-NF), un agoniste model de l'AhR, résultera en une augmentation du coût énergétique nécessitant la réorganisation du métabolisme cellulaire dans les hépatocytes de la truite arc-en-ciel. Tandis-que les résultats ne suggère aucune augmentation du coût énergétique associé à l'activation du AhR, l'analyse de l'activité enzymatique suggère, elle, une réorganisation du métabolisme. Cette étude montre aussi des changements dans les processus cellulaire qui n'ont pas été reporté dans le passé. De plus, l'approche d'*analyse du flux métabolique* (MFA) est utilisée pour la première fois sur les hépatocytes de poissons afin d'examiner le métabolisme intracellulaire dont l'applicabilité sera discutée.

Table of Contents

List of Figures

List of Table

List of Abbreviations

AAT - Alanine aminotransferase
ABC - ATP binding cassette
ADP - Adenosine diphosphate
AEC - Adenylate energy charge
AHH - Aryl hydrocarbon hydroxylase
AhR - Aryl hydrocarbon receptor
AMP - Adenosine monophosphate
ARNT - Aryl hydrocarbon receptor nuclear translocator
ATP - Adenosine triphosphate
HOAD - β-Hydroxyacyl CoA-dehydrogenase
β-NF - β-Naphthoflavone
CLRTAP - Committee on long range transport air pollution
CS - Citrate synthase
CYP - Cytochrome P450
DDT - Dichlorodiphenyltrichloroethane
DHAA - Dehydroabietic acid
EROD - Ethoxyresorufin-*O*-deethylase
FBA - Flux balance analysis
G-3PDH - Glyceraldehyde-3-phosphate dehydrogenase
G6PDH - Glucose-6-phosphate dehydrogenase
GST - Glutathione-*S*-transferase
HSP90 - Heat-shock protein 90
LDH - Lactate dehydrogenase
MFA - Metabolic flux analysis
MFNA - Metabolic flux network analysis
MFO - Mixed function oxidase
PAHs - Polyaromatic hydrocarbons
PBDE - Polybrominated diphenyl ether
PCB - Polychlorinated biphenyl
PFC - Perfluoroalkyl chemicals
PFK - Phosphofructokinase
P-gp - P-glycoprotein
PHH - Polyhalogenated hydrocarbon
POPs - Persistent organic pollutants
PPCPs - Pharmaceuticals and personal care products
SDA - Specific dynamic action
SULT - Sulfanotransferase
UDPGT - Uridine diphosphate glucoronyltransferase
UNECE - United Nation economic commission for Europe
XRE - Xenobiotic response element

Acknowledgements

First of all, I wish to express my sincere thanks to my supervisor Dr. Thomas W. Moon for providing me with an opportunity to learn and grow as a member of his lab. His guidance, expertise and support were invaluable to me throughout this project and as I pursue a career in research. I am also grateful for his openness to allow me to explore novel techniques in the course of this study which has been a great learning experience.

I would also like to thank my committee members, Drs. Jules Blais, Steven J. Cooke and Jean-Michel Weber for their valuable input throughout this project. I would also like to express thanks to Maryam Haghighi whose expertise linear programming was greatly appreciated.

Furthermore, I would also like to thank my colleagues in the Moon lab, Aziz Al-Habsi, Paul Craig, Shahram Eisa-Beygi, Andrey Massarsky, Kim Mitchell and Pamela Stroud who have always been ready to lend a hand when needed and have been great friends. Special thanks also to Hiba Al-Hafizi and Jessica Taylor who have provided important contributions in biochemical assays as well as Bill Fletcher at the aquatics care facility for providing care and maintenance for the fish and aquatic facilities.

Finally, I would like to thank my family and friends for their continuous support in every endeavour I undertake and without whom I could not have made it this far.

Funding for this research was provided by the Natural Science and Engineering Council (NSERC) to Dr. Thomas W. Moon.

Chapter 1 – General Introduction

1.0. The Basic Problem

Persistent organic pollutants (POPs) enter the aquatic environment through a number of sources including industrial and urban sewage effluents, atmospheric deposition, and run-off and groundwater leading to their ubiquitous distribution in aquatic environments (Zhou et al., 2010). Properties of POPs including their ability to bioaccumulate in organisms based upon their lipophility, their potential for long-range transport, their persistence and their toxicity make these contaminants a particular concern within aquatic systems (Schwarzenbach et al., 2010) and those aquatic organisms that inhabit them (Miranda et al., 2008). Many of these contaminants are banned including the 'legacy chemicals' identified by the Stockholm convention (Kaiser and Enserink, 2000; Kelly et al., 2007; Weber et al., 2011), yet these chemicals continue to be detected in aquatic ecosystems (Bhavsar et al., 2007; Miranda et al., 2008). Polychlorinated biphenyls (PCBs) for example have reached stable levels in the Great Lakes almost 40 years after their production was banned in North America (Bhavsar et al., 2007). In addition to these 'legacy chemicals', emerging POPs which were not originally identified by the Stockholm convention are now detected in the environment (Weber et al., 2011) and the release of significant amounts of polyaromatic hydrocarbons (PAHs) found in fossil fuels continue to occur (Incardona et al., 2005; Kerr et al., 2010).

Organisms, to cope with exposure to these environmental pollutants, are believed to have evolved mechanisms to detect and respond to these chemicals by increasing cellular defence and detoxification systems (Bains and Kennedy, 2004; DuRant et al., 2007). Of particular importance for POPs, the aryl hydrocarbon receptor (AhR) detects and responds to exposure to many of these

chemicals (Zhou et al., 2010). Activation of the AhR by specific POPs leads to the transcription of genes leading to production of xenobiotic detoxification enzymes such as cytochrome P4501A1 which incorporates oxygen into the xenobiotic molecule to increase its water solubility and facilitate its excretion (Matsuo et al., 2008; Široká and Drastichová, 2004). This system is well characterised in fish (Andersson and Förlin, 1992; Goksøyr and Förlin, 1992; Hahn, 2002; Van der Oost et al., 2003) to the point where activity of CYP1A1 is often considered a useful biomarker of exposure to these AhR agonists (Reynaud and Deschaux, 2006; Van der Oost et al., 2003).

Exposure to these contaminants is considered to pose a significant energetic challenge to the intoxicated organism (Beyers et al., 1999; Handy et al., 1999; Levesque et al., 2002; Sherwood et al., 2000). In a typical scenario, organisms gain energy from food intake and allocate this energy to physiological processes including maintenance metabolism, growth, activity and reproduction (Beyers et al., 1999; Calow, 1991; Knops et al., 2001; Rombough, 1994). With exposure to contaminants, induction of detoxification processes becomes a necessity for survival and a part of the daily energy demands thus potentially increasing maintenance metabolic costs and presumably decreasing energy availability for other physiological processes (Beyers et al., 1999). The quantification of the energy demands due to contaminant exposure has been a challenge at the whole organism level as there are a suite of behavioural and physiological changes that render these processes complex (DuRant et al., 2007).

One can use cellular models to potentially overcome these challenges (Bains and Kennedy, 2004). Fish liver cells or hepatocytes are considered a useful tool in toxicological studies (Pesonen and Andersson, 1997) as the liver is the main organ for detoxification (Pacheco and Santos, 2001). There is evidence that changes in energy demand can be observed at this level either as increased oxygen consumption (Bains and Kennedy, 2004), heat production (Rissanen et

al., 2003) or the use of ATP resulting in decreased adenylate energy charge values (Hildebrand et al., 2009). These studies provided evidence that exposure to toxicants leads to increased energetic costs although few such studies focus on costs stemming from detoxification with the exception of those looking at P-glycoprotein (P-gp) induction in rainbow trout hepatocytes (Bains and Kennedy, 2005; Hildebrand et al., 2009). Given the importance of these detoxification mechanisms and in particular the importance of CYP1A1 induction by exposure to AhR agonists, it is important to examine the energetic costs that may translate to whole animal metabolism and thus impact the overall fitness of the intoxicated organism.

This study will therefore examine the cellular energetic costs of activation of the AhR by the model AhR agonist β-Naphthoflavone (β-NF) which is a potent AhR agonist (Gesto et al., 2009; Tintos et al., 2008). Using innovative approaches including *in silico* modeling of cellular metabolism as well as traditional approaches examining perturbations of the adenylate pool and activity of the energetically costly processes of protein synthesis and Na^+/K^+-ATPase activities as well as examining metabolic enzyme activities, this research will provide insights into the possible costs of AhR induction and detoxification of AhR agonists.

1.1. Environmental pollutants

1.1.1. Persistent organic pollutants in the environment

The aquatic environment acts as a sink for environmental pollutants (Van der Oost et al., 2003). The number of different chemicals being released to the environment is vast and this complex mixture of contaminants poses major challenges when assessing the health of our aquatic ecosystems (Schwarzenbach et al., 2010). These chemicals can range from organic pollutants generated by industries and agriculture to toxic metals from mining and even pharmaceuticals and personal care products (PPCPs) produced from anthropogenic sources

(Grans et al., 2010). However, some of the most important contaminants on a global scale are persistent organic pollutants (POPs) which, as their name suggests, persist in the environment and are often subjected to long-range transport (Schwarzenbach et al., 2010; Weber et al., 2011). In fact, POPs are detected in some of the most remote regions of the world (Jorgensen et al., 2006; Lang, 1992) and are reported at some of the highest tissue loads in many Arctic species including the Arctic char, *Salvelinus alpines* (Vijayan et al., 2006).

Classification of chemicals as POPs is generally delineated by four key characteristics (Schwarzenbach et al., 2010). As previously described, two of these categories are persistence in the environment and their potential for long range transport. This means that these chemicals are not significantly degraded by chemical, photochemical or biological processes in addition to being volatile (Schwarzenbach et al., 2010). Additionally, POPs bioaccumulate and biomagnify in organisms and within food-webs (Schwarzenbach et al., 2010) which makes POPs of particular concern. These chemicals accumulate in fatty tissues of organisms and result in high tissue loads despite the presence of low or trace amounts in the environment (Miranda et al., 2008; Van der Oost et al., 2003). Finally, exposure to POPs elicits toxic effects in organisms from wildlife to humans (Schwarzenbach et al., 2010). Taken together, these characteristics make these compounds of significant environmental and toxicological concern.

A number of POPs exert many if not most of their toxic effects in fish through activation of the AhR (Zhou et al., 2010). Indeed, AhR activation is observed upon exposure to dioxin and dioxin-like PCBs (Safe et al., 1985) as well as planar PAHs (Reynaud and Deschaux, 2006) supporting this claim, at least for these planar compounds in which all atoms lie in the same plane allowing ligand-receptor interaction (Denison et al., 2002). Reported toxic effects of these planar AhR agonists in fish are numerous. Mutations, heritable reproductive effects, deformities, neural cell death, anaemia and impaired growth and swimming are reported in several studies (Barron et

al., 2004; Billiard et al., 1999; Brinkworth et al., 2003; Incardona et al., 2005; White et al., 1999), symptoms that are characteristic of blue-sac disease resulting from the exposure in early life stages of fish to dioxin and dioxin-like chemicals (Barron et al., 2004; Billiard et al., 1999). While these results are generally indicative of acute exposures, chronic effects on the other hand include immunotoxicity and hepatotoxicity in fish (Reynaud and Deschaux, 2006; Wills et al., 2010) and in mammals as well (Kopec et al., 2008).

The Stockholm convention and the POP protocol under the United Nation Economic Commission for Europe's (UNECE) Convention on Long Range Transboundary Air Pollution (CLRTAP) are two examples of international efforts to regulate environmental levels of POPs (Choi et al., 2009; Kaiser and Enserink, 2000; Kelly et al., 2007). Originally, the POPs of most concern were those identified in the Stockholm convention which was ratified in 2004 by 131 countries and were called the "dirty dozen" and now called "legacy chemicals" (Kelly et al., 2007; Weber et al., 2011). These included the pesticides DDT, Aldrin, Dieldrin, Endrin, Chlordane, Heptachlor, Mirex and Toxaphene as well as the polyhalogenated hydrocarbons (PHHs) hexachlorobenzene, dioxin, furans and PCBs which were targeted for elimination or reduction (Kaiser and Enserink, 2000). Since the ratification of the Stockholm convention several other chemicals were added to the list of POPs including polybrominated diphenyl ethers (PBDEs) and perfluoroalkyl chemicals (PFCs) (Weber et al., 2011). Similarly, the UNECE's CLRTAP included many of those covered by the Stockholm convention but also identifies PAHs as POPs of concern (Choi et al., 2009).

Despite these regulatory efforts to control POPs, these contaminants remain a threat to wildlife and humans. Although the production of PCBs for example was banned in North America in the late 1970's and environmental levels almost 40 years later are lower, they appear to have reached stable levels (Bhavsar et al., 2007) thus presenting a chronic sublethal

toxicological risk. PAHs as well pose a serious threat as they are important by-products of fossil fuels and are produced through fuel combustion (Correia et al., 2007). Studies observing acute effects of early life-stage exposure to PAHs were in large part seen following the 1989 Exxon Valdez crude oil spill in Prince William Sound, Alaska, which contaminated fish spawning grounds (Incardona et al., 2005). Events in April 2010 where large amounts of oil were released at the Deepwater Horizon oil drilling platform into the Gulf of Mexico (Kerr et al., 2010) is a reminder that these contaminants are of important environmental concern and that efforts must continue towards understanding the consequences of PAH exposure in aquatic organisms.

1.1.2. The AhR receptor pathway

Organisms have evolved inducible mechanisms to detect and respond to the presence of environmental contaminants (Bains and Kennedy, 2004; Hahn, 2002; Pascussi et al., 2008). Among these defence mechanisms, the AhR pathway has been extensively studied in vertebrates including mammals and fish (Goksøyr and Förlin, 1992; Hahn, 2002; Široká and Drastichová, 2004; Van der Oost et al., 2003) and is of particular importance for POPs (Reynaud and Deschaux, 2006; Safe et al., 1985; Schwarzenbach et al., 2010). As was previously mentioned, most of the toxicological effects observed from exposure to POPs including dioxin and PCBs are believed to be mediated through activation of the AhR (Kopec et al., 2008; Zhou et al., 2010). The importance of the AhR in mediating toxicity may explain the observed adaptation of Atlantic killifish (*Fundulus heteroclitus*) and Atlantic tomcod (*Microgradus tomcod*) populations from highly AhR-agonist contaminated sites to have reduced receptor sensitivity to these agonists (Bello et al., 2001; Wirgin et al., 2011).

The AhR, a member of the basic-helix-loop-helix (bhlh)-Per-ARNT-Sim (PAS) gene superfamily (Hahn, 2002), is activated by agonist molecules or ligands in the cytosol of cells

(Kopec, 2008; Safe, 2001) leading to conformational changes of stabilizing proteins (see Fig. 1.1) including chaperone p23, immunophilin like XAP2 (also known as ARA9 or AIP) and 90kDa heat-shock protein (HSP90). These conformational changes cause HSP90 to unmask a nuclear localization sequence (Hahn, 2002; Zhou et al., 2010) which leads to the translocation of the AhR with its associated proteins into the nucleus where dissociation of these proteins is believed to occur (Heid et al., 2000). Once in the nucleus, the AhR forms a heterodimer with the aryl hydrocarbon receptor nuclear translocator (ARNT) (Barouki et al., 2007; Heid et al., 2000) and this ligand-AhR-ARNT complex then acts as a transcription factor, binding to the xenobiotic response element (XRE; also known as the dioxin response element, DRE). This results in the transcription of a number of xenobiotic metabolizing enzymes including cytochrome P4501A(CYP1A), UDP glucuronosyltransferase (UDPGT) and glutathione-S-transferase (GST) together known as the AhR 'gene battery' (Reynaud and Deschaux, 2006) (Fig. 1.1). CYP1A is possibly the best characterized target gene of AhR activation and is commonly used as a biomarker of exposure to AhR agonists/ligands assessing its induction by rates of deethylation of ethoxyresorufin known as the ethoxyresorufin-O-deethylase (EROD) activity (Pacheco and Santos, 2001; Reynaud and Deschaux, 2006).

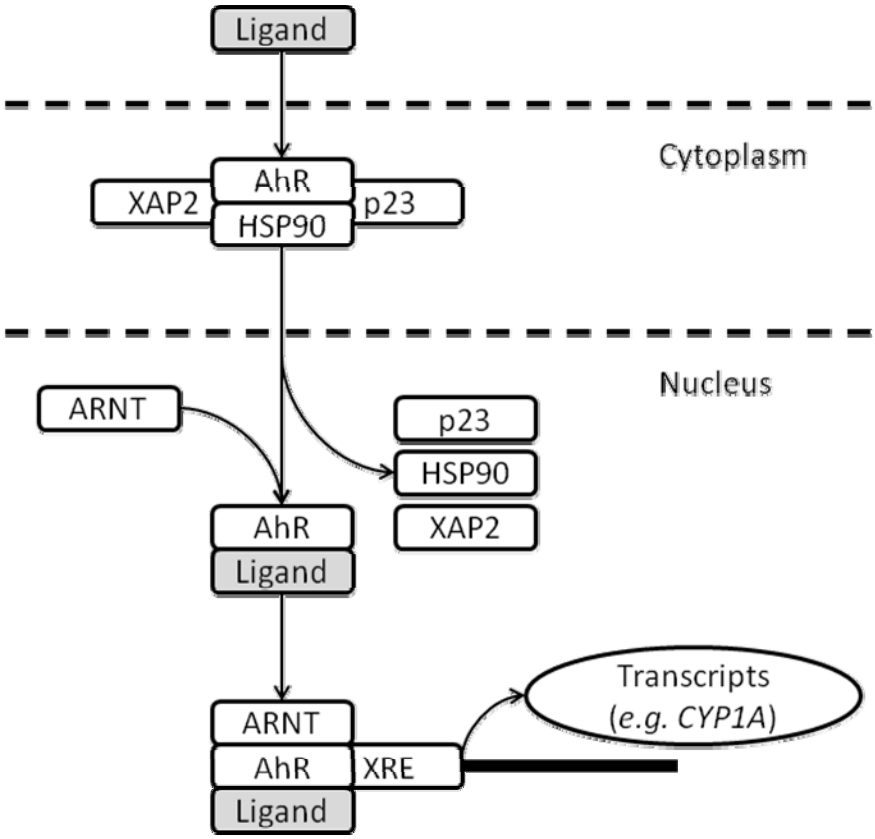

Figure 1.1. The aryl hydrocarbon receptor (AhR) activation pathway; see text for abbreviations. Modified from Zhou et al. (2010).

Although the role of the AhR in response to environmental contaminants is thought to be an adaptive one, its adaptive function is thought to have evolved in early vertebrates where it may have played a role in the development of sensory structures (Hahn, 2002) although it appears to maintain important roles in development and physiological homeostasis in addition to its adaptive role in mammals (Mitchell and Elferink, 2009; Hahn, 2002). This appears to be the case in fish as well given the developmental toxic effects observed in blue-sac disease and it is believed that among the two isoforms found in fish (AhR1 and AhR2), AhR2 is the main isoform mediating both toxicity of AhR agonists and the developmental role of AhRs (Zhou et al. 2010). Interestingly, the AhR2 appears to be the main target in the selection of AhR agonist resistant Atlantic tomcod (Wirgin et al., 2011).

1.1.3. Xenobiotic detoxification

Xenobiotic detoxification is classified into two mechanisms known as phase I and phase II biotransformations (Andersson and Förlin, 1992; Goksøyr and Förlin, 1992; Matsuo et al., 2008) and, in some instances a third mechanism known as phase III biotransformation exists (Kennedy and Tierney, 2008; Nakata et al., 2006). Enzymes that make-up these phases work in concert in an attempt to render the xenobiotic molecule more water soluble allowing it to be excreted either in the bile or through the urine (Xu et al., 2005). For a comprehensive review on xenobiotic detoxification in fish see Van der Oost et al. (2003).

Phase I biotransformation enzymes, perhaps the most important as they serve as a first line of defence, are those that incorporate oxygen into the target molecule or xenobiotic. These enzymes are generally members of the cytochrome P450 (CYP) superfamily (Xu et al., 2005) which are monomeric hemeproteins with a loosely bound protoporphyrin IX group and catalyze mixed function oxidase (MFO) or mono-oxygenase reactions (Matsuo et al., 2008; Široká and Drastichová, 2004). These enzymes use NADPH as an electron donor to a cytochrome P450

reductase enzyme; CYPs incorporate an atom of oxygen from dioxygen into the molecule with the second oxygen atom reduced to water (Široká and Drastichová, 2004) (see Fig. 1.2) rendering the molecule slightly more soluble and ready for phase II biotransformation enzymes.

It must be noted however that not all CYPs are involved in xenobiotic detoxification or are induced by the AhR. CYPs are a large gene superfamily, identified by CYP which describes the gene followed by an Arabic number identifying the family (and the wavelength of light which the protein absorbs), a letter identifying the subfamily and lastly, a second Arabic number to identify the individual gene (Goksøyr and Förlin, 1992). Xenobiotic activation of the AhR in mammals induces two CYP isoforms, specifically CYP1A1 and CYP1A2 (Goksøyr and Förlin, 1992; Hahn and Stegeman, 1994). In fish however, only the CYP1A1 form is apparently induced by AhR activation (Goksøyr and Förlin, 1992; Hahn and Stegeman, 1994) whose induction is considered to be a reliable biomarker of exposure to AhR agonists (Pacheco and Santos, 2001; Reynaud and Deschaux, 2006; Van der Oost et al., 2003).

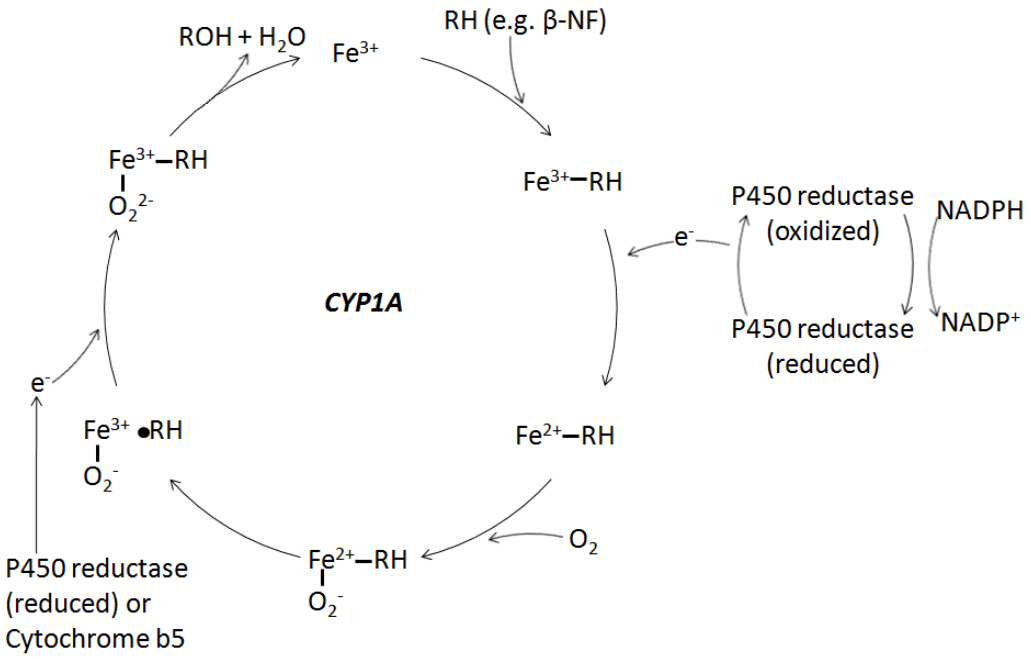

Figure 1.2. The cytochrome P450 catalytic cycle; adapted from Plant (2003)

Phase II biotransformation enzymes are those which, following oxygenation by phase I enzymes (Kennedy and Tierney, 2008), render the molecule more soluble through conjugation with an endogenous molecule including glucuronic acid, sulphate or glutathione (Nakata et al., 2006) by enzymes including UDP-glucuronosyltransferases (UDPGTs), sulfanotransferases (SULTs) and glutathione-*S*-transferase (GST), respectively. Although it is believed that some of these phase II enzymes are also induced through AhR activation, this appears to be less significant than the activation of the phase I enzymes (Van der Oost et al., 2003). Finally, phase III metabolism, unlike the previous two phases, does not result in transformation of the molecule. This phase of xenobiotic defence consists of enzymes that transport these molecules out of cells and comprises proteins including ATP-binding cassette (ABC), P-glycoproteins (P-gp) and multidrug resistance proteins (Nakata et al., 2006; Xu et al., 2005).

The liver is the major xenobiotic detoxification organ in animals (Aly and Domènech, 2009; Pacheco and Santos, 2001; Van der Oost et al., 2003). Tissue specific EROD activities in the European eel (*Anguilla anguilla*) for example are 10-20 times higher in the liver than the kidney, gills and intestine following exposure to an AhR agonist (Pacheco and Santos, 2001) as is also the case in gilthead seabream (*Sparus aurata*) liver in comparison to the kidney and gills (Sandvik et al., 1998). The importance of the liver in these detoxification pathways makes the liver and primary hepatocyte cell cultures a popular and useful model for toxicological studies (Pesonen and Andersson, 1997).

1.2. Bioenergetics

1.2.1. Whole animal energetics

Bioenergetics as defined by Ney (1993), describes energy acquisition in animals and its subsequent use for physiological processes. These processes rely upon the laws of

thermodynamics and more specifically, conform to the first law of thermodynamics which describes the conservation of energy within a system (Beyers et al., 1999). Energy can therefore be considered as the currency of ecology and physiology as, not unlike monetary currency, the gain of product such as mass or reproductive success must come with certain energetic costs (Beyers et al., 1999; Rombough, 1994; Smolders et al., 2003; Widdows and Donkin, 1991). As with any currency however, organisms are limited in the amount of energy that can be used by the amount gained through feeding which implies that organisms operate on an energetic "budget" and allocate specific amounts of energy to specific physiological processes such as maintenance metabolism, growth, activity and reproduction (Knops et al., 2001; Rombough, 1994; Smolders et al., 2003).

These energetic budgets or, in other words, energy allocation in animal bioenergetic studies are examined using a factorial approach dividing nutrient requirements for physiological processes into a number of fractions or components that can be examined independently (Bureau et al., 2003; Dumas et al., 2008) and are described in the following equation (or other similar) based on the nomenclature developed by the Committee on Animal Nutrition of the U.S. National Research Council:

$$\mathbf{IE = FE + UE + ZE + HiE + HeE + HjE + RE} \text{ (Eq. 1)}$$

where **IE** is energy intake; **FE** the energy lost as feces; **UE** and **ZE** are the loss through urinary and branchial nitrogen excretion, respectively; **HiE** the energy loss from feeding (often referred to as the Specific Dynamic Action or SDA); **HeE** the standard or maintenance metabolism; **HjE** the energy loss due to activity; and, **RE** is the recovered energy or the energy available for growth, reproduction and other anabolic processes.

It is evident that the principal determinant of energy allocation lies in energy intake (**IE**). Regulation of **IE** or feeding behaviour is accomplished through orexigenic (stimulates food

intake) and anorexigenic (inhibits food intake) endocrine signals generally produced within the hypothalamus (Volkoff et al., 2005). These signals are of increasing interest in toxicology as endocrine disruptors are believed to lead to energy imbalances and possibly lead to metabolic disorders such as obesity and diabetes (Migliarini et al., 2010)**.** Interestingly, dioxin and dioxin-like molecules have been shown to result in significant declines in feeding followed by weight loss of up to 50% with lethal doses of dioxin in rats (Linden et al., 2010). This type of response, hypophagia and cessation of weight gain in young animals or weight loss in adults, is known as the 'wasting syndrome' (Linden et al., 2010; Seefeld et al., 1984). In fact, cessation of weight gain is seen in larval fathead minnows (*Pimephales promelas*) (Olivieri et al., 1997) and swim-up rainbow trout (Carvalho et al., 2004) indicating the occurrence of a 'wasting syndrome' in fish. This type of dysregulation of feeding outlines the importance of **IE** in the bioenergetic equation (Eq. 1).

The amount of **IE** available for metabolic processes is commonly referred to as metabolizable energy (**ME**) and is estimated to account for 40-80% of total energy intake (Brett and Groves, 1979) although this amount appears to be highly dependent on the quality (e.g. plant vs. animal) rather than the quantity of the diet as was demonstrated by Hofer et al. (1985) in the common roach (*Rutilus rutilus*). **ME** is believed to be allocated in a hierarchal manner where requirements for **HiE** and **HeE** are fulfilled first and foremost. This comes as no surprise as both of these factors represent energetic requirements for survival. The latter energy fraction, **HeE**, is particularly important from an animal energetics view and for this study as it encompasses basal metabolic requirements including detoxification mechanisms which may impact the survival of the organism (Beyers et al., 1999). This is evident from studies with fasted fish where these fish consume stored energy rather than stop using energy. Because of the importance and

prioritization of **HeE**, it seems apparent that increases in this fraction will come at the expense of production processes **HjE** and **RE**.

Exposure to environmental pollutants is reported to alter energy allocation to these processes in fish (Beyers et al., 1999; Sherwood et al., 2000). The presence of pollutants is perceived by an organism as a stressor that triggers a series of physiological responses (Beyers et al., 1999; Calow, 1991; DuRant et al., 2007) including increases in defence mechanisms, detoxification processes and hormonal changes (DuRant et al., 2007). The concept where an organism attempts to regain homeostasis following the application of a stressor was described by Selye (1950) as the *general adaptation syndrome* (GAS) and is an indication of the energy requirements needed to overcome this physiological disturbance (Beyers et al., 1999; Selye, 1950).

The GAS response is comprised of three phases namely the alarm, resistance and exhaustion phases. The alarm phase refers to the immediate physiological response to the external stressor mediated by the hypothalamic-pituitary-interrenal axis leading to secretion of catecholamines and cortisol into the blood stream (Iwama, 1998) and ultimately increased energy mobilization (Beyers et al., 1999). Secondly, the resistance phase occurs once all immediate physiological mechanisms to regain homeostasis have occurred and the presence of the stressor has become part of daily energy expenditure or incorporated into the energy of maintenance metabolism (Beyers et al., 1999). This, for example may be the continuous activity of detoxification mechanisms which, in the case of POPs is likely to remain important due to their persistence and ability to bioaccumulate (Schwarzenbach et al., 2010). Finally, the exhaustion phase occurs when the organism is no longer able to compensate or cope with the increased energetic costs potentially leading to disease and pre-mature death (Beyers et al., 1999). This relationship between a toxicant and the GAS was clearly demonstrated by Beyers et al. (1999);

they reported an increased maintenance metabolic rate (**HeE**) in largemouth bass (*Micropterus salmoides*) when exposed to the pesticide Dieldrin that, when examined on a temporal scale, showed an energetic response similar to that of the alarm and resistance phases of the GAS.

As previously described, an increase in **HeE** requirements is likely to come at the expense of **HjE** and **RE** which has been reported in a number of studies (Beyers et al., 1999; Knops et al., 2001; Rombough, 1994). Beyers et al. (1999) observed a decreased growth rate in addition to increased standard metabolism in Dieldrin-exposed largemouth bass. Similarly, Bellehumeur (2010) demonstrated a reduction in the aerobic scope for activity in PCB 126 exposed rainbow trout which is indicative of a decreased ability to allocate energy to activity and appears to be related with a high standard metabolism. Furthermore, Sherwood et al. (2000) and Levesque et al. (2002) observed decreased growth rates in yellow perch (*Perca flavescens*) in toxic metal contaminated lakes even though energy intake remained the same as fish from a reference lake. On the other hand, rainbow trout exposed to chronic dietary copper did not show growth rates changes but reduced swimming activity and increased gill surface area which were hypothesised to occur in order to improve respiratory efficiency although whole-animal respiration was not altered (Handy et al., 1999).

There is also evidence that fish mobilize tissue energy reserves to cope with exposure to pollutants in addition to impaired growth and increased respiration. Smolders et al. (2003) examined tissue glycogen, protein and lipid stores and showed that zebrafish (*Danio rerio*) exposed to effluents from an industrial plant depleted glycogen and lipid stores and, more importantly, that depletion of lipid stores had a significant impact on growth and reproduction further supporting a trade-off between detoxification and reproduction. Furthermore, rainbow trout exposed to β-NF increased plasma glucose as early as 24 h following intraperitoneal injection suggesting enhanced glycogenolysis to fulfill increased energy demands (Al-Hameedi,

2008; Tintos et al., 2008) at least in the short term as this increase is no longer apparent at 6 days and later (Aluru and Vijayan, 2004; Basu et al., 2001).

The variability observed in energetics costs and energy mobilization at the whole animal level as noted between detoxification and swimming (Handy et al., 1999), the absence of an increased plasma glucose (Aluru and Vijayan, 2004; Basu et al., 2001) as well as changes in energy intake such as in the wasting syndrome (Linden et al., 2010; Seefeld et al., 1984) highlights the complexities associated with examining energetic costs at the whole animal level. Energy allocation in whole animals is influenced by a suite of behavioural, environmental and hormonal factors (Aluru and Vijayan, 2004; Beyers et al., 1999; Handy et al., 1999) and consists of interactions between several organs. The examination of energetic costs at the cellular level where many of these external influences can be controlled may provide more definitive answers.

1.2.2. Cellular energetics

Energy at the cellular level is stored in a chemical form (Atkinson, 1977). While typically this chemical form is adenosine triphosphate (ATP) and its metabolites adenosine diphosphate (ADP) and adenosine monophosphate (AMP), there are a number of other molecules that are capable of storing energy including phosphocreatine (in vertebrates), phosphoarginine (in invertebrates) and acetyl-CoA (Moyes and Schulte, 2006). However, ATP is considered to be the most abundant and most accessed of these energy storage molecules as it is either consumed or produced in many metabolic pathways (Atkinson, 1977). In fact, ATP is one of three fundamental requirements for living cells along with reducing power and biosynthetic substrate (Atkinson, 1977).

ATP production (catabolic) and consumption (anabolic) processes in cells are highly regulated leading to closely matched catabolic and anabolic rates (Krumschnabel and Wieser, 1994; Wieser and Krumschnabel, 2001). It was hypothesized by Atkinson (1977) that, similar to

the whole animal energy allocation (see Eq. 1), activity of anabolic processes were hierarchically depressed under limited energy conditions or reduced energy production by catabolic processes. It was suggested that storage pathways would be the first to be depressed followed by biosynthesis of macromolecules then maintenance activities such as ion pumps. Perhaps one of the first studies that strongly supported this hypothesis was that of Buttgereit and Brand (1995) for rat thymocytes which examined activities of the anabolic processes of protein synthesis, Na^+/K^+-ATPase, Ca^{2+}-ATPase, RNA/DNA synthesis and proton leak upon gradual reduction of mitochondrial ATP synthesis achieved by inhibition of complex III using myxothiazol, although earlier studies did provide evidence of this in fish hepatocytes (Krumschnabel et al., 1994a; Krumschnabel et al., 1994b; Krumschnabel and Wieser, 1994).

While studies examining hierarchal organization of ATP consuming processes in fish hepatocytes are not as robust as the report of Buttgereit and Brand (1995), these fish studies are informative nonetheless. Using chemical anoxia (cyanide exposure) to induce a state of low energy, Krumschnabel et al. (2001) examined the contribution of the two principal sources of ATP synthesis, namely glycolysis and oxidative phosphorylation (Moyes and Schulte, 2006), on the two most important energy consuming activities, namely protein synthesis and activities of the Na^+/K^+-ATPase (Krumschnabel et al., 1994b; Pannevis and Houlihan, 1992; Wieser and Krumschnabel, 2001) in rainbow trout hepatocytes. These studies demonstrated that energy limitation as a result of chemical anoxia resulted in decreased Na^+/K^+-ATPase activities while protein synthesis remained unaffected. Interestingly, the authors suggested that this may be a result of spatial distribution of ATP consuming processes as was suggested to occur in rat hepatocytes (Aw and Jones, 1985). In fact, decreased Na^+/K^+-ATPase activity in rainbow trout is associated with energy limitations in a number of studies (Krumschnabel et al., 2000; Krumschnabel et al., 1998; Krumschnabel et al., 1999) although the opposite, a decrease in

protein synthesis and little effect on Na^+/K^+-ATPase, is also observed (Wieser and Krumschnabel, 2001) suggesting that there may be more than decreased ATP availability influencing ATP consuming processes and that the support for Atkinson's (1977) hierarchal organization hypothesis by Buttgereit and Brand (1995) may not be applicable in all cells or under all conditions.

When the adenylate pool is perturbed, cells attempt to re-establish steady state by altering the balance between ATP synthesis and consumption processes where some of these processes may actually overshoot the other for a short time before regaining balance (Wieser and Krumschnabel, 2001). This concept is highlighted in the adenylate energy charge (AEC) concept described by equation 2

$$\mathbf{AEC = ([ATP] + 0.5[ADP]) / ([AMP] + [ADP] + [ATP])} \text{ (Eq. 2)}$$

proposed by Atkinson based upon the observation that regulation of enzyme reaction rates was not vested in only ATP but also its metabolites ADP and AMP (Atkinson and Walton, 1967; Klungsoy et al., 1968; Ramaiah et al., 1964; Shen et al., 1968). For example, yeast phosphofructokinase (PFK) which plays a role in the catabolic pathway glycolysis was shown to be negatively regulated by ATP while an increase in AMP levels increased PFK catalytic rate (Ramaiah et al., 1964). Conversely, activity of rat liver citrate cleavage enzyme which plays a role in anabolic processes (lipid synthesis) is positively regulated by ATP and negatively regulated by ADP (Atkinson and Walton, 1967). These observations led to the hypothesis that the AEC may serve as a metabolic control parameter ensuring that cells do not deplete energy stores in the absence of large energy requirements or allocate all energy to storage resulting in a dearth of energy when it is required (Atkinson, 1977; Atkinson and Walton, 1967; Klungsoy et al., 1968; Shen et al., 1968).

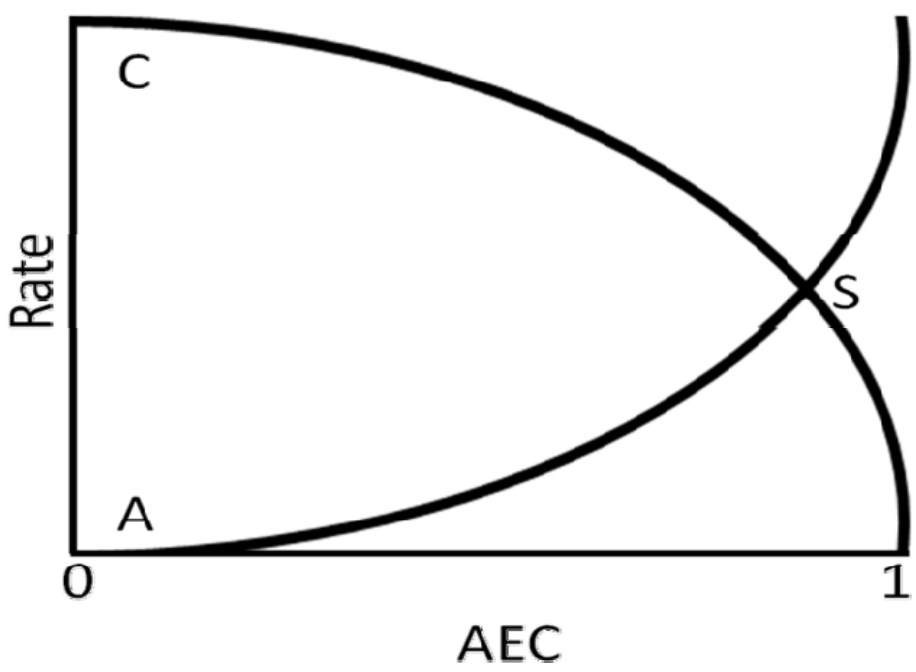

Figure 1.3. Adenylate energy charge (AEC) regulation of catabolic (C), anabolic (A) enzyme activities to achieve steady state (S); adapted from Atkinson (1968).

Recent evidence has identified AMP-activated protein kinase (AMPK) as an energy sensing protein that may be responsible for maintaining steady-state adenylate levels and thus the AEC; AMPK is regulated by ADP/ATP ratios in addition to its original observed regulation by AMP/ATP ratios (Oakhill et al., 2011). AMPK, which is regulated by the phosphorylation of a threonine (Thr^{172} of the α subunit), is known to play a role in mediating both anabolic and catabolic metabolism (Mantovani et al., 2011; Oakhill et al., 2011) providing a clear link between the AEC and energy metabolism. Therefore, the AEC, which falls between a value of zero and one can be considered as an indicator of the energetic status of cells identifying whether it is in a catabolic (C), anabolic (A) or at steady (S) state (see Fig. 1.3) (Atkinson, 1968, 1977; Atkinson and Walton, 1967) although these processes are likely regulated by AMPK (Oakhill et al., 2011).

The examination of toxicity at the cellular level is often examined in isolated hepatocytes in rainbow trout which are considered a valuable model to examine the toxicity of environmental chemicals (Pesonen and Andersson, 1997). Indeed, the liver accounts for a significant proportion of whole animal metabolism (Moon, 2004; Pacheco and Santos, 2001). Although a number of studies have examined O_2 consumption rates in isolated tissue/cells, very few indicate the contribution made by the liver to whole animal respiration. Prasada Rao et al. (1985) estimated the contribution of the liver to whole animal metabolism at about 24% in tilapia (*Tilapia mossambica*). This value is supported by evidence that the fractional protein synthesis rate in the liver in fasted and re-fed rainbow trout accounted for 17.9 and 30.6% day^{-1}, respectively using the ^{3}H-phenylalanine 'flooding-dose' technique to estimate protein synthesis (McMillan and Houlihan, 1989). These studies provide evidence that the liver is indeed a significant contributor to whole animal metabolism in addition to its importance in detoxification processes and that isolated hepatocytes are in fact a valuable model.

Studies using rainbow trout hepatocytes provided evidence that there are energetic costs associated with toxicant exposure and activation of detoxification systems. Typically these studies employed oxygen consumption or heat generation as indicators of energetic costs. For example, Bains and Kennedy (2004) reported increased oxygen consumption upon exposure of rainbow trout hepatocytes to the PAH pyrene supporting an increased energetic cost, but isolated mitochondrial respiration was largely unaffected. This increased oxygen consumption may arise directly from phase I metabolism that uses molecular O_2 as a substrate but the study provided no information as to whether ATP turnover was altered. On the other hand, energetic costs as demonstrated by increased oxygen consumption occurred specifically from activation of the phase III biotransformation system P-gp (Bains and Kennedy, 2005) as well as a decreased AEC (Hildebrand et al., 2009) suggesting that these rainbow trout hepatocytes were in a catabolic state. Additionally, increased glycolytic rate, O_2 consumption, and heat production in addition to a decreased ATP content was observed in rainbow trout hepatocytes exposed to dehydroabietic acid (DHAA) found in wood industry effluent (Rissanen et al., 2003) further supporting that exposure to pollutants and induction of detoxification mechanisms alter energetic costs in isolated fish hepatocytes incubated *in vitro*.

These studies generally support changes in whole fish and hepatocyte energetics when exposed to contaminants. My thesis will examine these issues in trout hepatocytes using a metabolic modelling approach.

1.3. Mathematical modelling of cellular metabolism

The quantitative understanding of metabolism is particularly important for the optimization of bioprocesses and several attempts to model the dynamics of metabolism are reported (Chan et al., 2003a; Lee et al., 1999; Nielsen, 1998; Varma and Palsson, 1994).

However, to completely describe these dynamics one must know the fine details of metabolic regulation which is often difficult to obtain (Uygun et al., 2007; Varma and Palsson, 1994). To overcome these challenges, models are developed based on the pathway stoichiometry and the assumption that the systems studied are in a pseudo steady-state where accumulation of intracellular metabolites is negligible in comparison to the rates at which metabolites are generated and consumed (Uygun et al., 2007; Varma and Palsson, 1994).

Several variants of these stoichiometry-based models are available, the simplest of which is known as *metabolic flux analysis* (MFA) (Nielsen, 1998). Other models have expanded on MFA; *flux balance analysis* (FBA) for example incorporates all known reactions by including genes encoding enzymes to construct a more robust MFA model (Orth et al., 2010) while *metabolic network flexibility analysis (*MNFA) incorporates thermodynamic constraints (Iyer et al., 2010). Despite these differences, mathematically these models all estimate intracellular fluxes based on extracellular measurements using a series of linear equations based on reaction stoichiometry that calculate intracellular rates that result in all uptakes of metabolites being equal to the rates of removal of the eventual metabolite of the substrates as described by equation 3

$$-\sum_{j\in O} S_{ij} V_j^m - \sum_{j\ni O} S_{ij} V_j \quad \text{(Eq. 3)}$$

where the negative sum of the stoichiometry S for metabolite i and reaction j multiplied by the measured flux (denoted V_j^m in Eq. 3) in which flux j is an element of the known fluxes ($j \in O$) is equal to the sum of the fluxes (j) that are not an element of known fluxes ($j \ni O$) multiplied by their respective stoichiometries (Uygun et al., 2007).

Generally, metabolic systems modelled are 'under-determined' meaning that the number of mass balances is smaller than the actual number of fluxes resulting in a system where there are an infinite number of solutions (Bonarius et al., 1996; Lee et al., 1999). Because of this, these

systems are solved using linear programming which is used to optimize specific objective equations (e.g. maximize or minimize elimination of lactic acid) which can be applied to each flux in order to determine the feasible flux ranges of each reaction that fall within the measured flux ranges which are used to constrain flux range estimations (Iyer et al., 2010).

Although these models are generally applied to microorganisms, especially those used in biotechnology applications (Edwards et al., 2001; Klamt et al., 2002; Mavrovouniotis and Stephanopoulos, 1990), this approach has been expanded to a number of other systems. For example, Bonarius et al. (1996) used this approach for mammalian hybridoma cells to try to improve production of pharmaceuticals by improving nutrient supplementation that would maximize specific pathways. Similarly, rat hepatocytes were used as a possible tool to explore the metabolism of bio-artificial livers (Chan et al., 2003a, b; Nolan et al., 2006) as well as to examine metabolic changes that occur upon exposure to the pesticide Triadimefon (Iyer et al., 2010).

This study will use an approach similar to that of Iyer et al. (2010) using the same metabolic network (Fig. 1.4) developed for rat hepatocytes as, although flux rates are likely to differ, reaction stoichiometry remains the same. The advantage of this approach is that these pathways and their respective stoichiometry are well known allowing the modeller to describe metabolic pathways as networks rather than a series of individual reactions and thus individual metabolic fluxes can be considered in the context of whole cell metabolism (Lee et al., 1999). Furthermore, this allows the examination of all metabolic fluxes simultaneously rather than using various radiolabelled substrates which may be done in varying culture conditions (Bonarius et al., 1996). Nevertheless, using a computational model remains highly theoretical relying strongly on the constraints defined and therefore estimates should be confirmed with experimental data as was done in Iyer et al. (2010).

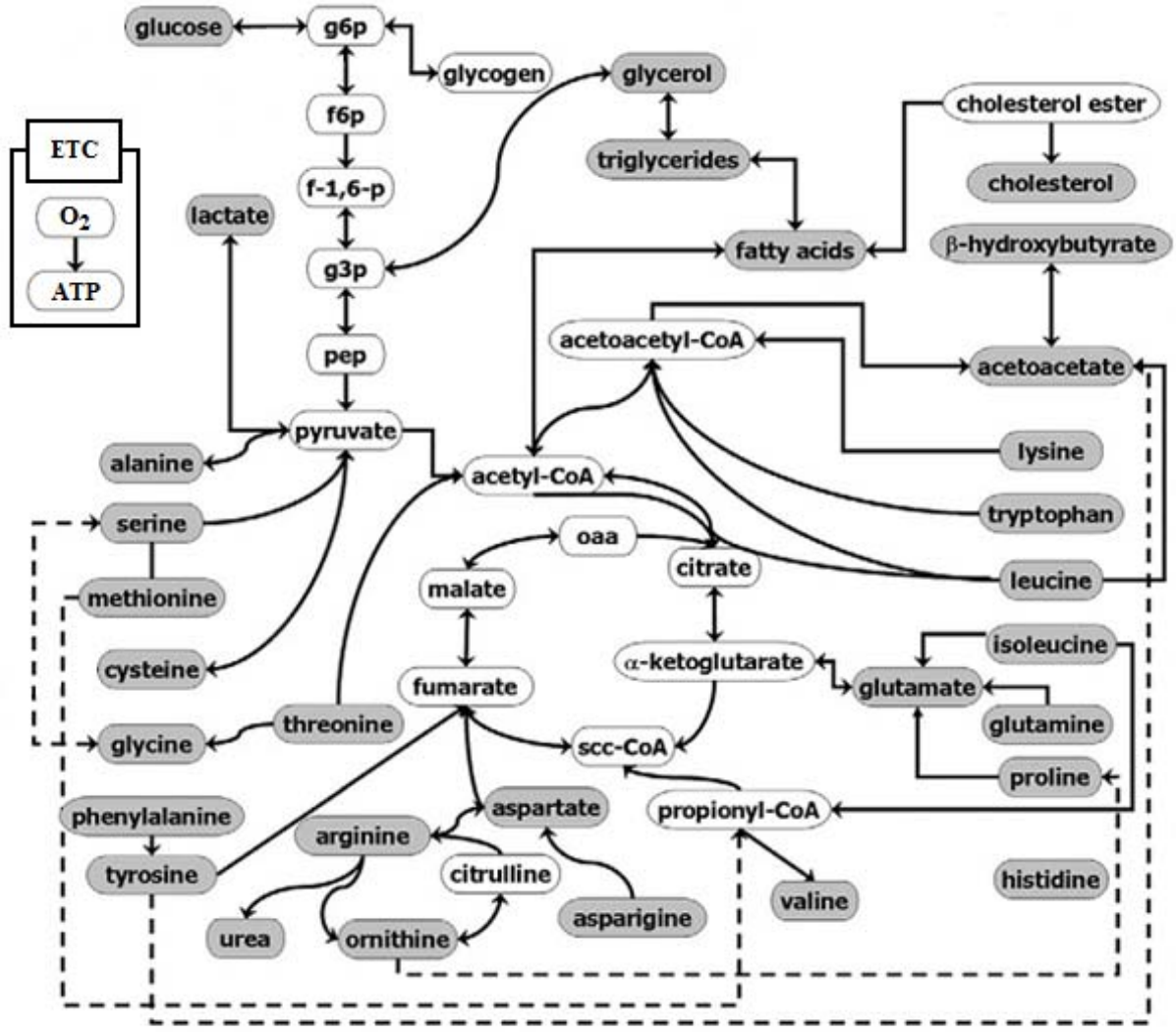

Figure 1.4. Metabolic network for metabolic flux analysis used in this study; adapted from Iyer et al. (2010).

1.4. Goals of this study

The continuous presence of pollutants in aquatic environments at sublethal levels is of concern to the health and welfare of aquatic organisms. In particular, as previously highlighted, induction of detoxification mechanisms such as CYP1A by AhR agonists is likely to result in increased energetic costs as an organism attempts to detoxify and eventually eliminate these molecules. Such increases in daily energetic requirements could result in impaired growth and reproduction and decreased activity which could impair the long-term survival and fitness of the organism.

Given the evidence presented throughout this Introduction, I hypothesize that activation of the AhR by β-NF (Fig. 1.5), a PAH and potent AhR agonist, will result in increased energetic costs leading to the metabolic reorganization of trout hepatocyte metabolism. This hypothesis can be separated into two fundamental questions which will be addressed in this thesis:

(1) Does AhR activation by β-NF increase energetic costs in rainbow trout hepatocytes?

(2) Do rainbow trout hepatocytes reorganize their metabolism to cope with β-NF-induced AhR activation?

β-NF was chosen as it is commonly used as the prototypical AhR agonist in a number of studies assessing its mode of action (Aluru and Vijayan, 2004; Navas and Segner, 2000; Tintos et al., 2008).

These questions will be assessed using a combination of traditional approaches including the estimation of the adenylate energy charge (AEC) and enzyme activities as well as using the novel approach of *in silico* modelling of metabolism. To my knowledge, this is the first study using this modelling approach in fish cells and one of the very few that have used metabolic flux analysis in a toxicological study. This combination of approaches will hopefully lead to an in depth analysis of the metabolic response of the trout liver to exposure to an AhR agonist and will

provide insights into the energetic costs that may occur in this tissue that may reflect upon the whole organism level.

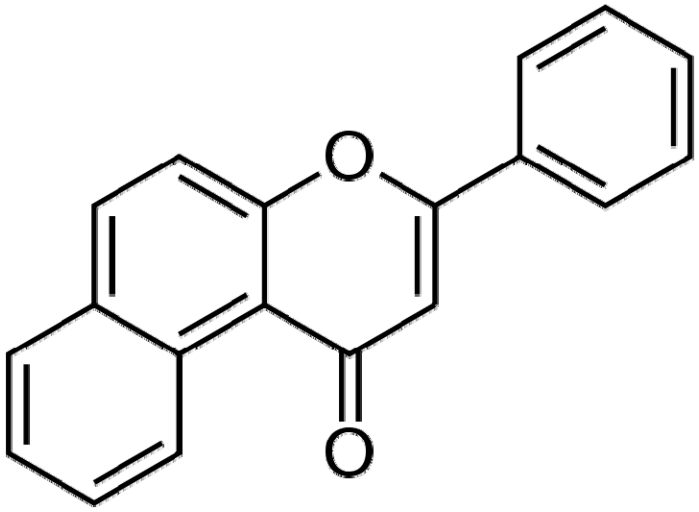

Figure 1.5 Structure of β-Naphthoflavone

Chapter 2 – Materials and Methods

2.0. Chemicals

Antibiotic-antimycotic and de-fatted bovine serum albumin (BSA) was purchased from Invitrogen Life Technologies (Carlsbad, CA) and MP Biomedical, LLC (Solon, OH), respectively. L-4,5[^{3}H]leucine was purchased from PerkinElmer Inc. (Waltham, MA). All other chemicals were purchased from Sigma-Aldrich Chemical Co. (St. Louis, MO) unless stated otherwise.

2.1. Fish

Female rainbow trout *Oncorhynchus mykiss* weighing 150 to 300 g were obtained from Linwood Acres Trout Farm (Campbellcroft, ON, Canada) and transported to the University of Ottawa Aquatic Care Facility where they were acclimated at least 2 weeks in 1185 L fibreglass circular tanks. Fish were fed commercial trout pellets and held under a 12 h light:12 h dark photoperiod in 13˚C dechloraminated City of Ottawa tap water. Trout used in experiments were juveniles and possessed no mature gonads. All experiments followed a protocol approved by the University of Ottawa Animal Care Protocol Review Committee and adhere to guidelines established by the Canadian Council on Animal Care for the use of animals in research and teaching.

2.2. Hepatocyte isolation

Rainbow trout were randomly chosen from the 1185 L tank and hepatocytes were isolated as described by Dugan and Moon (1998). In short, rainbow trout were anaesthetized in

benzocaine, cannulated through the portal vein and the liver perfused at 2 mL min^{-1} with modified Hanks' medium (in mM: 0.33 Na_2HPO_4, 0.44 KH_2PO_4, 0.8 $MgSO_4$, 136.9 NaCl, 5.4 KCl, 5 Hepes, 5 Na-Hepes, pH 7.63) containing 1 mM EGTA until no sign of blood leaving the liver was observed. This was followed by perfusion with a collagenase solution (modified Hanks' medium + 0.15 mg mL^{-1} Sigma type IV Collagenase) for 10-15 min or until the liver appeared soft to touch. The liver was removed from the fish carefully avoiding the gall bladder, chopped using a razor blade and the resulting cells passed through a 250 mm followed by a 75 mm nylon mesh screen. Cells were then transferred to a 50 mL centrifuge tube and rinsed 4 times by centrifugation at 90 x g at 4˚C for 2 min, once in modified Hanks' medium with EGTA (1 mM), once more in half modified Hanks' medium with EGTA and half re-suspension medium (modified Hanks' medium; 1.0% BSA and 1.5 mM $CaCl_2$) and twice more with only the final re-suspension medium. Hepatocyte viability was assessed using Trypan Blue exclusion and used only when initial viabilities > 90%. The final hepatocyte suspension was set to the desired concentration in Hanks' culture media (Hanks' resuspension medium; 5 mM glucose, antibiotic-antimycotic, essential amino acid and non-essential amino acids). Antibiotic-antimycotic (Invitrogen Life Technologies, 15240), essential amino acid mixture (Sigma-Aldrich, M5550) and non-essential amino acid mixture (Sigma-Aldrich, M7145) were used at a final concentration of 1X.

2.3. Hepatocyte exposure and protein content

Final hepatocyte suspensions at the desired concentration for a particular protocol were aliquoted into 96 well plates (adenylate energy charge; 90 μL), 6 well plates (metabolic flux analysis; 3 mL) or 48 well plates (all other experiments; 500 μL) using a repeater pipette and a sample from the final suspension randomly aliquoted into duplicate plastic conical centrifuge

tubes for protein content determination. Hepatocytes were then pre-incubated for 24 h at 13°C prior to exposures. At the end of the pre-incubation period the hepatocytes were exposed to the toxin or the DMSO vehicle control maintaining a constant DMSO content of 0.01% in all experiments.

Hepatocyte protein content was determined by centrifuging the conical tubes at 80 x g for 2 min at 4°C and rinsed twice with Sodium Phosphate Buffer (PBS) (pH 7.4) to remove BSA from the Hanks' culture media. Cells were then sonicated in 500 µL 6% PCA (perchloric acid). Following sonication, the tubes were again centrifuged at 10,000 x g for 30 sec and the supernatant was removed. The pellet was resuspended in 0.5 M NaOH by sonication and assayed for protein using the BCA (bicinchoninic acid) assay (Sigma-Aldrich) with BSA in 0.5 M NaOH to generate a standard curve.

2.4. Hepatocyte membrane integrity

Hepatocyte membrane integrity was assessed by estimating lactate dehydrogenase (LDH) activity in the extracellular culture media according to Bains and Kennedy (2004). Triton-X 100 (final 1% v/v) was used as a positive control to completely permeabilize the hepatocyte leading to the release of all LDH from the cell into the culture media (Bains and Kennedy, 2004). LDH activity was estimated spectrophotometrically using a SPECTRAmax PLUS 384 microplate spectrophotometer (Molecular Devices, Sunnyvale, CA) using 10 µL of sample; the sample was added in triplicate to 200 µL pyruvate (5 mM) in imidazole buffer (50 mM, pH 7.4) in a 96-well microtitre plate. Plates were then read kinetically for 5 min at 340 nm followed by the addition of 10 µL NADH (2 mM) in imidazole buffer. Absorbance was monitored at 340 nm for 20 min or until reactions were complete. Absorbance values were converted to µmoles NADH oxidized min^{-1} using the NADH molar extinction coefficient 6.22. Values in the medium were compared

to those of the medium in the positive control as an estimate of membrane integrity and thus hepatocytes viability.

2.5. EROD assay

EROD activities were assessed in hepatocytes plated into 48 well plates at approximately 15 mg mL^{-1}. Following toxin exposure, the culture media was aspirated and plates frozen at -80°C for no more than one week. EROD activities were estimated using a slightly modified method described by Kennedy et al. (1995). Briefly, 150 µL PBS (phosphate-buffered saline) was added to each well of the thawed 48 well plates containing hepatocytes. Resorufin standards were prepared in methanol (0.54 mM) and diluted to concentrations ranging from 0.1 to 0.5 µM in PBS. 150 µL of each standard was plated into empty wells on the same plate. 7-Ethoxyresorufin solution (1 mM) was prepared in methanol and diluted to 0.63 µM in PBS immediately prior to use and 25 µL was added to each well. Plates were incubated in the dark for 5 min and then reactions were initiated by the addition of 25 µL NADPH (1.2 mM) and read kinetically for 20 min at 530/590 nm excitation/emission filters using a SpectraMax GeminiXS fluorometer (Molecular Devices, Sunnyvale, CA). Activity was estimated for the linear part of the reaction curve and calculated from the generated resorufin standard curve. All activities were normalised to cell protein content.

2.6. Adenylate energy charge

Adenylate energy charge (AEC) was assessed as described by Hildebrand et al. (2009) using the commercial kit available from Lonza (Basel, Switzerland). Briefly, 90 µL of hepatocyte suspension adjusted to 10 mg mL^{-1} was aliquoted into wells of a 96 well plate (ADP and AMP assays) or a 96 well plate for luminometer (ATP assay) provided with the kit. Following a 24 h

pre-incubation, hepatocytes were exposed to solutions of either actinomycin D (1 μM), cycloheximide (1 μM), resveratrol (10 μM) or DMSO vehicle control for 30 min after which cells were exposed either to DMSO vehicle control or 1 μM β-NF for 48 h at 13^{o}C. For measurements of AMP, this protocol was performed 1 h prior to the wells used for ADP and ATP to compensate for incubation time of the AMP assay. At the end of the 48 h exposure, cell suspensions were lysed with the lysis solution provided with the kit and then incubated for 10 min at room temperature.

Wells for AMP and ADP were then converted to ATP using myokinase (rabbit muscle; Sigma-Aldrich) and pyruvate kinase (rabbit muscle**;** Sigma-Aldrich). Briefly, 100 μL cell lysate was added to 300 μL 40 mM tricine buffer containing 0.04 mM phosphoenol pyruvate (PEP) and 10 mM KCl (pH 7.75) and myokinase (100 U mL^{-1}) plus pyruvate kinase (40 U mL^{-1}); this was incubated at room temperature for 120 min. ADP was converted to ATP by excluding myokinase from the tricine buffer and requiring an incubation time of only 5 min. Finally, AMP and ADP were converted to ATP and ATP was measured according to manufacturer's directions using ATP to generate a standard curve. ADP was then estimated by subtracting ATP levels and AMP levels were estimated by subtracting levels of ADP and ATP. Adenylate levels were normalized to the cell mass.

2.7. Protein synthesis

Protein synthesis was assessed using L-4,5[^{3}H]leucine incorporation into the trichloroacetic acid (TCA) insoluble protein fraction similar to the method described by Krumschnabel et al. (2000) and Kwast and Hand (1993). In short, L-4,5[^{3}H]leucine was added to a concentration of 0.5 μCi mL^{-1} in each well of a microtitre plate (0.25 μCi well^{-1}) containing hepatocytes (25 mg mL^{-1}). Hepatocytes were then resuspended by gently pipetting and incubated

for 2 and 4 h at 13°C and sampled at 0, 2 and 4 h post [^{3}H]leucine addition by aliquoting 30 µL of the radioactive hepatocyte suspensions onto G6 glass fibre filters (Fisher Scientific, Pittsburgh, PA) in duplicate. Filters were allowed to air-dry for several seconds and then placed into ice-cold 10% TCA containing 5 mM unlabelled L-leucine for 10 min followed by two 15 min washes in 5% TCA at room temperature to precipitate proteins onto the filter. This was followed by two 10 min washes in 99% ethanol. Filters were then air-dried and were added to scintillation vials for counting using 5 mL Ready-Safe scintillation fluid (Beckman Coulter, Brea, CA). [^{3}H]Leucine incorporation was calculated based on specific activity (54.1 Ci mMole^{-1}) normalized to protein content and expressed relative to control at 0 h.

2.8. Rubidium uptake

Rb^+ uptake was assessed as an indicator of Na^+/K^+-ATPase activity by replacing culture media K^+ with Rb^+ (in mM: 0.33 Na_2HPO_4, 0.44 H_3PO_4, 0.8 $MgSO_4$, 136.9 NaCl, 5.4 RbCl, 5 Hepes, 5 Na-Hepes, 1.5 $CaCl_2$, 1.0% BSA, pH 7.63) in each well of a microtitre plate containing hepatocytes (25 mg mL^{-1}). Following a 10 min incubation with K^+ free culture media, 150 µL cell suspension was added to a 1.5 mL plastic conical tube and centrifuged for 2 min at 10,000 x g. The supernatant was immediately aspirated and the pellet washed 3 times with ice-cold $MgCl_2$ medium (in mM: 95 $MgCl_2$, 10 imidazole) to remove all extracellular Rb^+. Cell pellets were lysed in 5% PCA with 0.05% Triton-X 100 (250 µL) then centrifuged for 2 min at 10,000 x g. Supernatants were transferred to a new plastic centrifuge tube and diluted 10 times in KCl (26.8 mM). Samples were then analyzed for Rb^+ using a Varian AA240 atomic absorption spectrometer (Agilent technologies, Santa Clara, CA) with acetylene carrier gas at 780 nm with a slit width of 0.2 nm using RbCl in KCl (26.8 mM) to generate a standard curve. Concentrations

of intracellular Rb^+ were divided by duration of incubation, related to protein content and expressed relative to control at 0 h.

2.9. Metabolic flux analysis: Metabolite assays

Metabolite flux measurements were performed as described by Iyer et al. (2010) adjusted for a slower metabolic rate in rainbow trout compared with rat hepatocytes. Hepatocytes were isolated as in 2.3 above and hepatocytes from 2 fish were combined and adjusted to a concentration of 25 mg mL^{-1} and aliquoted into a 6 well plate in duplicate. Following the 24 h pre-incubation, the culture media was renewed with fresh culture media and hepatocytes were exposed to either β-NF or DMSO vehicle control. For each treatment, culture media in one of the duplicates was removed at 24 h post-exposure with a pipette and transferred to a plastic tube for metabolite analysis and replaced with fresh culture media with β-NF or DMSO vehicle control for a second 24 h period of incubation (total of 48 h exposure). Media was then removed as was done at 24 h for metabolite analyses in both duplicates at 48 h post initial exposure (see Fig. 2.1). Metabolic fluxes were then determined by estimating individual metabolites at 24 and 48 h post-exposure and levels found in hepatocyte free culture media were subtracted. The difference in metabolite level was divided by the hours of exposure and the protein content.

Metabolite assays for metabolic flux analysis were performed using either a SPECTRAmax PLUS 384 microplate spectrophotometer (Molecular devices, Sunnyvale, CA) or a 6890N network gas chromatograph system (Agilent technologies, Santa Clara, CA). Metabolites were analyzed in culture media de-proteinized using PCA (6% final), followed by centrifugation at 10,000 x g for 2 min and neutralizing the supernatant with the addition of 5 M K_2CO_3.

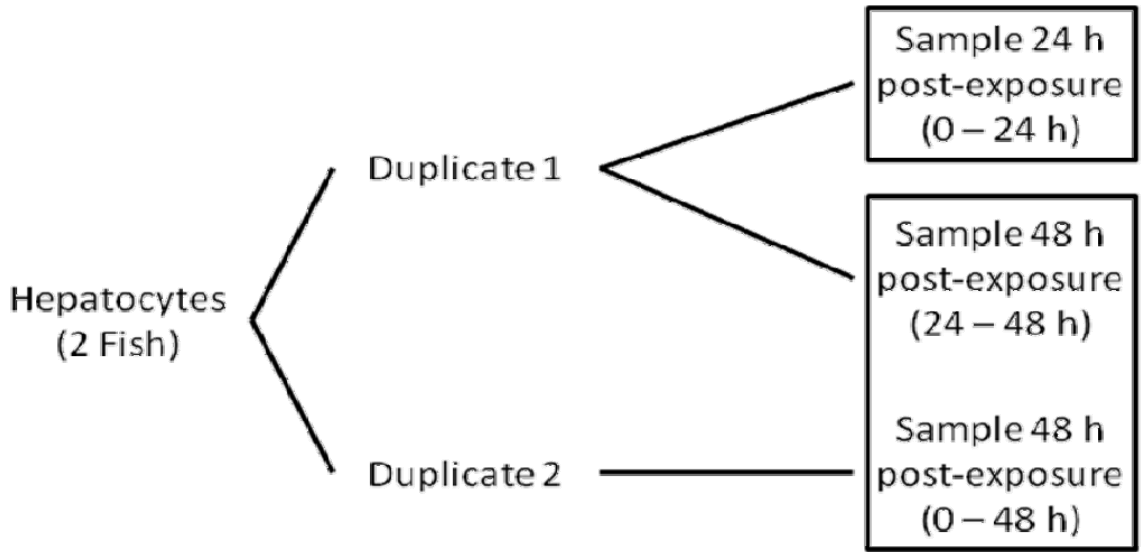

Figure 2.1. Metabolic flux analysis sampling flow chart for isolated hepatocytes of 2 fish combined.

2.9.1. Ammonia

Ammonia in the culture media was assessed according to Verdouw et al. (1978). In a 2 mL glass test tube, 280 µL sample or standard was added followed by 60 µL salicylate (2.5 M), 60 µL sodium nitroprusside (0.8 mM) and 60 µL alkaline hypochlorite (1:1 v/v 6% bleach and 1.6 M sodium citrate in 1 M NaOH). Tubes were immediately vortexed for 5 sec after each addition. Reactions were incubated at room temperature in the dark for 3 h and 200 µL of the medium was added to a 96-well plate in duplicate and read spectrophotometrically at 650 nm. Ammonia levels were calculated based on a standard curve generated using ammonium chloride.

2.9.2. Free Fatty Acids

Media free fatty acids (FFA) were determined using a gas chromatography similar to the method described by Vaillancourt et al. (2009) for rat plasma although separation of lipid fractions was unnecessary due to the simplicity of the culture media. Briefly, culture media lipids (350 µL) were extracted in 50 mL glass tubes by adding 15 mL chloroform:methanol (2:1 v/v; Folch medium) after addition of 30 µL 17:0 fatty acid (0.3 µg μL^{-1}) as an internal standard. Samples were vortexed then centrifuged for 10 min at 2,500 x g. The supernatant was filtered through a GF/C glass fibre filter and the pellet was re-extracted twice more with 10 mL Folch and a final time in 5 mL Folch. Supernatants were combined and 0.25 volumes of 0.25% KCl added to the combined supernatants; the tubes were centrifuged at 2,500 x g after which the aqueous phase was aspirated and the organic phase was transferred to a rotavapor flask and the organic solvent evaporated using a rotavapor (Büchi, Flawil, Switzerland) at 70°C. The remaining lipids were resuspended in hexane:isopropanol (3:2) and transferred to a 15 mL glass tube filled with N_2 gas, capped and stored at -20°.

Free fatty acids were methylated by evaporating the hexane:isopropanol under N_2 gas at 50°C and 100 µL methanol was added followed by 1 mL dimethoxypropane and 40 µL HCl (12 N) and vortexed following each addition. Samples were left at room temperature for 30 min and then dried under N_2 gas at 50°C. Lipids were resuspended in 50 µL isooctane and transferred to an autosampler tube and analyzed using a 6890N network gas chromatograph system (Agilent technologies, Santa Clara, CA) and compared to pure fatty acid standards (Sigma-Aldrich) for retention time and concentrations were determined as the area under individual peaks for all peaks that represented more than 1% of total free fatty acids and calculated based on the known concentration and area of the internal standard.

2.9.3. Glucose

Media glucose was estimated by the production of NADH generated through phosphorylation of glucose to glucose-6-phosphate (G6P) followed by the reduction of G6P byglucose-6-phosphate dehydrogenase (G6PDH) with NAD^+. Glucose was assessed in 10 µL samples or D-Glucose standards using a 96-well plate in triplicate. To each well 200 µL assay mix (in mM; 60 Trizma base, 40 Tris-HCl, 1 $MgSO_4$, 2 NAD^+, 1 ATP) with G6PDH (0.1 U mL^{-1}) (*Leuconostoc mesenteroides*; Sigma-Aldrich) was added and the plate was incubated at room temperature for 5 min and pre-read at 340 nm. Reactions were initiated by the addition of 10 µL hexokinase (0.3 U mL^{-1}) (Bakers yeast, Sigma-Aldrich) and the plate was allowed to sit at room temperature for 30 min and once again read at 340 nm. Values of the pre-read were subtracted from the final reading and glucose concentrations were calculated from a standard curve.

2.9.4. Glutamine and Glutamate

L-Glutamine and L-glutamate was estimated in 70 µL neutralized samples where L-glutamine was first deaminated in 20 µL acetate buffer (50 mM) and 10 µL glutaminase (4 U mL^{-1}) (*Escherichia coli*, Sigma-Aldrich) in acetate buffer and incubated at 37°C for 1 h. L-Glutamate

samples were manipulated in the same way but the glutaminase enzyme was replaced with acetate buffer. Samples (25 µL) containing L-glutamine and L-glutamate as well as L-glutamic acid standards were plated in triplicate in a 96-well plate and 25 µL assay soup (in mM; 8.01 NAD^+, 2.67 ADP) and 50 µL 1:20 (v/v) hydrazine in Tris-EDTA buffer (in mM; 100 Tris-HCl, 2 EDTA) was added to each well and read kinetically at 340 nm for 5 min to estimate background activities. Thereafter 10 µL L-glutamic dehydrogenase (1235 U mL^{-1}) (Bovine liver, Sigma-Aldrich) in ddH_2O was added to initiate the reaction and the formation of NADH was followed kinetically at 340 nm until absorbance no longer changed. L-glutamate levels were then calculated from standard curves while L-glutamine was calculated from the same standard curve and levels of L-glutamate were subtracted.

2.9.5. Ketone Bodies

Acetoacetate and β-hydroxybutyrate were assessed as described by Bergmeyer (1985). Acetoacetate in 240 µL neutralized samples was enzymatically reduced to β-hydroxybutyrate with the addition of 12 µL D-3-hydroxybutyrate dehydrogenase (3-HBDH) (15 U mL^{-1}) (*Pseudomonas lemoignei*; Sigma-Aldrich) and 90 µL buffer (in mM; 100 Triethanolamine, 5 EDTA, 8 NADH, pH 7.5) and incubated at room temperature for 1 h. Samples for β-hydroxybutyrate measurements were manipulated in the same manner except the 3-HBDH was replaced with ddH_2O. Acetoacetate and β-hydroxybutyrate were then estimated by following the reduction of an Fe^{3+}-BPS complex to Fe^{2+}-BPS measured at 546 nm mediated by phenazine methosulfate and reduced by NADH which is generated by the oxidation of β-hydroxybutyrate by 3-HBDH and NAD^+. Briefly, thawed samples and β-hydroxybutyrate standards were heated at 56°C for 15 min and 150 µL was plated in a 96-well plate in duplicate. To each well, 20 µL NAD^+/phosphate buffer (in mM; 25 NAD^+, 1000 KH_2PO_4, pH 8.5) followed by 20 µL Fe^{3+}-BPS (in mM; 5 $FeCl_3$, 20 BPS) and 10 µL phenazine methosulftate (63 µM) were added. The plate

was read kinetically for 5 min at 546 nm to observe background absorbance and the reaction was then initiated by the addition of 3-HBDH (15 U mL^{-1}) and read kinetically at 546 nm until absorbance no longer changed. β-Hydroxybutyrate levels were then calculated from a standard curve while acetoacetate was calculated from the same standard curve and levels of β-hydroxubutyrate were subtracted.

2.9.6. Lactic Acid

Lactic acid was assessed by following the production of NADH generated from the reduction of lactic acid by lactic dehydrogenase (LDH) (Bovine heart, Sigma-Aldrich) and NAD^+. Briefly, 5 µL deproteinized sample or standard was added to a 96-well plate in triplicate and 250 µL glycine 1:2 (v/v) with NAD^+ (2.5 mM) and 10 µL LDH (1500 U mL^{-1}) was added to each well. Plates were incubated for 30 min and then read at 340 nm. Lactic acid levels were quantified based on a lactic acid standard curve.

2.9.7. Intracellular Glycogen

Intracellular glycogen was assessed according to the method described by Keppler and Decker (1974). In short, hepatocytes were sonicated in ice-cold 6% PCA then centrifuged at 10,000 x g for 5 min. One hundred µL of the supernatant was transferred to a small glass tube and 50 µL $NaHCO_3$ (1 M) and 1 mL amyloglucosidase (11.6 U mL^{-1}) in acetate buffer (0.1 M) was added to the glass tube and incubated at 35-40°C for 2 h. At the end of the incubation the reaction was stopped by the addition of 25 µL 70% PCA, vortexed and centrifuged at 6,250 x g. Glycogen was then assayed using the glucose assay (section 2.9.3) corrected for the presence of glucose in the cell and in the amyloglucosidase solution and expressed as glycosyl units.

2.9.8. Cholesterol and Triglycerides

Cholesterol and triglycerides were determined using commercially available kits from Teco Diagnostics (Anaheim, CA, USA) adjusted for 96-well plates and glycerol was measured using the free glycerol reagent (Sigma-Aldrich) and adjusted for 96-well plates.

2.10. Metabolic flux analysis

The mathematical model for metabolic flux analysis was developed based on the pathways described by Iyer et al. (2010) and Yang et al. (2010). Using CellNetAnalyzer (Klamt et al., 2007) implemented in MATLAB (MathWorks Inc., Natick, MA), a stoichiometry table for each reaction was developed by entering individual reactions (Appendix A) and exported as a stoichiometry matrix into the mathematical program GAMS integrated development environment version 26.6.3 (GAMS, Washington, DC; downloaded from www.gams.com).

Flux constraints for measured metabolites (Table A.2) were determined by calculating maximum and minimum fluxes as the average flux plus or minus standard deviation, respectively. On the other hand, constraints for unknown uptake and output of amino acids were set to a range of -10 to 10 nmol h^{-1} mg^{-1} protein as incorporation of many amino acids into glucose and CO_2 production in rainbow trout hepatocytes was shown to be less important than lactate (French et al., 1981) which shows an average flux of 11.23 to 19.91 (Table 3.1) while flux ranges for glycerol, cholesterol and triglyceride were set at -5 to 5 nmol h^{-1} mg^{-1} protein as these were the smallest ranges that allowed a feasible model and may fall within the undetectable range of the assays used to measure them. Similarly, constraints for unknown intracellular fluxes were set to a range of -50 to 50 nmol h^{-1} mg^{-1} protein as glucose fluxes were observed to show maximal rates of 58.2 nmol h^{-1} mg^{-1} protein (Table A.2) although the constraint was set to 50

nmol h^{-1} mg^{-1} protein as most other metabolite fluxes were well below this value. Irreversible fluxes were given a minimum flux rate of 0 nmol h^{-1} mg^{-1} protein.

Finally, because CYP1A metabolism of β-NF was not directly assessed, CYP1A constraints (Table A.2) were set to a range of 0 to 1 nmol h^{-1} mg^{-1} protein (assuming a very low control CYP1A rate) with the control group constraints and to 4 to 5 nmol h^{-1} mg^{-1} protein for the low CYP1A activity estimates based on an increase in EROD activity of about 5 times control values (Fig. 3.1). Additionally, in order to determined the metabolic consequences of unlimited CYP1A activity, maximal CYP1A under the given constraints was estimated and rounded to the closest 100 and to a range of 1 nmol h^{-1} mg^{-1} protein. These constraints were incorporated into the GAMS program and fluxes were then maximized and minimized using linear programming solved by GAMS with CPLEX 12 solver (IBM Corporation, Armonk, NY) for each individual reaction (Table A.4).

2.11. Enzyme activities

Hepatocytes (15 mg mL^{-1}) incubated in 48 well plates were transferred to plastic conical centrifuge tubes and centrifuged at 80 x g for 2 min. Culture media was removed and replaced with 1:15 w/v homogenisation buffer described by Sanden et al. (2003) (in mM: 20 Tris-HCl, 5 EDTA, 5 $MgCl_2$, 150 KCl, 5 β–mercaptoethanol, pH 7.4) based on the original cell mass in microtitre plate (7.5 mg cells $well^{-1}$). There were no signs of hepatocytes remaining in wells as they had formed a layer adhering to each other. Cells were sonicated, centrifuged at 10,000 x g for 2 min and enzyme activities analyzed in the supernatant. All estimates used a SPECTRAmax PLUS 384 microplate spectrophotometer (Molecular Devices, Sunnyvale, CA) in 96 well plates and each sample was plated in triplicate. Rates were maximum activities determinate at saturating substrate concentrations and were calculated after subtracting background activities (rates in the

absence of substrate) from the steepest linear part of the slope and on extinction coefficients (molar extinction coefficients: NADH/NADPH, 6.22; DTNB, 13.7).

2.11.1. Alanine Aminotransferase (AAT; *E.C. 2.6.1.2*)

Alanine aminotransferase was assessed by the disappearance of NADH measured at 340 nm. Assay mix (final in mM: 200 alanine, 50 imidazole, 0.2 NADH, 0.05 Pyridoxal-5-phosphate, pH 7.4) with LDH (48 U mL^{-1}) is added to each well and plates are measured kinetically for 5 min to observe background rates. Reactions were initiated by the addition of the substrate α-ketoglutarate (final; 10 mM) and measured for 20 min.

2.11.2. Glyceraldehyde-3-Phosphate Dehydrogenase (G-3PDH; *E.C. 1.2.1.12*)

Glyceraldehyde-3-phosphate dehydrogenase was assessed by the disappearance of NADH measured at 340 nm. Assay mix (final in mM: 20 imidazole, 0.15 NADH, pH 7.6) is added to each well and plates are measured kinetically for 5 min to observe background rates. The reaction was initiated by the addition of the substrate dihydroxyacetone phosphate (final; 0.1 mM) and measured for 20 min.

2.11. 3. Glucose-6-Phosphate Dehydrogenase (G6PDH; *E.C. 1.1.1.49*)

Glucose-6-phosphate dehydrogenase was assessed by the appearance of NADPH measured at 340 nm. Assay mix (final in mM: 50 imidazole, 7 $MgCl_2$, 0.4 NADP, pH 7.4) is added to each well and plates are measured kinetically for 5 min to observe background activities. The reaction was initiated by the addition of substrate G6P (final; 1 mM) and measured for 20 min.

2.11. 4. Citrate Synthase (CS; *E.C. 2.3.3.1*)

Citrate synthase was assessed by the appearance of 5-thio-2-nitrobenzoic acid measured at 412 nm. Assay mix (final in mM: 50 Tris-HCl, 0.3 acetyl-CoA, 0.1 5,5'-dithiobis-(2-nitrobenzoic acid), pH 8.0) is added to each well and plates with and without oxaloacetate (0.5 mM) and are

immediately measured kinetically for 20 min. Rates in the absence of oxaloacetate are subtracted from those with oxaloacetate.

2.11. 5. β-Hydroxyacyl CoA-Dehydrogenase (HOAD; *E.C. 1.1.1.35*)

β-Hydroxyacyl CoA-dehydrogenase was assessed by the disappearance of NADH measured at 340 nm. Assay mix (final in mM: 50 imidazole, 0.05 NADH, pH 7.4) is added to each well and plates are measured kinetically for 5 min to observe background activities. The reaction was initiated by the addition of substrate acetoacetyl-CoA (final; 0.1 mM) and measured for 20 min.

2.11. 6. Phophoenolpyruvate Carboxykinase (PEPCK; *E.C. 4.1.1.32*)

Phosphoenolpyruvate carboxykinase was assessed by the disappearance of NADH measured at 340 nm. Assay mix (final in mM: 80 Tris-HCl, 1 $MgCl_2$, 1 $MnCl_2$, 1.5 IDP, 0.17 NADH, 1 phosphoenolpyruvate (PEP), pH 7.4) with malate dehydrogenase (19 U mL^{-1}) is added to each well and plates are measured kinetically for 5 min to observe background activities. The reaction was initiated by the addition of the substrate $NaHCO_3$ (final; 20 mM) and measured for 20 min.

2.11. 7. Pyruvate Kinase (PK; *E.C. 2.7.1.40*)

Pyruvate kinase was assessed by the disappearance of NADH measured at 340 nm. Assay mix (final in mM: 50 MOPS, 5 ADP, 100 KCl, 10 $MgCl_2$, 0.1 F-1,6-P_2, 0.15 NADH, pH 7.4) with LDH (80 U mL^{-1}) is added to each well and plates are measured kinetically for 5 min to observe background activities. The reaction was initiated by the addition of the substrate PEP (final; 5 mM) and measured 20 min.

2.11. 8. Isocitrate Dehydrogenase (IDH; *E.C. 1.1.1.42*)

Isocitrate dehydrogenase was assessed by the appearance of NADPH measured at 340 nm. Assay mix (final in mM: 50 imidazole, 4 $MgCl_2$, 0.4 NADP, pH 7.4) is added to each well

and plates are measured kinetically for 5 min to observe background rates. The reaction was initiated by the addition of substrate isocitrate (final; 0.6 mM) and measured for 20 min.

2.11. 9. Malic Enzyme (ME; *E.C. 1.1.1.40*)

Malic enzyme was assessed by the appearance of NADPH measured at 340 nm. Assay mix (final in mM: 50 imidazole, 1 $MgCl_2$, 0.4 NADP, pH 7.4) is added to each well and plates are measured kinetically for 5 min to observe background rates. The reaction was initiated by the addition of substrate malate (final; 1 mM) and measured for 20 min.

2.12. Statistical analysis

Statistical analyses and graphs used Sigma Plot 11 (Systat Software Inc., San Jose, CA). Statistically significant differences were determined using a two-way repeated measures ANOVA when examined for effects of time and treatment, a one-way repeated measures ANOVA when examined for effect of treatment or a two-way ANOVA when sample size for treatment or time points are not equal. Upon determination of significant difference ($p<0.05$), a Holm-Sidak post-hoc test was performed.

Chapter 3 - Results

3.0. Characterization of AhR activation and cytotoxicity

Hepatocyte EROD activities increased with increasing β-NF concentration at both 24 and 48 h post-exposure reaching a maximum activity of 27.4 ± 4.0 pmol min^{-1} mg^{-1} protein (n = 4) at 24 h and 34.1 ± 4.1 pmol min^{-1} mg^{-1} protein (n = 4) at 48 h; these maximum activities were achieved at 1 μM β-NF in both cases (Fig. 3.1A). Exposure to a concentration of 10 μM β-NF did not significantly change EROD activities. EROD activity at 48 h post-exposure was also significantly higher ($p<0.05$) than the 24 h post-exposure at concentrations of 0.1 to 10 μM β-NF. Although EROD activities at 6 and 12 h are reported at 1 μM β-NF, statistical analysis was not performed on these measurements as these were not estimated at other β-NF concentrations; these values are shown to demonstrate a continuous increase in EROD activity over the 48 h period. Conversely, extracellular media LDH activity showed no significant differences among concentrations of β-NF or over time while activity was significantly lower ($p<0.001$**)** than the Triton X-100 positive control (Fig. 3.1B).

Inhibitors of protein synthesis actinomycin D (Fig. 3.2) and cycloheximide (Fig. 3.3) also showed no significant differences in medium LDH activities suggesting neither agent affected cell viability while EROD activities were significantly lower at 1 μM for actinomycin D (Fig. 3.2A) and at 1 and 10 μM for cycloheximide (Fig. 3.3A). Resveratrol exposure as well did not show any effect on cell viability but also did not result in significant differences in EROD activities (Fig. 3.4).

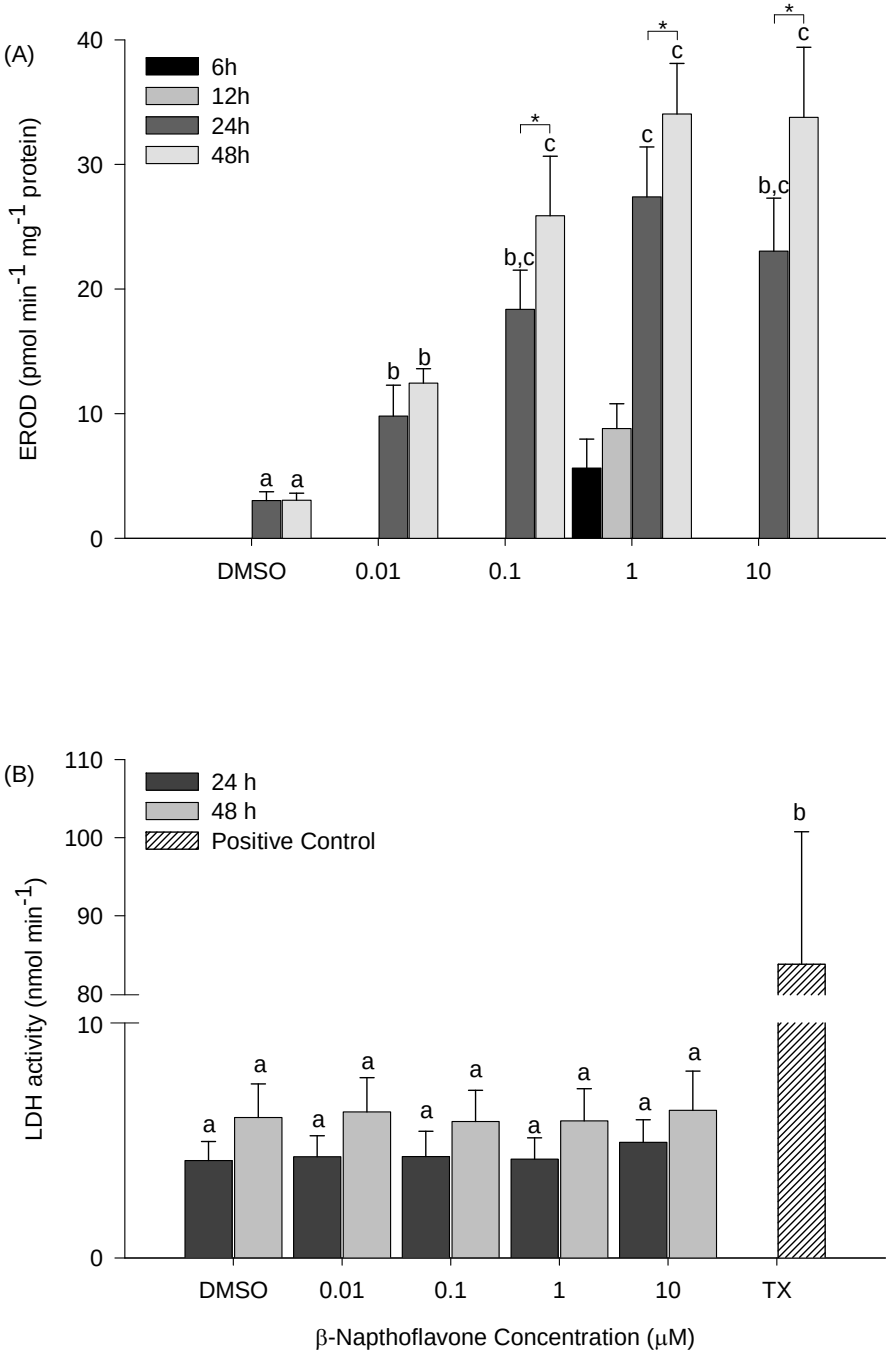

Figure 3.1. EROD activities (A) and culture media LDH activities (B) for isolated rainbow trout hepatocytes at various incubation times and concentrations of β-NF or 1% Triton X-100 (TX) as a positive control for cell disruption. Data represent mean + S.E.M. (n = 4). Statistical analysis consisted of a repeated measures two-way ANOVA and significant difference ($p<0.05$) are represented by different letters within time points while statistical differences within doses are indicated by an asterisk.

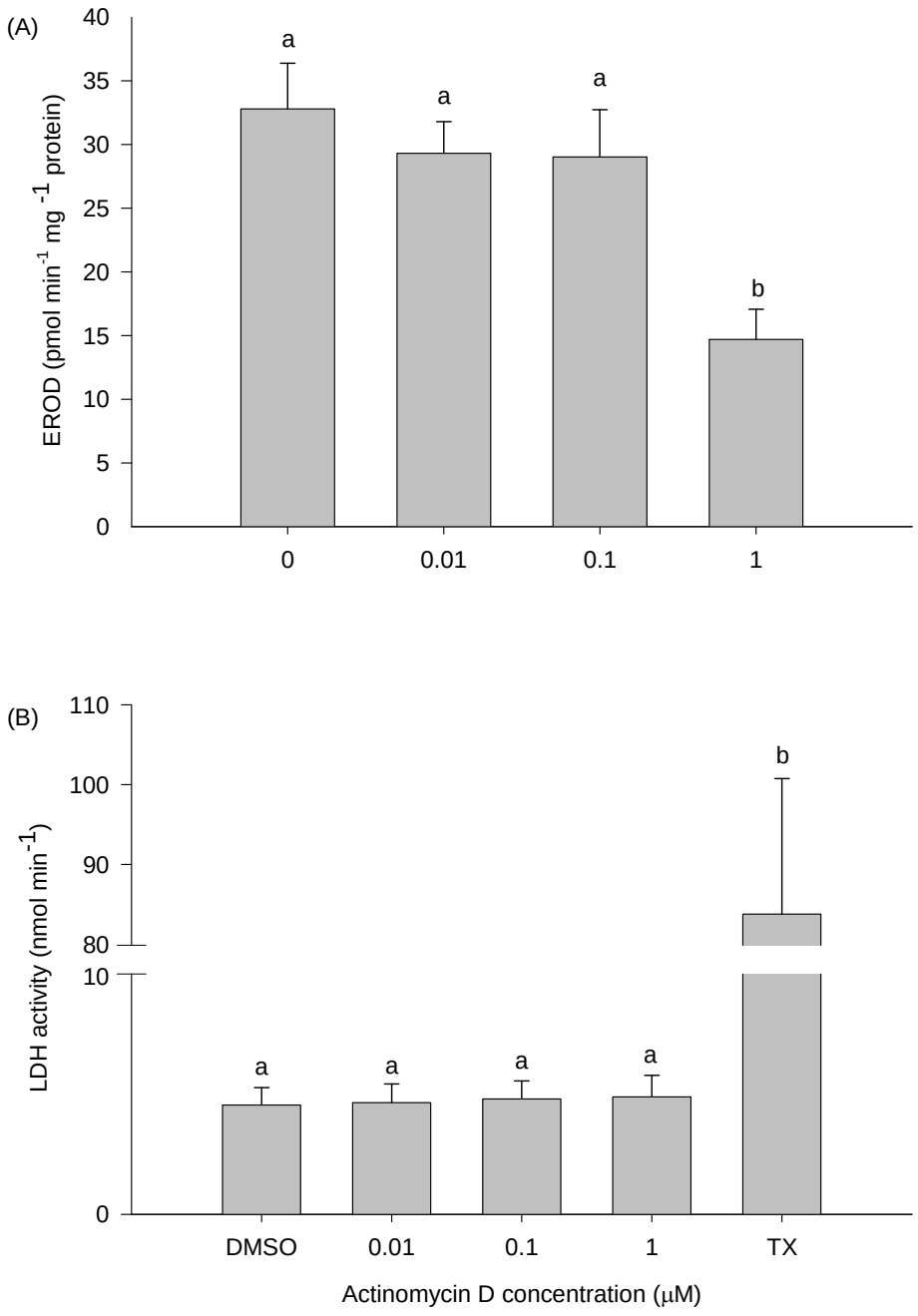

Figure 3.2. EROD activities (A) and culture media LDH activities (B) for isolated rainbow hepatocytes at 1 μM β-NF and various concentrations of actinomycin D or 1% Triton X-100 (TX) as a positive control for cell disruption at 48 h post-exposure. Data represent mean + S.E.M. (n = 5). Statistical analysis consisted of a repeated measures one-way ANOVA and significant difference ($p<0.001$) are represented by different letters.

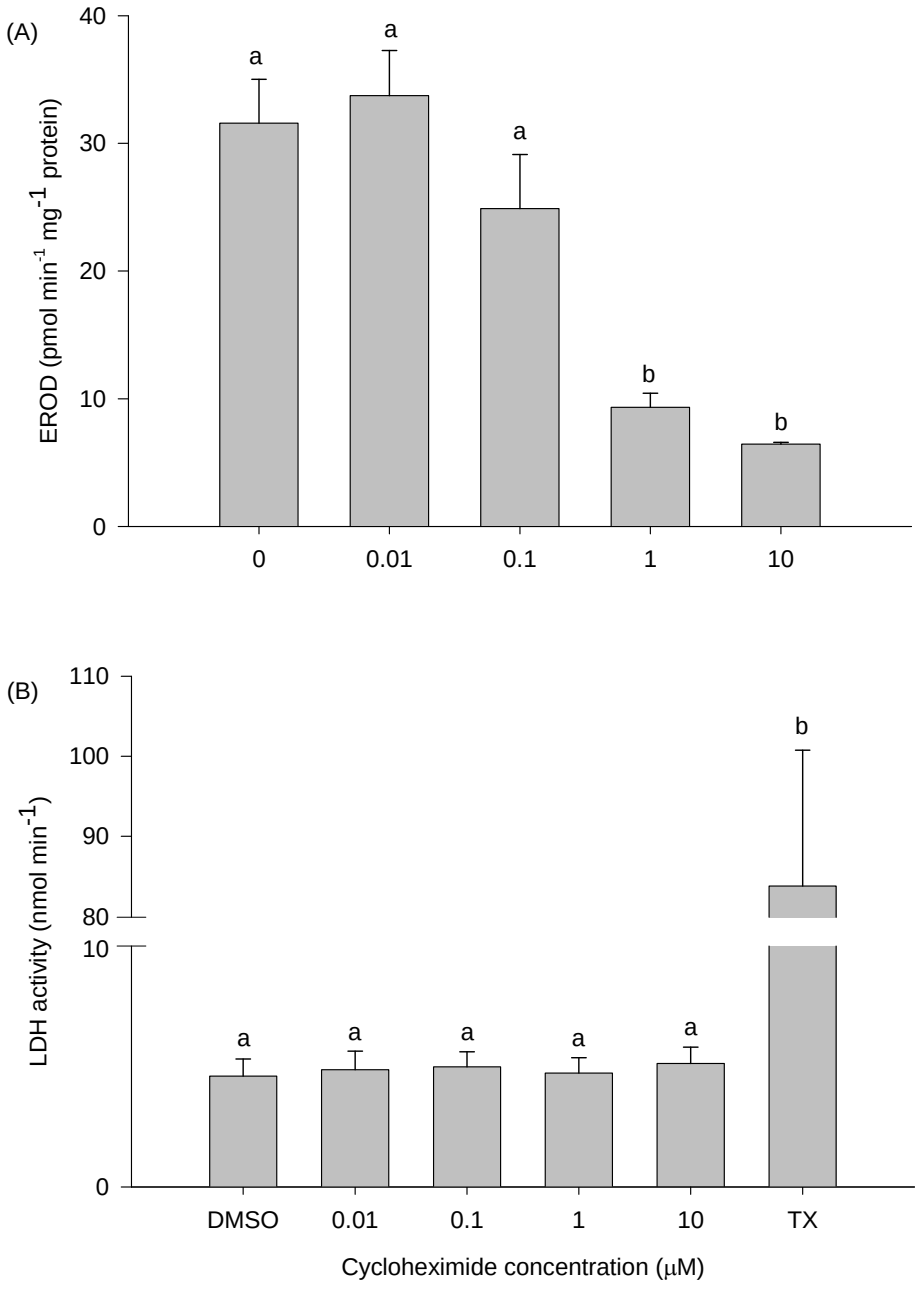

Figure 3.3. EROD activities (A) and culture media LDH activities (B) for isolated rainbow hepatocytes at 1 μM β-NF and various concentrations of cycloheximide or 1% Triton X-100 (TX) as a positive control for cell disruption at 48 h post-exposure. Data represent mean + S.E.M. (n = 5). Statistical analysis consisted of a repeated measures one-way ANOVA and significant difference ($p<0.001$) are represented by different letters.

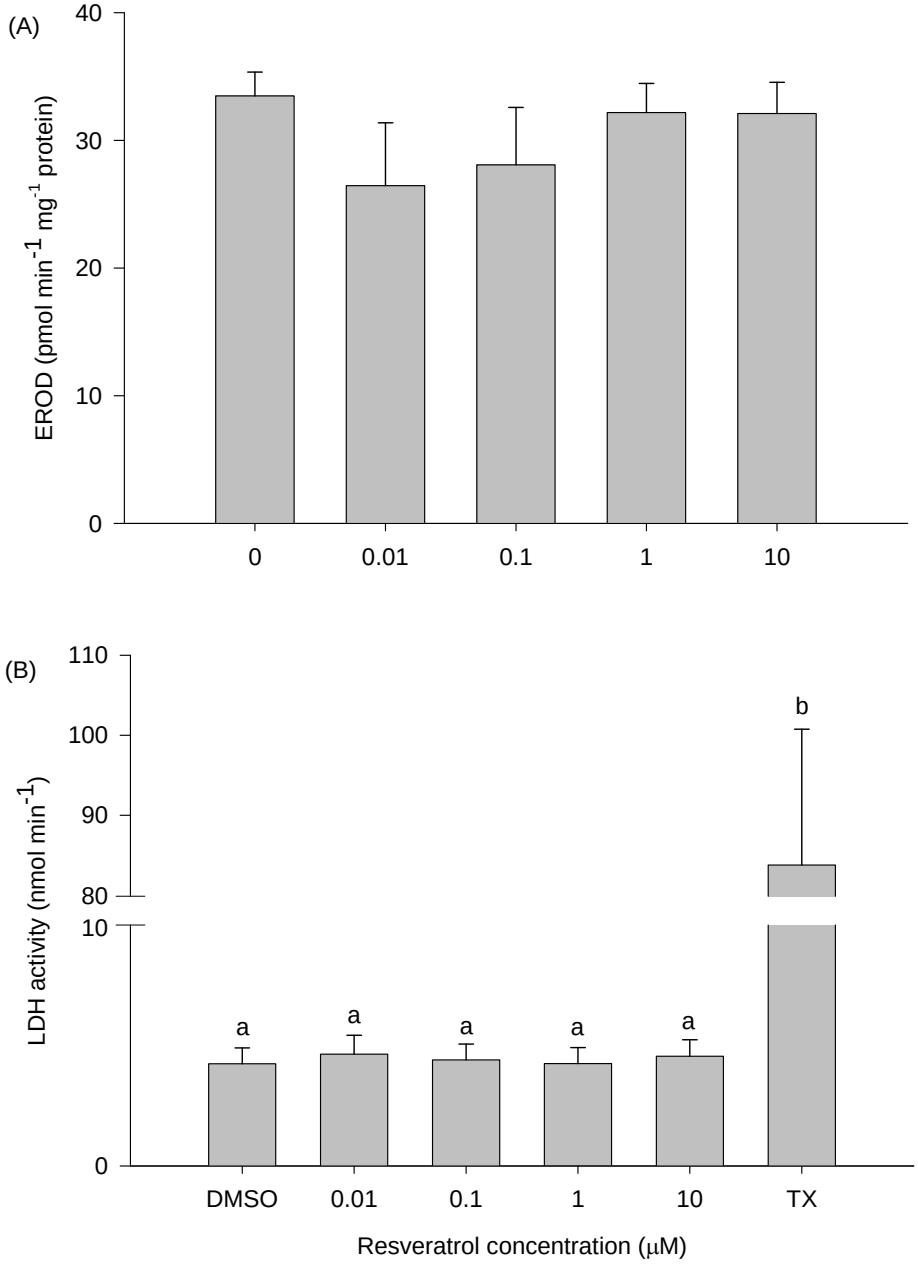

Figure 3.4. EROD activities (A) and culture media LDH activities (B) for isolated rainbow hepatocytes at 1 μM β-NF and various concentrations of resveratrol or 1% Triton X-100 (TX) as a positive control for cell disruption at 48 h post-exposure. Data represent mean + S.E.M. (n = 5). Statistical analysis consisted of a repeated measures one-way ANOVA and significant difference ($p<0.001$) are represented by different letters.

3.1. Adenylate energy charge (AEC)

Exposure of isolated hepatocytes to actinomycin D, cycloheximide or resveratrol in the presence or absence of β-NF (1 μM) or β-NF alone did not result in any significant differences either in the AEC (Fig. 3.5A) or in levels of any of the individual adenylates (Fig. 3.5B) assessed. AEC values in these hepatocytes ranged from 0.6 ± 0.04 to 0.66 ± 0.01 while total adenylates ranged from 1.24 ± 0.08 to 1.40 ± 0.10 nmol mg^{-1} cells.

3.2. Protein synthesis

Incorporation of L-4,5[^{3}H]leucine into the TCA-insoluble protein fraction showed no significant differences either from exposure to β-NF or over the duration of exposure (Fig 3.6). Values, relative to the 0 h control, range from 0.84 ± 0.16 to 1.26 ± 0.39.

3.3. Rubidium uptake

Uptake of rubidium (Rb^+), an indicator of K^+ influx through the Na^+/K^+-ATPase, showed no significant differences from exposure to β-NF at any of the examined time points (Fig. 3.7). However, Rb^+ uptake was significantly different ($p<0.05$) at 24 h for both control and β-NF-exposed hepatocytes. Although the Holm-Sidak post-hoc test does not show significant differences at 48 h post-exposure, the less conservative Student-Newman-Keuls post-hoc test indicates a statistically significant difference ($p<0.05$) at this time point as well.

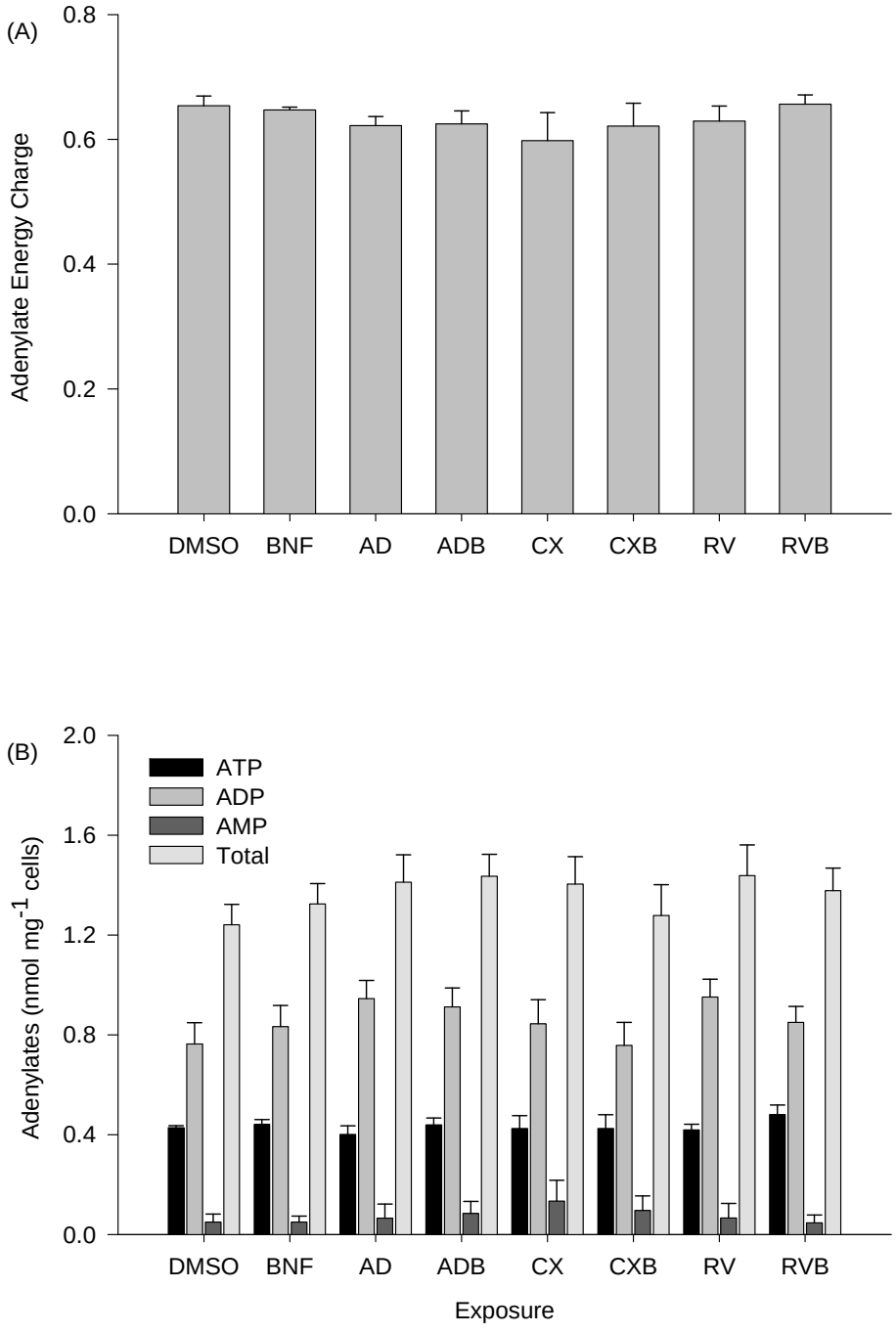

Figure 3.5. Adenylate energy charge (A) and levels of individual or total adenylates (B) in isolated hepatocytes exposed to actinomycin D (AD; 1 μM), cycloheximide (CX; 1 μM) or resveratrol (RV; 10 μM) and in the presence of β-NF (1 μM) with actinomycin D (ADB), cycloheximide (CXB) or resveratrol (RVB). Data represent mean + S.E.M. (n = 5). Statistical analysis consisted of a repeated measures two-way ANOVA; no significant differences were observed.

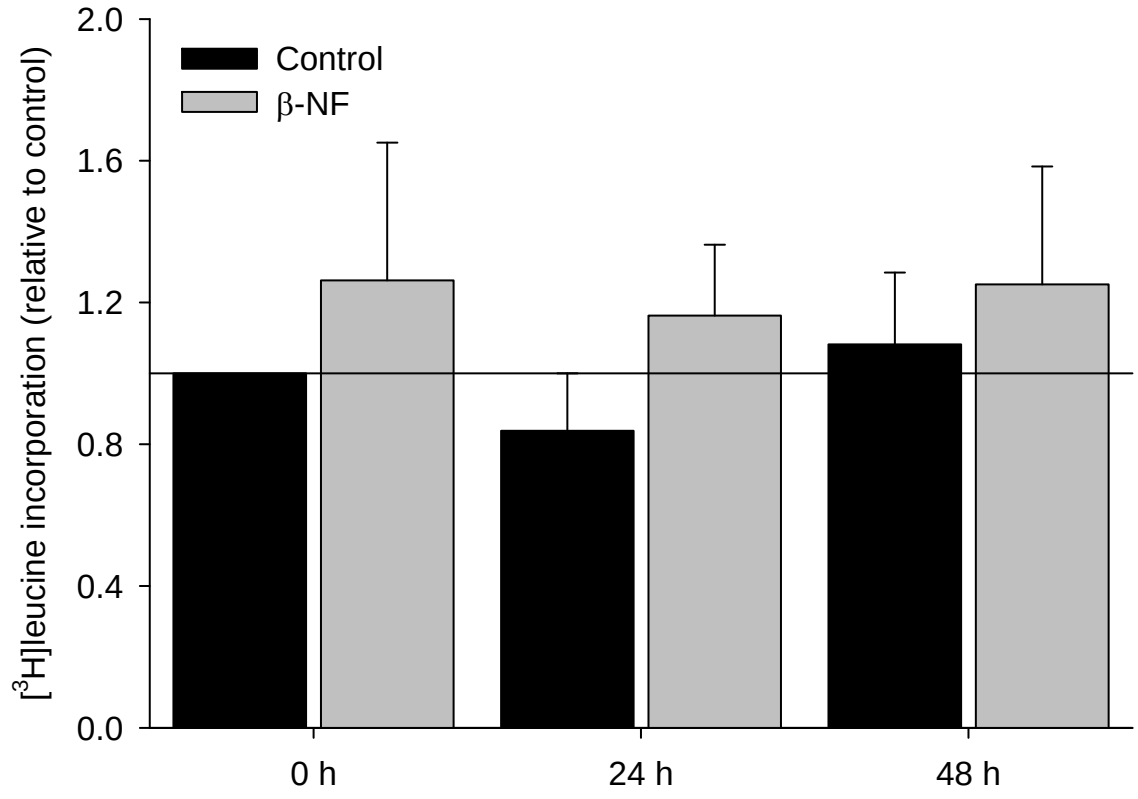

Figure 3.6. L-4,5[^{3}H]Leucine incorporation into the TCA-insoluble protein fraction at 0, 24 and 48 h post-exposure to DMSO vehicle control or β-NF (1 μM). Data represent mean + S.E.M. (n = 2-4) relative to the 0 h control (8.0 ± 2.6 nmol h^{-1} mg^{-1} protein). Statistical analysis consisted of a two-way ANOVA; no significant differences were observed.

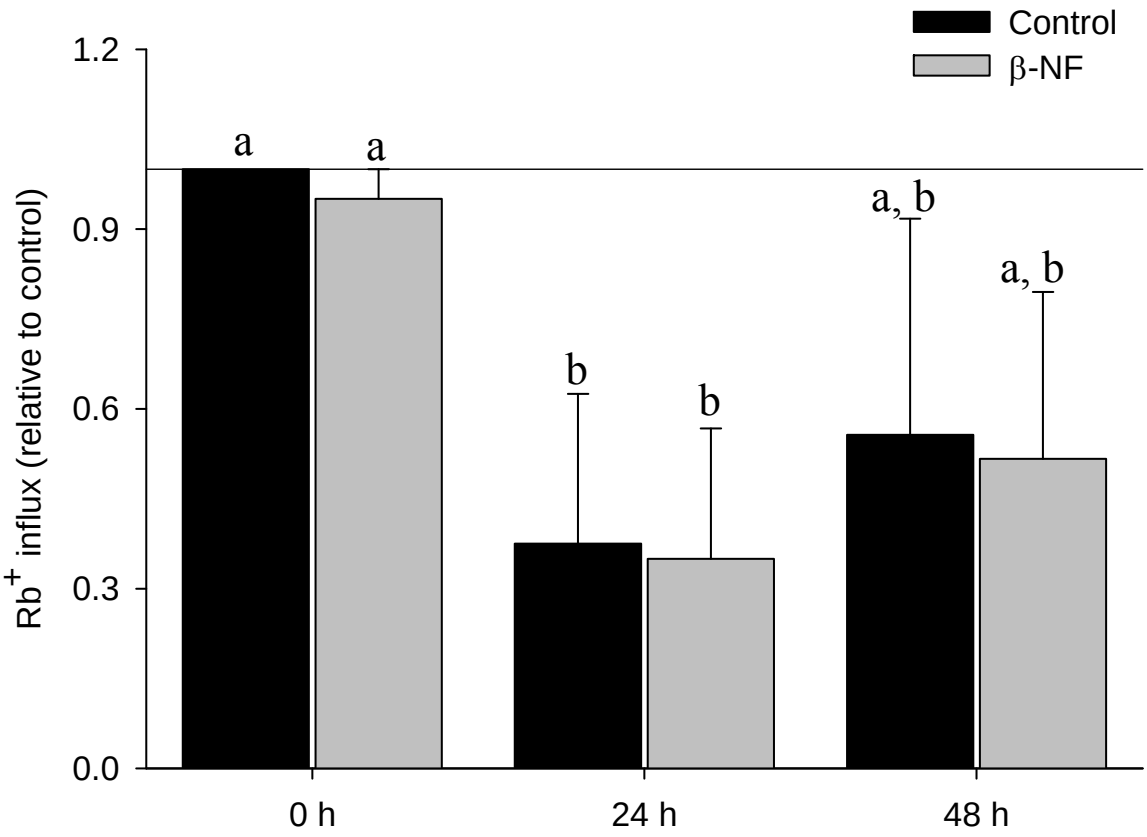

Figure 3.7. Rubidium (Rb^+) uptake into isolated rainbow trout hepatocytes at 0, 24 and 48 h post-exposure to DMSO vehicle control or β-NF (1 μM). Data represent mean + S.E.M. (n = 4) relative to the 0 h control (0.6 ± 0.1 nmol Rb^+ min^{-1} mg^{-1} protein). Statistical analysis consisted of a repeated measures two-way ANOVA; significant differences are indicated by different letters for time and treatment (see text).

3.4. Metabolite flux

Metabolite fluxes for all measured extracellular metabolites are shown on Table 3.1. Among examined metabolite fluxes, ammonia, glycerol, triglyceride and cholesterol were at undetectable levels in the extracellular media at all time points including the continuous 48 h exposure; therefore, rates could not be calculated. The flux for β-hydroxybutyrate and acetoacetate were also relatively low and are presented in pmol h^{-1} mg^{-1} protein range and showed no significant differences. The fluxes estimated for glutamate, glutamine and lactate were not significantly different across durations of exposure or treatment although lactate fluxes were much higher than those for glutamate and glutamine as were glucose and free fatty acid fluxes.

Glucose flux was significantly different ($p<0.05$) at every time point assessed; glucose was produced and released over the first 24 h period and was close to 0 in the second 24 h period. No differences were noted between control and β-NF-exposed hepatocytes. Glucose flux in the continuous exposure was significantly different ($p<0.05$) as well at values that are intermediate to the first and second 24 h period of exposure. On the other hand, free fatty acid flux was only significantly different in the continuous exposure control hepatocytes versus the second 24 h exposure. No significant differences were observed between control and β-NF-exposed hepatocytes for free fatty acid fluxes. Fluxes were variable and this variability may have masked any significant differences especially between control and β-NF exposures.

3.5. Hepatocyte glycogen content

Hepatocyte glycogen levels were unchanged 24 h post-exposure for both control and β-NF-exposed hepatocytes and at 48 h post-exposure control hepatocytes showed lower levels of glycogen that were statistically significant ($p<0.05$). β-NF-exposed hepatocytes demonstrated no significant decrease in glycogen levels at 48 h post-exposure.

Table 3.1. Metabolite flux estimates for assessed metabolites in the medium of control or 1 μM β-NF-exposed hepatocytes. Values presented are means (± S.E.M.) for n = 4-5. Significant differences ($p<0.05$), determined by a repeated measures two-way ANOVA, are indicated by different letters among exposure times. No significant differences were observed within treatments. Negative values indicate uptake of metabolite.

Metabolite (nmol h^{-1} mg^{-1} protein)	Exposure Time (h)	Treatment	
		Control	β-Naphthoflavone
Ammonia	0-24	ND	ND
	24-48	ND	ND
	0-48	ND	ND
Glutamate	0-24	-0.22 (0.40)	-0.07 (0.38)
	24-48	0.11 (0.20)	0.02 (0.34)
	0-48	0.79 (0.34)	0.53 (0.24)
Glutamine	0-24	0.70 (0.55)	0.02 (0.31)
	24-48	-0.73 (0.47)	-0.51 (0.39)
	0-48	-0.39 (0.29)	0.81 (0.42)
D-3-β-Hydroxybutyrate‡	0-24	-0.06 (0.17)	0.08 (0.08)
	24-48	-0.06 (0.1)	0.10 (0.07)
	0-48	-0.01 (0.29)	-0.23 (0.19)
Acetoacetate‡	0-24	0.28 (0.27)	-0.00 (0.01)
	24-48	0.30 (0.18)	-0.04 (0.03)
	0-48	0.05 (0.04)	0.38 (0.24)
Glucose	0-24	37.23 (9.36)[a]	32.56 (7.40)[a]
	24-48	1.79 (2.78)[b]	-4.71 (3.08)[b]
	0-48	23.95 (5.04)[c]	21.19 (5.21)[c]
Lactate	0-24	19.91 (8.07)	18.12 (7.30)
	24-48	14.65 (6.32)	11.23 (4.88)
	0-48	16.96 (7.59)	18.02 (7.17)
Glycerol	0-24	ND	ND
	24-48	ND	ND
	0-48	ND	ND
Triglyceride	0-24	ND	ND
	24-48	ND	ND
	0-48	ND	ND
Cholesterol	0-24	ND	ND
	24-48	ND	ND
	0-48	ND	ND
Free fatty acids	0-24	23.11 (14.12)[ab]	14.69 (10.45)
	24-48	-17.50 (16.25)[a]	-17.94 (5.15)
	0-48	35.60 (20.57)[b]	13.04 (13.31)

‡ Rates are expressed as pmol h^{-1} mg^{-1} protein

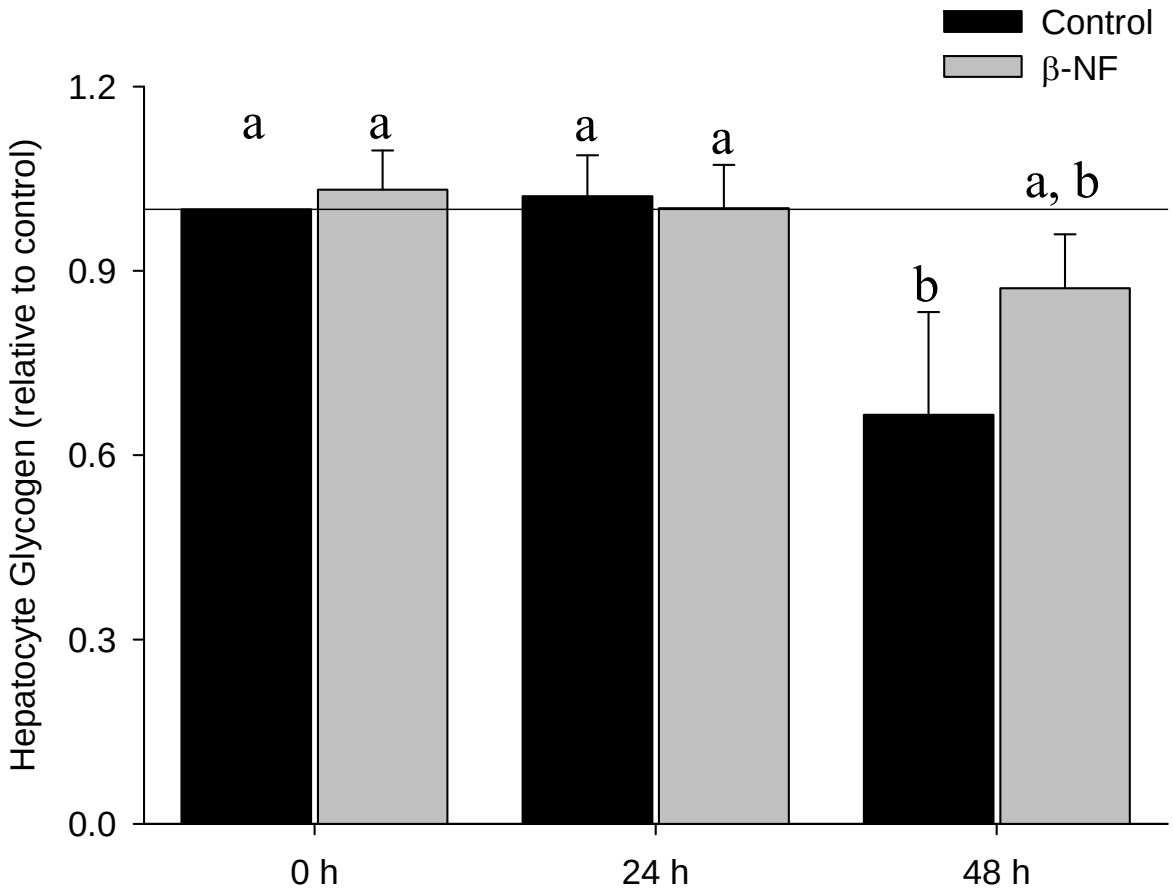

Figure 3.8. Hepatocyte glycogen content at 0, 24 and 48 h post-exposure to DMSO vehicle control or β-NF (1 μM). Data represent mean + S.E.M. (n = 4) relative to control at 0 h (2.73 ± 0.66 mg glycogen mg^{-1} protein). Statistical analysis consisted of a repeated measures two-way ANOVA; significant differences are indicated by different letters for time and treatment.

3.5. Metabolic flux analysis

Given the constraints set within the model as described in section 2.10 (see Tables A.2 and A.3), metabolic flux analysis indicated a large variability in the metabolic fluxes analyzed (all calculated flux range values are described in Table A.4). Glucose metabolizing pathways in the initial 24 h period showed no impact of low CYP1A activities although high CYP1A activities resulted in an increase pentose phosphate pathway activity most likely for the generation of NADPH (Fig. 3.9A) used as a substrate in the CYP1A reaction. With the metabolic constraints of the second 24 h period of exposure however, low CYP1A activities narrowed the flux ranges while high CYP1A activities appeared to result in an increase in both glucogenic (production of glucose from any carbon source) pathways as well as the pentose phosphate pathway (Fig. 3.9B).

The fluxes reported for the tricarboxylic acid and urea cycles as well as the electron transport chain do not appear to be influenced by either low or high CYP1A activities both in the first or second 24 h period of exposure (Fig. 3.10). Similarly, fatty acid metabolic fluxes are generally unaffected by CYP1A activities although high CYP1A in the first 24 h period did restrict fluxes for fatty acid synthesis and G3P to the upper flux range of control and low CYP1A activity estimates (Fig. 3.11A; flux 47, 49). Furthermore, amino acid fluxes appear not to be influenced given the constraints of the initial 24 h of exposure (Fig. 3.12A) while high CYP1A activities within the constraints of the second 24 h period resulted in an increase in alanine and valine production (Fig. 3.12B; flux 21, 44).

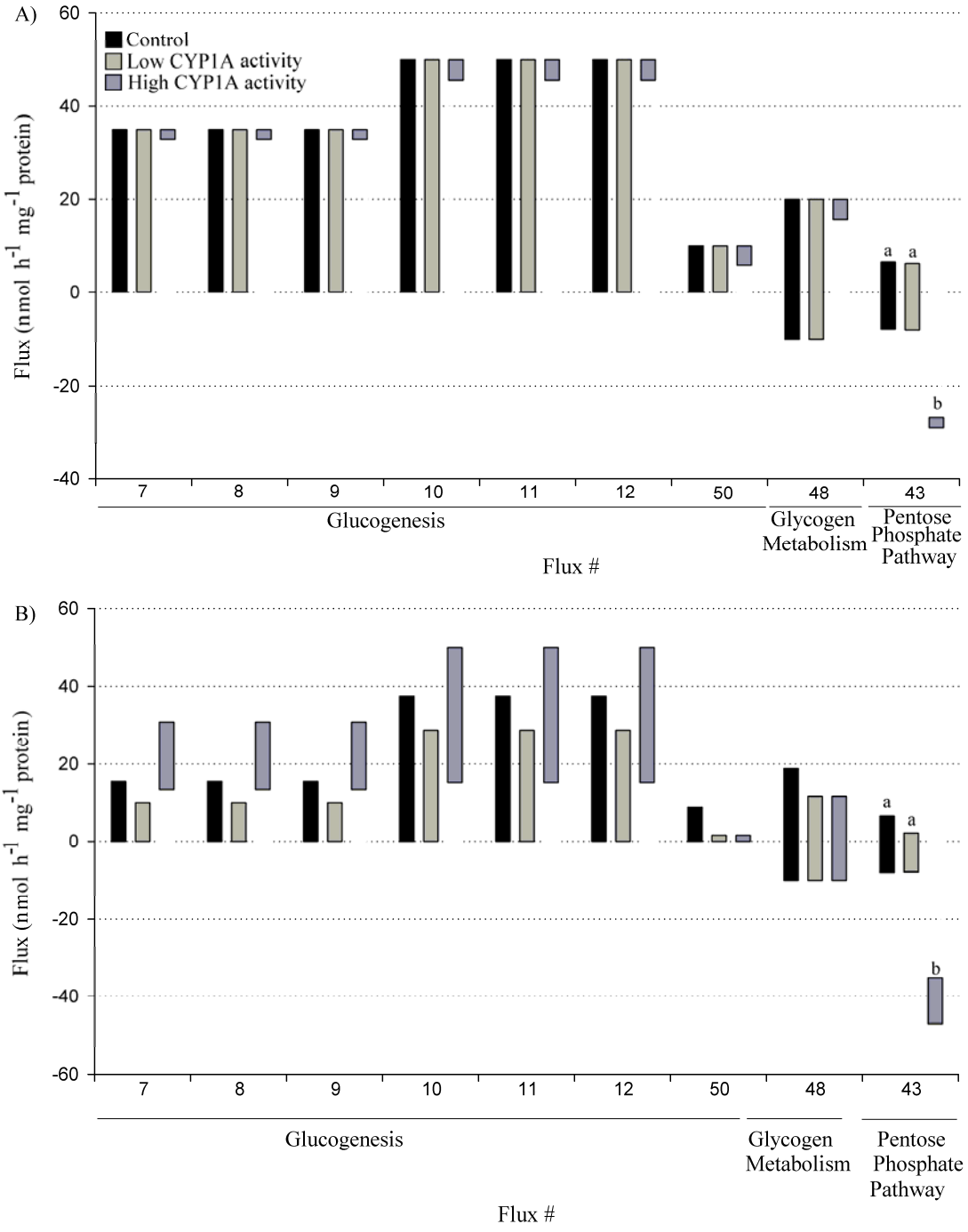

Figure 3.9. Metabolic flux ranges for glucose metabolizing pathways estimated using measured fluxes for the first 24 h of exposure (A) and second 24 h period (B) in control hepatocytes and β-NF-exposed hepatocytes constrained to low (4 – 5 nmol h^{-1} mg^{-1} protein) or maximum CYP1A activities. Numbers below bars (on x-axes) represent reactions described in Table A.1; non-overlapping fluxes are identified by different letters.

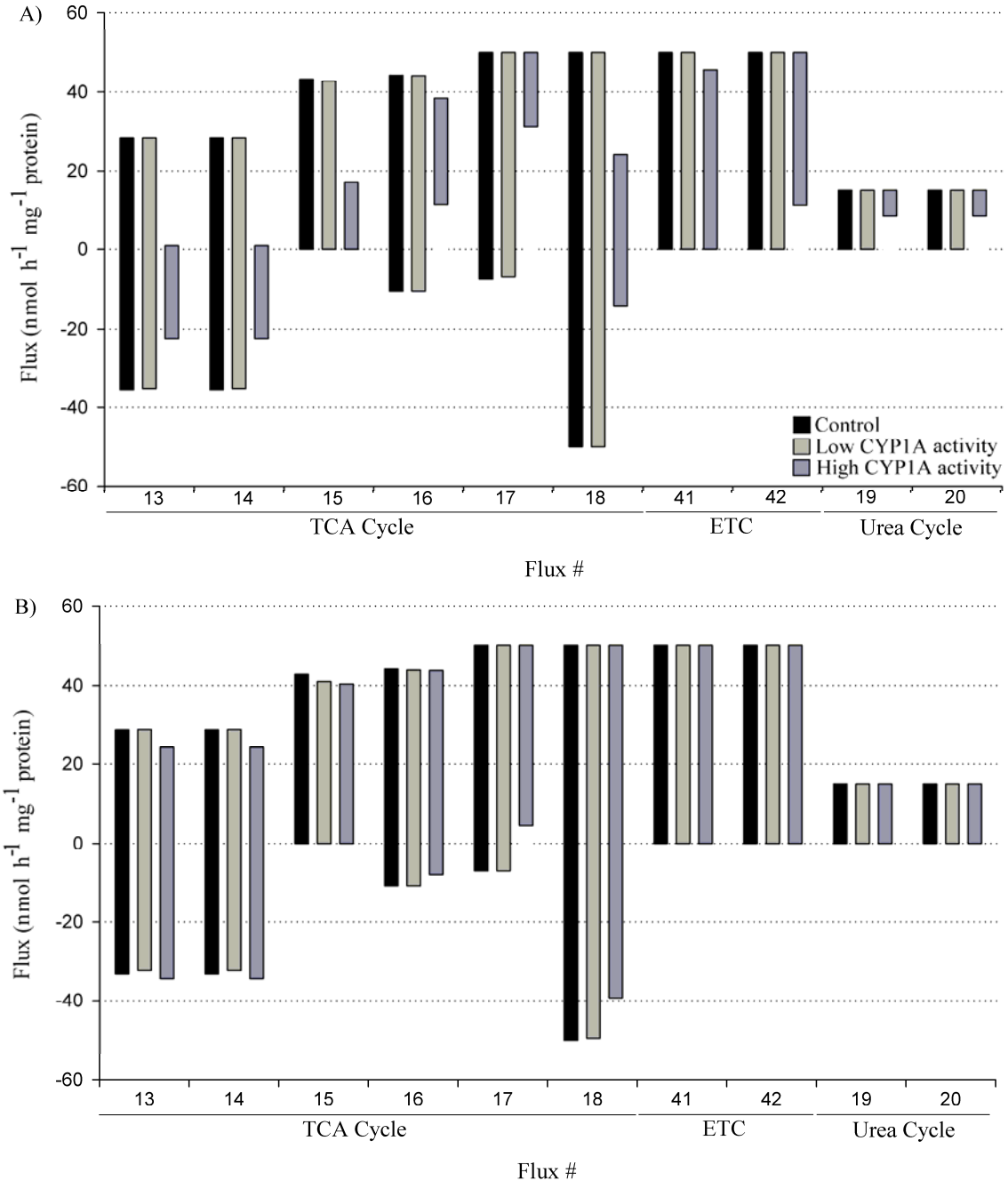

Figure 3.10. Metabolic flux ranges for the tricarboxylic acid and urea cycles and the electron transport chain estimated using measured fluxes for the first 24 h of exposure (A) and second 24 h period (B) in control hepatocytes and β-NF-exposed hepatocytes constrained to low (4 – 5 nmol h^{-1} mg^{-1} protein) or maximum CYP1A activity. Numbers below bars (on x-axes) represent reactions described in Table A.1; non-overlapping fluxes are identified by different letters.

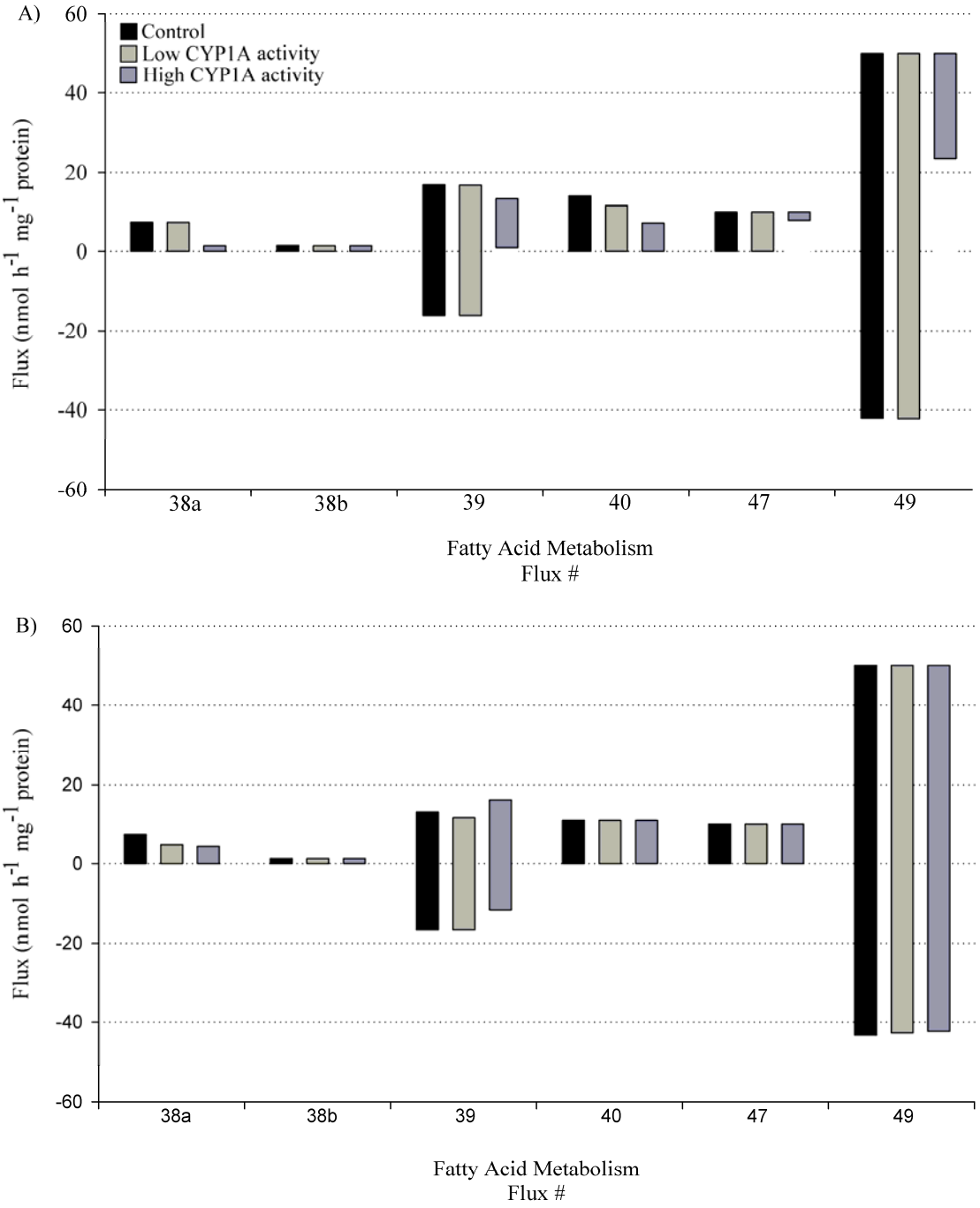

Figure 3.11. Metabolic flux ranges for fatty acid metabolizing pathways estimated using measured fluxes for the first 24 h of exposure (A) and second 24 h period (B) in control hepatocytes and β-NF-exposed hepatocytes constrained to low (4 – 5 nmol h^{-1} mg^{-1} protein) or maximum CYP1A activity. Numbers below bars (on x-axes) represent reactions described in Table A.1; non-overlapping fluxes are identified by different letters.

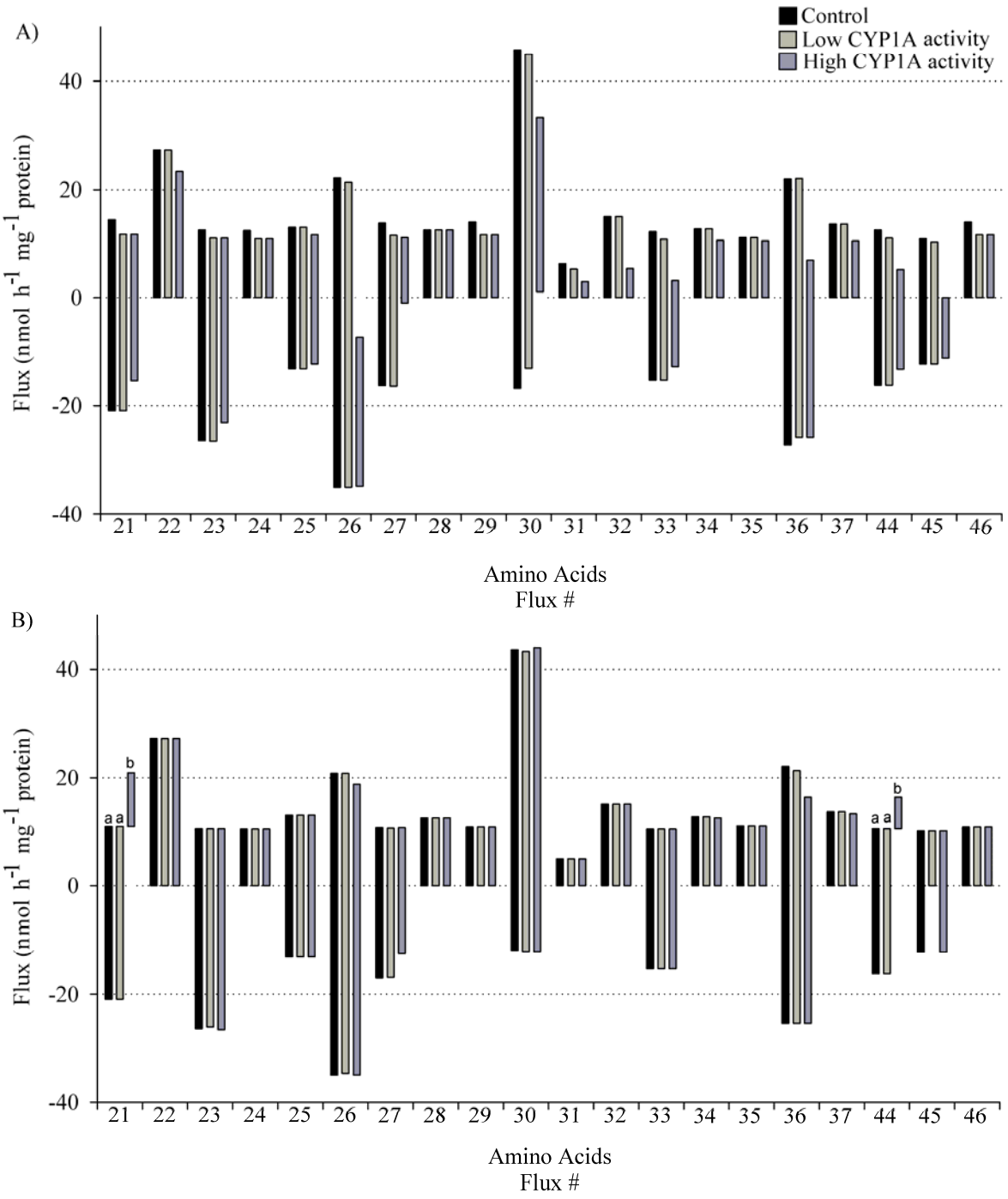

Figure 3.12. Metabolic flux ranges for amino acid metabolising pathways estimated using measured fluxes for the first 24 h of exposure (A) and second 24 h period (B) in control hepatocytes and β-NF-exposed hepatocytes constrained to low (4 – 5 nmol h^{-1} mg^{-1} protein) or maximum CYP1A activity. Numbers below bars (on x-axes) represent reactions described in Table A.1; non-overlapping fluxes are identified by different letters.

3.6. Enzyme activities

Among examined enzymes both alanine aminotransferase (AAT) and citrate synthase (CS) showed significant differences ($p<0.05$) in activities (Table 3.2). AAT activities were lower in β-NF-exposed hepatocytes at 24 h exposure and returned to control values at 48 h post-exposure. Conversely, CS activities were significantly higher in β-NF-treated hepatocytes at 48 h compared to control hepatocytes at that same time point. No other enzyme activities estimated differed significantly with β-NF treatment.

Table 3.2. Hepatocyte enzyme activities. Values presented are means (± S.E.M.) for n = 4. Significant differences ($p<0.05$) determined by a repeated measures two-way ANOVA, are indicated by different letters. No significant difference was observed across exposure times.

Enzyme (nmol min^{-1} mg^{-1} protein)	Exposure Time (h)	Treatment	
		Control	β-Naphthoflavone
Alanine aminotransferase	24	48 (5.53)[a]	38.78 (3.97)[b]
	48	52.21 (5.07)[a,b]	54.13 (7.43)[a,b]
Citrate synthase	24	165.3 (22.19)[a,b]	183.19 (28.34)[a,b]
	48	158.78 (14.83)[a]	190.87 (20.52)[b]
Glyceraldehyde-3-phosphate dehydrogenase	24	16.02 (2.11)	15.99 (2.18)
	48	15.99 (1.82)	16.28 (2.03)
Glucose-6-phosphate dehydrogenase	24	78.36 (16.12)	79.57 (16.77)
	48	79.25 (17.3)	80.53 (17.93)
β-Hydroxyacyl CoA dehydrogenase	24	10.71 (1.86)	10.7 (1.99)
	48	10.68 (1.84)	10.52 (1.99)
Isocitrate dehydrogenase	24	44.06 (3.09)	43.52 (3.34)
	48	45.48 (3.38)	45.82 (3.97)
Malic enzyme	24	6.79 (1.59)	6.64 (1.57)
	48	6.8 (1.55)	6.95 (1.56)
Phosphoenolpyruvate carboxykinase	24	13.68 (1.5)	17.09 (1.65)
	48	25.19 (8.43)	20.16 (6.85)
Pyruvate kinase	24	16.99 (2.61)	16.61 (3.18)
	48	17 (3.24)	17.44 (3.4)

Chapter 4 – Discussion and Conclusions

4.0. Discussion

The objective of this research was to examine the energetic costs of AhR activation in rainbow trout hepatocytes and the metabolic responses that might ensue. Therefore, it was essential that the β-NF concentration which resulted in maximal AhR activation be determined to observe maximal energetic costs. Analysis of EROD activities showed maximal activities at 48 h post-exposure and at a concentration of 1 μM β-NF (Fig. 3.1), a concentration used for all subsequent experiments. These results are consistent with reported values that demonstrated maximal EROD activities in rainbow trout hepatocytes at concentrations from 0.39 to 1.59 μM β-NF after a 48 h exposure (Navas and Segner, 2000) and a continuously increasing EROD activity over a period of 48 h in rainbow trout hepatocytes exposed to 0.36 μM β-NF (Pesonen et al., 1992). Furthermore, the absence of any significant changes in cell membrane integrity (assessed by LDH leakage) indicated that these β-NF concentrations are not cytotoxic.

Actinomycin D, cycloheximide and resveratrol were used to block protein transcription, translation and AhR activation, respectively (Aluru and Vijayan, 2006; Krumschnabel et al., 1994a; Krumschnabel et al. 1999; Wieser and Krumschnabel, 2001) to assess the energetic costs associated with individual steps of the AhR activation cascade. Although actinomycin D and cycloheximide at 1 μM inhibited β-NF-induced EROD activities, resveratrol did not inhibit the action of β-NF. Resveratrol, a proposed AhR antagonist (Aluru and Vijayan, 2006; Casper et al., 1999), resulted in both an increase and a decrease in CYP1A expression at low (≤ 0.01 μM) and high concentrations (≥ 0.1 μM), respectively in rainbow trout hepatocytes following a 24 h exposure to β-NF (Aluru and Vijayan, 2006); EROD activities however were not assessed in this study. Similarly, rainbow trout co-exposed to PCB 126 or β-NF and resveratrol for 10 days

showed either no change or inhibition of whole liver EROD activities, respectively (Al-Hameedi, 2008). These observed discrepancies suggest that the effectiveness of resveratrol as an AhR antagonist is unclear and may explain the absence of clear EROD inhibition observed in this study. As a result of the inability of resveratrol to inhibit AhR activation, these chemicals were included only when examining the adenylate energy charge (AEC) as actinomycin D and cycloheximide are both non-specific AhR antagonists unlike resveratrol which is shown to be specific, at least in mammalian cells (Casper et al., 1999; Ciolino et al., 1998). The use of these chemicals without a specific inhibitor of AhR activation could potentially lead to over-estimations of energetic costs as the non-specificity of the chemicals may cause unrelated and undetected toxic effects. For example, Wieser and Krumschnabel (2001) examined the energetic costs of protein synthesis using cycloheximide by assessing cellular respiration and [^{3}H]leucine incorporation and observed a 71-75% decrease in oxygen consumption while [^{3}H]leucine incorporation decreased energy use but only accounted for 10% of total oxygen consumption. This implies that the use of non-specific inhibitors such as cycloheximide or actinomycin D can be associated with a suite of additional effects as might be expected.

Once AhR activation was characterized, this study attempted to answer two questions regarding the costs of exposure to an AhR agonist. The first question was *does β-NF activation of the AhR result in increased energetic costs in rainbow trout hepatocytes?* To answer this question, the AEC was assessed as well as both protein synthesis and Rb^+ influx as an assessment of Na^+/K^+-ATPase, two of the most energetically costly processes in rainbow trout and goldfish (*Carassius auratus*) hepatocytes (Krumschnabel et al., 1994b; Pannevis and Houlihan, 1992; Wieser and Krumschnabel, 2001) as well as rat thymocytes (Buttgereit and Brand, 1995).

Although the validity of using AEC has been debated (Atkinson, 1977; Fromm, 1977), studies including those of Hildebrand et al. (2009) and Matsui et al. (1994) examining the AEC in

rainbow trout, rat and human hepatocytes as well as the recent evidence of AMPK as an energy sensing protein (Oakhill, 2011), support AEC as a viable indicator of the energetic status of cells. In my study, neither β-NF nor any of the other chemicals used caused a significant change in AEC values or in levels of individual or total adenylates following a 48 h exposure period. This was unexpected as the concentration of actinomycin D and cycloheximide used appeared to depress protein synthesis or at least EROD activities were significantly lower in β-NF-exposed than in control hepatocytes (Figs. 3.2-3.3). These results support a tightly regulated AEC in these trout hepatocytes at least under the conditions used in this study to maintain steady-state values.

It must be noted however that the estimated AEC values, which ranged from 0.6 to 0.7, are lower than the expected values of 0.8-0.9 for 'healthy' organisms that are in a steady-state (Cattani et al., 1996). Hildebrand et al. (2009) reported AEC values ranging from 0.8 to 0.9 in control rainbow trout hepatocytes when examined within hours of isolation. AEC values reported here were determined at 72 h post-isolation and this extended incubation may offer an explanation for the lower AEC values. On the other hand, Caldwell and Hinshaw (1994) measured the AEC of rainbow trout whole livers during an acclimation period of 77 days to hypoxic, normoxic and hyperoxic conditions and observed values of 0.4 to 0.75 which were not significantly different across treatments or times during the acclimation period. To confirm that the observed AEC values reported in my study were normal for our fish, adenylates from freshly isolated whole livers of trout taken from the same stock of trout as those used in the preparation of hepatocytes were examined and an AEC of 0.6 ± 0.04 (results not shown) was determined providing evidence that AEC values from whole trout liver and hepatocytes are maintained throughout the isolation and incubation process and that the reported hepatocyte values are reliable. Given the stability of the AEC throughout the isolation process, it is unlikely that the

different value reported by Hildebrand et al. (2009) is due to incubation time. As an alternate explanation it is possible that the size of rainbow trout may influence AEC values; Hildebrand et al. (2009) used fish weighing 600 – 800 g while those used by Caldwell and Hinshaw (1994) weighed 180 – 200 g, masses that are much closer to those used in my study. Although estimated values of routine metabolism in centrarchid fish for example including largemouth bass, smallmouth bass (*Micropterus dolomieui*), sunfish (*Lepomis gibbosus*) and bluegill (*Lepomis macrochirus*) do not show intra-species allometric scaling (Davies and Moyes, 2007) which would suggest no AEC scaling, it is possible that reduced energy use for growth in larger fish results in a higher AEC.

In vitro exposure of trout hepatocytes to β-NF had little impact on ATP consuming processes although significant differences were observed over the duration of the incubation period. Isolated hepatocytes at 24 h post-exposure (or 48 h post-isolation) had significantly lower Rb^+ influx, a direct estimate of Na^+/K^+-ATPase activity (Krumschnabel et al., 2001) than at 0 h (or 24 h post-isolation, Fig. 3.7). A decreased Rb^+ influx may be a response by the cells to reduce ATP consumption and suggests that cellular processes may be altered during the period of incubation to maintain a stable AEC (see Fig. 3.5A). In fact, decreased Na^+/K^+-ATPase activity, or channel arrest, coupled with an increase in passive Na^+ uptake is observed with energy limitation (hypoxia) in hepatocytes of hypoxia-tolerant fish species (Bogdonova et al., 2005) and hypoxia-intolerant species such as rainbow trout (Krumschnabel et al., 1996). At 48 h post-exposure (72 h post-isolation) however, Rb^+ influx returned towards their 0-time values although the less conservative Student-Newman-Keuls post-hoc test did indicate that values remained significantly below those at 0 h (24 h post-isolation). Intermediate Rb^+ influx values at 48 h, falling between the 0 h and 24 h values may be indicative of a deregulation of ion balance occurring over time whose regulation become more important than the conservation of cellular

energy by channel arrest. Rainbow trout being hypoxia-intolerant may not be able to regulate ion flux over long periods of time when energy is limited which could lead to increased Na^+/K^+-ATPase activities. Indeed, upon chemical anoxia (cyanide exposure) to create a state of limited energy, trout hepatocytes decreased Na^+/K^+-ATPase within 30 min but, unlike the hypoxia tolerant goldfish hepatocytes which are able to lower and maintain similar Rb^+ influx and K^+ efflux rates, rainbow trout hepatocyte K^+ efflux remained the same as control hepatocytes despite a reduction in Rb^+ influx (Krumschnabel et al., 1996) leading to an ion imbalance. To my knowledge, ion regulation has not been examined in trout hepatocytes over similar periods of incubation used in my study and therefore there is little literature support for ion regulation requirements becoming more important than the conservation of energy levels during the incubation period.

Protein synthesis as assessed by [^{3}H]leucine incorporation, on the other hand, showed no significant differences based on either treatment or duration of incubation. Under the hypothesized increased energy requirement of β-NF exposure it was predicted that protein synthesis would be decreased to conserve energy; the absence of differences in protein synthesis suggests that these hepatocytes either maintain adequate cellular energy levels to maintain this process or this process takes precedence over other processes and energy is thus conserved or directed preferrentially for this process. The impact of energy limitation on protein synthesis was reported to lead to either a decrease in protein synthesis and an unchanged Na^+/K^+-ATPase activity (Wieser and Krumschnabel, 2001) or vice-versa, an unchanged protein synthesis and a decreased Na^+/K^+-ATPase activity (Krumschnabel et al., 2001). Which of these possibilities occur with β-NF exposure is unclear but the observed decrease in Rb^+ influx supports the premise that protein synthesis may take precedence over ion regulation to maintain cellular energy status. It is known that activation of the AhR leads to an increase in expression of CYP1A followed by

an increase in CYP1A protein levels that peak at 48 h (Pesonen et al., 1992); a decreased protein synthesis rate would not be compatible with this protein increase. The observed mean values of protein synthesis in β-NF-exposed cells appeared to be consistently above those of control cells which, although not statistically significant, could be related to changes in translation of a number of proteins including those of the AhR gene 'battery'. It is also possible that a significantly increased protein synthesis upon β-NF exposure was masked by the depression of synthesis of AhR-unrelated proteins, an explanation that encompasses both predictions. β-NF-exposed rainbow trout did in fact show decreased gene expression for a number of genes in the brain (Aluru and Vijayan, 2008) and rat 5L hepatoma cells exposed to TCDD also showed decreased levels of a number of proteins (Sarioglu et al., 2008) supporting the idea that increased protein synthesis from AhR-related genes following a β-NF exposure was masked by decreased synthesis of other proteins.

The absence of β-NF-induced changes in AEC or specific adenylate levels and protein synthesis with significant differences in Rb^+ influx leads to two possible explanations. First, exposure to this AhR agonist and subsequent induction and action of xenobiotic detoxifying enzymes may not be associated with significant energetic costs or that these costs may be relatively small in comparison with overall cellular processes. Second, as hypothesized, rainbow trout hepatocytes may reorganize their metabolism to maintain that same balance between anabolic and catabolic processes which would allow the hepatocytes to cope with increased energetic costs while maintaining stable energy levels. This second possibility leads to the second question this study examined: *do rainbow trout hepatocytes reorganize their metabolism to cope with exposure to an AhR agonist?* To explore this question, a *metabolic flux analysis* (MFA) approach similar to that reported in Iyer et al. (2010) was used to examine intracellular metabolism.

Constraints used in the MFA model were generated by the assessment of a number of external fluxes presented in Table 3.1. Among the assessed metabolites, ammonia, cholesterol, glycerol and triglycerides were not detected in the extracellular culture media. Furthermore, as expected, metabolic fluxes for ketone bodies (acetoacetate and β-hydroxybutyrate) were much lower occurring in the pmol h^{-1} mg^{-1} protein range than all other metabolic fluxes assessed. Ketogenesis (production of ketone bodies) in teleost fish is not an important metabolic process as it is in mammals or elasmobranches as teleosts have a more efficient lipid β-oxidation and the tricarboxylic acid cycle to dispose of acetyl-CoA and apparently lack or have very low activities of the required enzymes for ketone production (Leblanc and Ballantyne, 1993; Segner et al., 1997); these features explain the low flux rates. Similarly, the amino acids glutamine and glutamate assessed spectrophotometrically also showed low flux with means < 1 nmol h^{-1} mg^{-1} protein. The MFA constraints used in this study were rounded to the first decimal thus these low fluxes had a negligible impact on the estimates.

Lactate, an indicator of glycolytic activities (Krumschnabel et al., 1994a; 1994b; Rissanen et al, 2003), showed much higher flux rates (Table 3.1) although no significant differences were observed between treatments or times. The absence of changed lactate production indicated that glycolysis was not increased in these hepatocytes either from β-NF exposure or over the duration of the incubation period. Additionally, estimated activity of glyceraldehyde-3-phosphate dehydrogenase (G-3PDH) was also unchanged (Table 3.2), further evidence that glycolysis was unchanged in these hepatocytes. This is not surprising as glycolysis in rainbow trout hepatocytes is estimated to account only for approximately 6% of total ATP production and inhibition of glycolysis by iodoacetic acid caused little impact on rates of Na^+/K^+-ATPase or protein synthesis (Krumschnabel et al., 2001) implying glycolysis plays a small role in energetics and functioning in these hypoxia-intolerant cells. However, the observed increase in glycolysis upon exposure to

DHAA observed by Rissanen et al. (2003) (see Introduction) does suggest that glycolysis can be increased when energy demands are increased in rainbow trout hepatocytes. Although glycolytic rates in isolated trout hepatocytes were maintained at a fixed rate across the β-NF exposure period, this consistency in metabolite flux did not occur for free fatty acids and glucose.

Although unaffected by β-NF exposure, free fatty acid fluxes changed over the incubation period although the differences were not statistically significant at each of the individual 24 h periods. The absence of difference is likely due to the high variability in these estimates (S.E.M. ≥ 50%). Nevertheless, it appeared that isolated hepatocytes changed from fatty acid release to fatty acid uptake over the initial 24 h period where fluxes ± S.E.M. remained above 0 and the last 24 h period where fluxes ± S.E.M. were below 0 (Table 3.1). This same trend, although achieving significant differences, occurred as well for glucogenesis in these isolated hepatocytes suggesting a likely link between glucose and fatty acid metabolism.

The observed initial high glucogenic flux was expected as isolated rainbow trout hepatocytes are in a 'negative glycogen balance' (Mommsen, 1986), meaning that glycogen is continuously broken down. Despite this negative glycogen balance however, hepatocytes maintained stable glycogen levels, at least for the first 24 h period (Fig. 3.8), likely due at least in part to the use of other glucogenic substrates including amino acids, glycerol or lactate (French et al., 1981; Renaud and Moon, 1980; Vijayan and Moon, 1992). Among these glucogenic substrates, glycerol was reported to be a preferred glucogenic substrate over lactate and alanine at least in American eel (*Anguilla rostrata*) hepatocytes and that glycerol, if added as a glucogenic substrate, could lead to sparing of glycogen reserves (Renaud and Moon, 1980). Indeed, Lech (1970) demonstrated that rainbow trout do incorporate glycerol into glycogen more so than into lipids. Therefore, the observed release of free fatty acids may be involved in maintaining the

stable glycogen levels through the breakdown of intracellular triglyceride stores increasing the availability of glycerol, something that is believed to occur in starving fish (Suarez and Mommsen, 1987). The absence of observable glycerol levels in the culture media (Table 3.1) may in fact support its immediate incorporation into glucogenesis rather than its release as liver glycerol kinase activities in rainbow trout are believed to be able to account for the turnover of all plasma glycerol within hours (Lech, 1970). It seems reasonable that glycerol metabolism does occur in these isolated hepatocytes. The subsequent reduction in glucogenesis and apparent switch from fatty acid release to uptake could therefore also occur due to the depletion of triglyceride reserves as it is evident that glycogen stores remain sufficient throughout the incubation (Fig. 3.8). However, no studies have examined triglyceride stores in rainbow trout hepatocytes to confirm this explanation.

The proposed depletion of intracellular triglycerides could also explain the large variation in fatty acid fluxes and the lack of significant differences as these rates may depend on initial triglyceride stores as reported for glycogen breakdown to glucose (Mommsen, 1986) in addition to the regulation of lipogenic activities by glycogen content reported in rainbow trout hepatocytes (Voss et al., 1986). Moreover, the depletion of intracellular triglyceride stores may explain the decreased glycogen stores for control hepatocytes as it is no longer being spared by glycerol, although β-NF appeared to provide some protective effect in this respect as glycogen stores were not significantly changed at 48 h post β-NF exposure (Fig 3.8) which is difficult to explain given the absence of significant differences in metabolite fluxes in β-NF exposed cells.

Regarding the apparent shift in fatty acid flux over time, hepatocytes isolated from fasted fish do metabolize fatty acids through β-oxidation (French, 1981; 1983) and in situations where energy becomes limited, as in the case of these hepatocytes given the observed changes in metabolic fuel use and the decreased Na^+/K^+-ATPase activities, hepatocytes may take up fatty

acids from the extracellular media to fuel cellular metabolism through β-oxidation. AMPK which is reported to be an AEC sensing protein (Oakhill et al., 2011) is known to result in an increase in β-oxidation in the liver when activated while also leading to a decrease in lipolysis in adipose tissue in mammals (Long and Zierath, 2006) and the functions of AMPK are believed to be conserved in rainbow trout (Polakof et al., 2011). It is possible that the observed changes in use of metabolic fuels is a result of AMPK activation due to decreasing cellular energy levels which allows the hepatocytes to return to the original AEC values. The absence of significant changes in β-hydroxyacyl-CoA dehydrogenase (HOAD) (Table 3.2) however does not support the idea of an increase in lipid β-oxidation unless HOAD activities are well above those necessary to increase lipid supplies to β-oxidation.

The MFA approach was used to provide further insight in the modulation of metabolic pathways within the trout hepatocytes. However, the large amount of variation observed in the metabolite fluxes assessed led to large flux ranges that, for the most part, are similar over time and treatment (see Figs. 3.9-3.12). Nevertheless, using theoretical constraints for CYP1A activities, the MFA model identified a few fluxes that may be modulated by exposure to β-NF (fluxes 21, 44 and 47). Among these fluxes, that of the pentose phosphate pathway (PPP) appears to show the largest difference upon maximal CYP1A activity constraints (Fig. 3.9, flux 47). This is not surprising as CYP1A requires NADPH for the metabolism of xenobiotics (Fig. 1.5) and the PPP is believed to be a primary source of NADPH (Sanden et al., 2003; Winzer et al., 2002). However analysis of G6PDH activities, a rate limiting enzyme of the PPP (Sanden et al., 2003) showed little effect of exposure to β-NF (Table 3.2). Interestingly, depressed G6PDH activities were observed in livers of β-NF-exposed rainbow trout (Tintos et al., 2008) and Aroclor 1254 (PCB mixture) exposed Arctic char (*Salvelinus alpinus*) (Vijayan et al., 2006) while Winzer et al. (2002) observed decreased G6PDH activities in European flounder (*Platichtys flesus L.*)

hepatocytes exposed to 100-400 μM benzo[a]pyrene, another AhR agonist. These results suggest that, contrary to the estimates of the MFA model, increased NADPH requirements may not be met through increased PPP pathway flux and may result in changes in cellular reduction potential ([NADPH]/[$NADP^+$] ratio). Interestingly, a decreased flux through the PPP pathway could explain an unchanged glycogen level as was observed in this study as less glucose-6-phosphate would be consumed through this pathway.

Furthermore, the MFA identified an increase in the metabolism of the amino acids alanine and valine, both in the direction of amino acid production and release in the second 24 h period of exposure (Fig. 3.12B). Although enzyme activities involved in valine metabolism were not assessed in this study, alanine aminotransferase (AAT) which is responsible for the inter-conversion of pyruvate and alanine (Table A.1, flux 27) was examined and showed a significant decrease in activity (Table 3.2) which was observed only in the initial 24 h once again providing little support for the estimates of the MFA model. Decreased AAT activities were also observed in livers of PCB-exposed Arctic char which would suggest a decrease in gluconeogenesis from alanine (Vijayan et al., 2006). This AAT activity decrease does not conform to the results of this study as glucogenesis was unaffected (Table 3.1) nor do other possible glucose-yielding substrates such as glycogen, lactate or glycerol from lipolysis explain the observed glucogenic flux if alanine incorporation into glucose is in fact reduced in the initial 24 h exposure period.

On the other hand, analysis of enzyme activities showed a significant increase in citrate synthase (CS) upon exposure to β-NF at 48 h post-exposure (Table 3.2). CS is the first unique enzyme of the mitochondrial tricarboxylic acid cycle that generates NADH ultimately for ATP production (Gagnon, 2002). This observed increase implicates a possible increase in oxidative metabolism following a 48 h exposure of hepatocytes to β-NF. Again this is inconsistent with the MFA although the fluxes through the tricarboxylic acid cycle show some of the largest ranges

likely due to large flux ranges for free fatty acid uptake/release (Table A.2). However, metabolite flux of fatty acids observed during the continuous 48 h exposure was about half of control hepatocytes (Table 3.1) and, although this was not statistically significant, may represent a larger incorporation of carbons from fatty acids into the tricarboxylic acid cycle through β-oxidation. Evidence for this however, as was previously noted, is not convincing as HOAD showed no significant differences in activity. These results as well are not consistent with Vijayan et al. (2006) who observed a significant increase in HOAD activity in liver of Arctic char exposed to PCBs suggesting a possible shift from fatty acid synthesis to β-oxidation and likely resulted in an increase in activity of the tricarboxylic acid cycle.

4.1. Conclusions and Future Work

I hypothesized in this study that β-NF activation of the AhR would increase energetic costs leading to the reorganization of metabolism in rainbow trout hepatocytes. This hypothesis was broken down into two fundamental questions:

(1) Does AhR activation by β-NF increase energetic costs in rainbow trout hepatocytes?

(2) Do rainbow trout hepatocytes reorganize their metabolism to cope with β-NF induced AhR activation?

These questions were assessed by examining the AEC in rainbow trout hepatocytes as well as the activity of energetically costly processes including Na^+/K^+-ATPase and protein synthesis, and by using the mathematical modelling approach of MFA the results of which were supplemented by analysis of enzyme activities. The results obtained in this study provide little evidence that exposure of trout hepatocytes to β-NF increased energetic costs although the results do support some modulation of metabolism. Moreover, this study identified significant changes in energy

consumption and cellular metabolism over the duration of the incubation which, to my knowledge, has not been reported previously.

Among the results obtained in this study, one of the most striking is the maintenance of stable AEC values upon exposure to β-NF. Under the given culture conditions where substrates for energy production (amino acids and glucose) are not limited, rainbow trout hepatocytes efficiently balance energy use and production through processes that may include channel arrest (Rb^+ uptake). Interestingly, this maintenance of the AEC was achieved without modulating intracellular metabolism as no enzyme activities were changed in DMSO vehicle control hepatocytes at any time point. However, unchanged intracellular fluxes were supported by significant changes in use of fuel, possibly shifting from lipolysis to glycogenolysis. As was previously noted, AMPK has recently been identified as a modulator of anabolic and catabolic metabolism by basically sensing the AEC (Long and Zierath, 2006; Oakhill et al., 2011) and it was suggested that activation of AMPK may be involved in the apparent switch in metabolic fuel use reported in this study. Future studies should examine the phosphorylation status of AMPK in rainbow trout hepatocytes over a prolonged incubation periods as well as the impact of AMPK activation on lipolysis and glucogenesis in these hepatocytes. AMPK is believed to sense minor fluctuations in the AEC (Oakhill et al., 2010) and assessment of its activation upon exposure to β-NF may also be more sensitive than the technique used in this study. Furthermore, as these results were obtained under conditions with readily available substrates for energy production, the assessment of β-NF exposure under limited energy substrate availability would provide valuable information of its impact on cellular energy metabolism as well.

Similarly, with the exception of Segner et al. (1994), to my knowledge this is the only study examining metabolism of rainbow trout hepatocytes at 72 h post-isolation and the endpoints assessed by Segner et al. (1994) were quite different which makes comparison difficult.

Nevertheless, Segner et al. (1994) reported a high rate of lipogenesis from [^{14}C]-acetate for the entire 72 h incubation and rates were higher at 24 to 48 h in comparison to 48 to 72 h post-isolation. It does in fact appear that significant changes in metabolic fluxes occurred near the 48 h post-isolation. This aspect of isolated rainbow trout hepatocyte cultures should be further explored as it may have important implications in studies using these cells for longer incubation periods and could also prove useful in determining how these cells can be maintained for even longer periods of time to explore more long term effects of toxicant exposure.

On the other hand, β-NF exposure showed very little significant differences and observed results are, for the most part, inconsistent with literature studies. With the exception of depressed G6PDH activity observed in hepatocytes of the European flounder (Winzer et al., 2002), enzyme activity analyses were done in livers following a whole animal exposure (Tintos et al., 2008; Vijayan et al., 2006). As was mentioned in the Introduction, isolated hepatocytes were used in order to examine specific AhR-activation energetic costs in the absence of modulation by other factors such as hormones. Tintos et al. (2008) and Vijayan et al. (2006) in their whole animal β-NF exposure studies observed significant differences in plasma cortisol and glucocorticoid receptor levels, respectively, which lead to the hypothesis that an AhR agonist by itself has little impact on energy metabolism but may result in significant differences in the presence of endocrine or other factors. However, transient changes in activities of AAT and CS support the modulation of gluconeogenesis and oxidative metabolism in isolated hepatocytes exposed to β-NF but how such changes impact the energetic status of the cells remains unclear. An additional advantage however of using a primary hepatocyte culture is that these endocrine factors can be added, an approach which could test the proposed hypothesis and may provide further insight on the mode of toxicity of AhR agonists.

This study is also, to my knowledge, the first to use a MFA approach in fish cells in order to examine intracellular metabolism and among very few that used this approach to examine the impact of toxicant exposure. It is evident in this study that the large variability in metabolic fluxes created large flux ranges which posed significant challenges in generating clear conclusions from the results obtained. Of all the fluxes examined, very few showed non-overlapping ranges and the noted changes were inconsistent with enzyme activities that are part of these fluxes as well as other reported studies in the literature. Further analyzing these values, those fluxes showing differences are generally involved in either consuming or producing NADPH and are therefore likely estimated to be different in order to maintain the assumption that intracellular metabolites, such as $NADP^+$ in this case, do not accumulate. Other studies reported inhibition of G6PDH upon exposure to AhR agonists (Tintos et al., 2008; Vijayan et al., 2006; Winzer et al., 2002), suggesting that the assumption of steady state may not be valid for NADPH and $NADP^+$. However, if this assumption was ignored, the absence of changes in external metabolite fluxes suggests that β-NF does not significantly change trout hepatocyte metabolism.

While the MFA model appears to be uninformative, the addition of more experimental constraints could only be of benefit and could lead to significant reduction in flux ranges making the model much more relevant. Due to challenges in regards to analysis of amino acid fluxes, these could not be incorporated in the MFA model which could be beneficial. Indeed, Zamorano et al. (2010) showed that the addition of as little as 3 more constraints helped in narrowing flux ranges in CHO-320 cells. Furthermore, although it was noted that the use of MFA has the advantage of not requiring the use of radiolabelled substrates, in combination with techniques such as GC-MS and NMR spectroscopy, the use of radiolabelled substrate could provide additional constraints to include in the MFA by following their incorporation in individual metabolites over time (Matsuoka et al., 2010).

Another point to consider when using MFA is the compartmentalization of metabolism that is found in eukaryotic cells, the separation of which is extremely challenging when measuring only extracellular metabolites (Allen et al., 2007; Nöh and Wiechert, 2011). In this study, compartmentalization was not considered as studies using mammalian models (Bonarius et al., 1996; Chan et al., 2003a, b; Uygun et al., 2007) have generated valuable information on intracellular flux without its consideration and in some cases, such as Iyer et al. (2010), were even validated by transcriptomic data as well. Compartmentalization leads to duplication of certain pathways and its respective metabolites (Nöh and Wiechert, 2011) which may be used differently under different conditions which cannot be assessed from external measurements only. An important difference that must be noted between rainbow trout hepatocytes and mammalian cells is the metabolic rates and fluxes which, in trout, are lower than in mammals. Such difference in rates could mean that metabolite accumulation in these cells is more pronounced which should be further examined. In particular, assessment of levels of metabolites which are used in a number of individual pathways such as oxidizer and reducers, or redox potential, should be examined as they impact a large number of fluxes.

Finally, the apparent shift in energy fuel use that occurred in this study may have impeded the use of an MFA approach. It is unlikely that the observed depression of glucogenesis and Na^+/K^+-ATPase and the uptake of fatty acids occurred simultaneously and at exactly 48 h post-isolation. This would suggests that these hepatocytes are not in fact in a steady state but rather that dramatic changes are occurring which could result in imprecise constraints and large flux ranges. Future studies looking to use an MFA approach in rainbow trout hepatocytes should consider these changes and determine when these changes in fuel use occur over such extended incubation periods. In fact, MFA using more and shorter intervals for flux analysis could be

useful to examine these changes if more sensitive techniques can be used to assess the slow metabolite fluxes.

Overall, this study provided little evidence that β-NF activation of the AhR leads to significant energetic challenges in isolated rainbow trout hepatocytes. Other challenges including the duration of incubation may be a larger challenge than the toxicant. There were changes in metabolism including gluconeogenesis (AAT) and oxidative metabolism (CS) with exposure to β-NF, but the noise in the data masked any potential significant changes on metabolic fluxes. These changes in enzyme activities however suggest that intracellular metabolism is in fact modulated upon exposure to β-NF which may allow the cells to maintain a stable AEC.

As for MFA in rainbow trout hepatocytes, it is clear that these cells do not behave as prokaryotic or mammalian cells and the application of this technique may be impeded by a number of factors including low metabolic fluxes, possible accumulation or depletion of intracellular metabolites and dramatic changes in overall metabolism that are largely unexplored in these cells. In this study, the inclusion of actual detoxification flux of CYP1A rather than theoretical ones could have also allowed more accurate constraints although sampling of metabolic fluxes at shorter time intervals may have more correctly integrated the change in fuel use. Nevertheless, with the inclusion of additional constraints and assessment of cellular redox potential to examine the apparent imbalance between need and use of NADPH by CYP1A, the use of MFA may prove to be useful in examining intracellular metabolism upon exposure to toxicants.

References

Al-Hameedi, S. 2008. Energetic costs of toxicant metabolism in rainbow trout (*Oncorynchus mykiss*), MSc thesis. University of Ottawa, Ottawa, p. 115.

Allen, D.K., Shachar-Hill, Y., Ohlrogge, J.B. 2007. Compartment-specific labeling information in ^{13}C metabolic flux analysis of plants. Phytochemistry 68, 2197-2210.

Aluru, N., Vijayan, M.M. 2004. β-naphthoflavone disrupts cortisol production and liver glucocorticoid responsiveness in rainbow trout. Aquat. Toxicol. 67, 273-285.

Aluru, N., Vijayan, M.M. 2006. Resveratrol affects CYP1A expression in rainbow trout hepatocytes. Aquat. Toxicol. 77, 291-297.

Aluru, N., Vijayan, M.M. 2008. Brain transcriptomics in response to β-naphthoflavone treatment in rainbow trout: The role of aryl hydrocarbon receptor signaling. Aquat. Toxicol. 87, 1-12.

Aly, H.A.A., Domènech, Ò. 2009. Aroclor 1254 induced cytotoxicity and mitochondrial dysfunction in isolated rat hepatocytes. Toxicology 262, 175-183.

Andersson, T., Förlin, L. 1992. Regulation of the cytochrome-P450 enzyme-system in fish. Aquat. Toxicol. 24, 1-19.

Atkinson, D.E. 1977. Cellular energy metabolism and its regulation. Academic Press, New York.

Atkinson, D.E., Walton, G.M. 1967. Adenosine triphosphate conservation in metabolic regulation - rat liver citrate cleavage enzyme. J. Biol. Chem. 242, 3239-3241.

Aw, T.Y., Jones, D.P. 1985. ATP concentration gradients in cytosol of liver-cells during hypoxia. Am. J. Physiol. 249, C385-C392.

Bains, O.S., Kennedy, C.J. 2004. Energetic costs of pyrene metabolism in isolated hepatocytes of rainbow trout, *Oncorhynchus mykiss*. Aquat. Toxicol. 67, 217-226.

Bains, O.S., Kennedy, C.J. 2005. Alterations in respiration rate of isolated rainbow trout hepatocytes exposed to the P-glycoprotein substrate rhodamine 123. Toxicology 214, 87-98.

Barouki, R., Coumoul, X., Fernandez-Salgueroc, P.M. 2007. The aryl hydrocarbon receptor, more than a xenobiotic-interacting protein. FEBS Lett. 581, 3608-3615.

Barron, M.G., Carls, M.G., Heintz, R., Rice, S.D. 2004. Evaluation of fish early life-stage toxicity models of chronic embryonic exposures to complex polycyclic aromatic hydrocarbon mixtures. Toxicol. Sci. 78, 60-67.

Basu, N., Kennedy, C.J., Hodson, P.V., Iwama, G.K. 2001. Altered stress responses in rainbow trout following a dietary administration of cortisol and β-napthoflavone. Fish Physiol. Biochem. 25, 131-140.

Bellehumeur, K. 2010. Consequences of sublethal polychlorinated biphenyl exposure on the swimming performance of rainbow trout *Oncorhynchus mykiss*, MSc thesis. University of Ottawa, Ottawa, p. 103.

Bello, S.M., Franks, D.G., Stegeman, J.J., Hahn, M.E. 2001. Acquired resistance to ah receptor agonists in a population of Atlantic killifish (*Fundulus heteroclitus*) inhabiting a marine superfund site: In vivo and in vitro studies on the inducibility of xenobiotic metabolizing enzymes. Toxicol. Sci. 60, 77-91.

Bergmeyer, H.U. 1986. Methods of enzymatic analysis: Metabolites 3, Lipids, amino acids and related compounds, 3rd edition. Academic Press, New York.

Beyers, D.W., Rice, J.A., Clements, W.H., Henry, C.J. 1999. Estimating physiological cost of chemical exposure: Integrating energetics and stress to quantify toxic effects in fish. Can. J. Fish. Aquat. Sci. 56, 814-822.

Bhavsar, S.P., Jackson, D.A., Hayton, A., Reiner, E.J., Chen, T., Bodnar, J. 2007. Are PCB levels in fish from the canadian great lakes still declining? J. Gt. Lakes Res. 33, 592-605.

Billiard, S.M., Querbach, K., Hodson, P.V. 1999. Toxicity of retene to early life stages of two freshwater fish species. Environ. Toxicol. Chem. 18, 2070-2077.

Bogdanova, A., Grenacher, B., Nikinmaa, M., Gassmann, M. 2005. Hypoxic responses of Na^+/K^+ ATPase in trout hepatocytes. J. Exp. Biol. 208, 1793-1801.

Bonarius, H.P.J., Hatzimanikatis, V., Meesters, K.P.H., deGooijer, C.D., Schmid, G., Tramper, J. 1996. Metabolic flux analysis of hybridoma cells in different culture media using mass balances. Biotechnol. Bioeng. 50, 299-318.

Brett, J.R., Groves, T.D.D. 1979. Physiological energetics, in: W.S. Hoar, D.J.R., Brett, J.R. (Eds.) Fish physiology. Academic Press, pp. 279-352.

Brinkworth, L.C., Hodson, P.V., Tabash, S., Lee, P. 2003. CYP1A induction and blue sac disease in early developmental stages of rainbow trout (*Oncorhynchus mykiss*) exposed to retene. J. Toxicol. Env. Health. A. 66, 627-646.

Bureau, D.P., Kaushik, S.J., Cho, C.Y. 2003. Bioenergetics, in: John, E.H., Ronald, W.H. (Eds.), Fish nutrition (third edition). Academic Press, San Diego, pp. 1-59.

Buttgereit, F., Brand, M.D. 1995. A hierarchy of ATP-consuming processes in mammalian-cells. Biochem. J. 312, 163-167.

Caldwell, C.A., Hinshaw, J.M. 1994. Nucleotides and the adenylate energy-charge as indicators of stress in rainbow-trout (*Oncorhynchus mykiss*) subjected to a range of dissolved-oxygen concentrations. Comp. Biochem. Physiol. 109B, 313-323.

Calow, P. 1991. Physiological costs of combating chemical toxicants - ecological implications. Comp. Biochem. Physiol., Part C: Toxicol. Pharmacol. 100, 3-6.

Carvalho, P.S.M., Noltie, D.B., Tillitt, D.E. 2004. Intra-strain dioxin sensitivity and morphometric effects in swim-up rainbow trout (*Oncorhynchus mykiss*). Comp. Biochem. Physiol. C-Toxicol. Pharmacol. 137, 133-142.

Casper, R.F., Quesne, M., Rogers, I.M., Shirota, T., Jolivet, A., Milgrom, E., Savouret, J.-F. 1999. Resveratrol has antagonist activity on the aryl hydrocarbon receptor: Implications for prevention of dioxin toxicity. Mol. Pharmacol. 56, 784-790.

Cattani, O., Serra, R., Isani, G., Raggi, G., Cortesi, P., Carpene, E. 1996. Correlation between metallothionein and energy metabolism in sea bass, *Dicentrarchus labrax*, exposed to cadmium. Comp. Biochem. Physiol., Part C: Toxicol. Pharmacol. 113, 193-199.

Chan, C., Berthiaume, F., Lee, K., Yarmush, M.L. 2003a. Metabolic flux analysis of cultured hepatocytes exposed to plasma. Biotechnol. Bioeng. 81, 33-49.

Chan, C., Berthiaume, F., Lee, K., Yarmush, M.L. 2003b. Metabolic flux analysis of hepatocyte function in hormone- and amino acid-supplemented plasma. Metab. Eng. 5, 1-15.

Choi, M.P.K., Kang, Y.H., Peng, X.L., Ng, K.W., Wong, M.H. 2009. Stockholm convention organochlorine pesticides and polycyclic aromatic hydrocarbons in hong kong air. Chemosphere 77, 714-719.

Ciolino, H.P., Daschner, P.J., Yeh, G.C. 1998. Resveratrol inhibits transcription of CYP1A1 in vitro by preventing activation of the aryl hydrocarbon receptor. Cancer Res. 58, 5707-5712.

Correia, A.D., Goncalves, R., Scholze, M., Ferreira, M., Henriques, M.A.R. 2007. Biochemical and behavioral responses in gilthead seabream (*Sparus aurata*) to phenanthrene. J. Exp. Mar. Biol. Ecol. 347, 109-122.

Davies, R., Moyes, C.D. 2007. Allometric scaling in centrarchid fish: Origins of intra- and inter-specific variation in oxidative and glycolytic enzyme levels in muscle. J. Exp. Biol. 210, 3798-3804.

Denison, M.S., Pandini, A., Nagy, S.R., Baldwin, E.P., Bonati, L. 2002. Ligand binding and activation of the ah receptor. Chem. Biol. Interact. 141, 3-24.

Dugan, S.G., Moon, T.W. 1998. Cortisol does not affect hepatic α- and β-adrenoceptor properties in rainbow trout (*Oncorhynchus mykiss*). Fish Physiol. Biochem. 18, 343-352.

Dumas, A., Dijkstra, J., France, J. 2008. Mathematical modelling in animal nutrition: A centenary review. J. Agric. Sci. 146, 123-142.

DuRant, S.E., Hopkins, W.A., Talent, L.G. 2007. Energy acquisition and allocation in an ectothermic predator exposed to a common environmental stressor. Comp. Biochem. Physiol. C-Toxicol. Pharmacol. 145, 442-448.

Edwards, J.S., Ibarra, R.U., Palsson, B.O. 2001. In silico predictions of escherichia coli metabolic capabilities are consistent with experimental data. Nat. Biotechnol. 19, 125-130.

French, C.J., Hochachka, P.W., Mommsen, T.P. 1983. Metabolic organization of liver during spawning migration of sockeye salmon. Am. J. Physiol. 245, R827-R830.

French, C.J., Mommsen, T.P., Hochachka, P.W. 1981. Amino-acid utilization in isolated hepatocytes from rainbow-trout. Eur. J. Biochem. 113, 311-317.

Fromm, H.J. 1977. Herbert fromm--control by energy charge is an untenable theory. Trends Biochem. Sci. 2, N198-N200.

Gagnon, M.M. 2002. Metabolic disturbances in fish exposed to sodium pentachlorophenate (NAPCP) and 3,3',4,4',5-pentachlorobiphenyl (PCB126), individually or combined. Comp. Biochem. Physiol. 132C, 425-435.

Gesto, M., Tintos, A., Rodriguez-Illamola, A., Soengas, J.L., Miguez, J.M. 2009. Effects of naphthalene, β-naphthoflavone and benzo(a)pyrene on the diurnal and nocturnal indoleamine metabolism and melatonin content in the pineal organ of rainbow trout, *Oncorhynchus mykiss*. Aquat. Toxicol. 92, 1-8.

Goksøyr, A., Förlin, L. 1992. The cytochrome-p-450 system in fish, aquatic toxicology and environmental monitoring. Aquat. Toxicol. 22, 287-311.

Grans, J., Wassmur, B., Celander, M.C. 2010. One-way inhibiting cross-talk between arylhydrocarbon receptor (AhR) and estrogen receptor (ER) signaling in primary cultures of rainbow trout hepatocytes. Aquat. Toxicol. 100, 263-270.

Hahn, M.E. 2002. Aryl hydrocarbon receptors: Diversity and evolution. Chem. Biol. Interact. 141, 131-160.

Hahn, M.E., Stegeman, J.J. 1994. Regulation of cytochrome P4501A1 in teleosts - sustained induction of CYP1A1 messenger-RNA, protein, and catalytic activity by 2,3,7,8-tetrachlorodibenzofuran in the marine fish *Stenotomus chrysops*. Toxicol. Appl. Pharmacol. 127, 187-198.

Handy, R.D., Sims, D.W., Giles, A., Campbell, H.A., Musonda, M.M. 1999. Metabolic trade-off between locomotion and detoxification for maintenance of blood chemistry and growth parameters by rainbow trout (*Oncorhynchus mykiss*) during chronic dietary exposure to copper. Aquat. Toxicol. 47, 23-41.

Heid, S.E., Pollenz, R.S., Swanson, H.I. 2000. Role of heat shock protein 90 dissociation in mediating agonist-induced activation of the aryl hydrocarbon receptor. Mol. Pharmacol. 57, 82-92.

Hepher, B., Liao, I.C., Cheng, S.H., Hsieh, C.S. 1983. Food utilization by red tilapia - effects of diet composition, feeding level and temperature on utilization efficiencies for maintenance and growth. Aquaculture 32, 255-275.

Hildebrand, J.L., Bains, O.S., Lee, D.S.H., Kennedy, C.J. 2009. Functional and energetic characterization of P-gp-mediated doxorubicin transport in rainbow trout (*Oncorhynchus mykiss*) hepatocytes. Comp. Biochem. Physiol. C-Toxicol. Pharmacol. 149, 65-72.

Hofer, R., Krewedl, G., Koch, F. 1985. An energy budget for an omnivorous cyprinid: *Rutilus rutilus* (l.). Hydrobiologia 122, 53-59.

Incardona, J.P., Carls, M.G., Teraoka, H., Sloan, C.A., Collier, T.K., Scholz, N.L. 2005. Aryl hydrocarbon receptor-independent toxicity of weathered crude oil during fish development. Environ. Health Perspect. 113, 1755-1762.

Iwama, G.K. 1998. Stress in fish. Ann. N.Y. Acad. Sci. 851, 304-310.

Iyer, V.V., Ovacik, M.A., Androulakis, I.P., Roth, C.M., Ierapetritou, M.G. 2010. Transcriptional and metabolic flux profiling of triadimefon effects on cultured hepatocytes. Toxicol. Appl. Pharmacol. 248, 165-177.

Jorgensen, E.H., Vijayan, M.M., Killie, J.E.A., Aluru, N., Aas-Hansen, O., Maule, A. 2006. Toxicokinetics and effects of PCBs in arctic fish: A review of studies on Arctic charr. J. Toxicol. Env. Heal. A. 69, 37-52.

Kaiser, J., Enserink, M. 2000. Environmental toxicology - treaty takes a pop at the dirty dozen. Science 290, 2053-2053.

Kelly, B.C., Ikonomou, M.G., Blair, J.D., Morin, A.E., Gobas, F. 2007. Food web-specific biomagnification of persistent organic pollutants. Science 317, 236-239.

Kennedy, C.J., Tierney, K.B. 2008. Energy intake affects the biotransformation rate, scope for induction, and metabolite profile of benzo[a]pyrene in rainbow trout. Aquat. Toxicol. 90, 172-181.

Kennedy, S.W., Jones, S.P., Bastien, L.J. 1995. Efficient analysis of cytochrome P4501A catalytic activity, porphyrins, and total proteins in chicken embryo hepatocyte cultures with a fluorescence plate reader. Anal. Biochem. 226, 362-370.

Keppler, D., Decker, K. 1974. Glycogen determination with amyloglucosidase, in: Bergmeyer, H.U. (Ed.), Methods of enzymatic analysis. Academic Press, New York, pp. 1127-1131.

Kerr, R., Kintisch, E., Stokstad, E. 2010. Gulf oil spill will deepwater horizon set a new standard for catastrophe? Science 328, 674-675.

Klamt, S., Saez-Rodriguez, J., Gilles, E. 2007. Structural and functional analysis of cellular networks with cellnetanalyzer. BMC Sys. Biol. 1, 2.

Klamt, S., Schuster, S., Gilles, E.D. 2002. Calculability analysis in underdetermined metabolic networks illustrated by a model of the central metabolism in purple nonsulfur bacteria. Biotechnol. Bioeng. 77, 734-751.

Klungsoy, L., Hagemen, H.J., Fall, L., Atkinson, D.E. 1968. Interaction between energy charge and product feedback in regualation of biosynthetic enzymes. Aspartokinase phosphoribosyladenosine triphosphate synthetase and phosphoribosyl pyrophosphate synthetase. Biochemistry 7, 4035-4040.

Knops, M., Altenburger, R., Segner, H. 2001. Alterations of physiological energetics, growth and reproduction of daphnia magna under toxicant stress. Aquat. Toxicol. 53, 79-90.

Kopec, A.K., Boverhof, D.R., Burgoon, L.D., Ibrahim-Aibo, D., Harkema, J.R., Tashiro, C., Chittim, B., Zacharewski, T.R. 2008. Comparative toxicogenomic examination of the hepatic effects of PCB126 and TCDD in immature, ovariectomized C57BL/6 mice. Toxicol. Sci. 102, 61-75.

Krumschnabel, G., Biasi, C., Schwarzbaum, P.J., Wieser, W. 1996. Membrane-metabolic coupling and ion homeostasis in anoxia-tolerant and anoxia-intolerant hepatocytes. Am. J. Physiol. 270, R614-R620.

Krumschnabel, G., Biasi, C., Wieser, W. 2000. Action of adenosine on energetics, protein synthesis and K^+ homeostasis in teleost hepatocytes. J. Exp. Biol. 203, 2657-2665.

Krumschnabel, G., Frischmann, M.E., Schwarzbaum, P.J., Wieser, W. 1998. Loss of K^+ homeostasis in trout hepatocytes during chemical anoxia: A screening study for potential causes and mechanisms. Arch. Biochem. Biophys. 353, 199-206.

Krumschnabel, G., Malle, S., Schwarzbaum, P.J., Wieser, W. 1994a. Glycolytic function in goldfish hepatocytes at different temperatures - relevance for Na^+ pump activity and protein-synthesis. J. Exp. Biol. 192, 285-290.

Krumschnabel, G., Manzl, C., Schwarzbaum, P.J. 2001. Importance of glycolysis for the energetics of anoxia-tolerant and anoxia-intolerant teleost hepatocytes. Physiol. Biochem. Zool. 74, 413-419.

Krumschnabel, G., Schwarzbaum, P.J., Wieser, W. 1994b. Coupling of energy supply and energy demand in isolated goldfish hepatocytes. Physiol. Zool. 67, 438-448.

Krumschnabel, G., Schwarzbaum, P.J., Wieser, W. 1999. Energetics of trout hepatocytes during A23187-induced disruption of Ca^{2+} homeostasis. Comp. Biochem. Physiol., Part C: Toxicol. Pharmacol. 124, 187-195.

Krumschnabel, G., Wieser, W. 1994. Inhibition of the sodium-pump does not cause a stoichiometric decrease of ATP-production in energy limited fish hepatocytes. Experientia 50, 483-485.

Kwast, K.E., Hand, S.C. 1993. Regulatory features of protein-synthesis in isolated-mitochondria from *Artemia* embryos. Am. J. Physiol. 265, R1238-R1246.

Lang, V. 1992. Polychlorinated-biphenyls in the environment. J. Chromatogr. 595, 1-43.

Leblanc, P.J., Ballantyne, J.S. 1993. β-Hydroxybutyrate dehydrogenase in teleost fish. J. Exp. Zool. 267, 356-358.

Lech, J.J. 1970. Glycerol kinase and glycerol utilization in trout (*Salmo gairdneri*) liver. Comp. Biochem. Physiol. 34, 117-124.

Lee, K., Berthiaume, F., Stephanopoulos, G.N., Yarmush, M.L. 1999. Metabolic flux analysis: A powerful tool for monitoring tissue function. Tissue Eng. 5, 347-368.

Levesque, H.M., Moon, T.W., Campbell, P.G.C., Hontela, A. 2002. Seasonal variation in carbohydrate and lipid metabolism of yellow perch (*Perca flavescens*) chronically exposed to metals in the field. Aquat. Toxicol. 60, 257-267.

Linden, J., Lensu, S., Tuomisto, J., Pohjanvirta, R. 2010. Dioxins, the aryl hydrocarbon receptor and the central regulation of energy balance. Front. Neuroendocrinol. 31, 452-478.

Long, Y.C., Zierath, J.R. 2006. AMP-activated protein kinase signaling in metabolic regulation. J. Clin. Invest. 116, 1776-1783.

Lupatsch, I., Kissil, G.W., Sklan, D. 2003. Comparison of energy and protein efficiency among three fish species gilthead sea bream (*Sparus aurata*), european sea bass (*Dicentrarchus labrax*) and white grouper (*Epinephelus aeneus*): Energy expenditure for protein and lipid deposition. Aquaculture 225, 175-189.

Lupatsch, I., Kissil, G.W., Sklan, D., Pfeffer, E. 1998. Energy and protein requirements for maintenance and growth in gilthead seabream (*Sparus aurata* L.). Aquacul. Nutr. 4, 165-173.

Mantovani, J., Roy, R. 2011. Re-evaluating the general(ized) roles of AMPK in cellular metabolism. FEBS Lett. 585, 967-972.

Matsuo, A.Y.O., Gallagher, E.P., Trute, M., Stapleton, P.L., Levado, R., Schlenk, D. 2008. Characterization of phase I biotransformation enzymes in coho salmon (*Oncorhynchus kisutch*). Comp. Biochem. Physiol. C-Toxicol. Pharmacol. 147, 78-84.

Matsuoka, Y., Shimizu, K. 2010. Current status of ^{13}C-metabolic flux analysis and future perspectives. Process. Biochem. 45, 1873-1881.

Mavrovouniotis, M.L., Stephanopoulos, G. 1990. Computer-aided synthesis of biochemical pathways. Biotechnol. Bioeng. 36, 1119-1132.

McMillan, D.N., Houlihan, D.F. 1989. Short-term responses of protein-synthesis to re-feeding in rainbow-trout. Aquaculture 79, 37-46.

Migliarini, B., Piccinetti, C.C., Martella, A., Maradonna, F., Gioacchini, G., Carnevali, O. 2011. Perspectives on endocrine disruptor effects on metabolic sensors. Gen. Comp. Endocrinol. 170, 416-423.

Miranda, A.L., Roche, H., Randi, M.A.F., Menezes, M.L., Ribeiro, C.A.O. 2008. Bioaccumulation of chlorinated pesticides and PCBs in the tropical freshwater fish *Hoplias malabaricus*: Histopathological, physiological, and immunological findings. Environ. Int. 34, 939-949.

Mitchell, K.A., Elferink, C.J. 2009. Timing is everything: Consequences of transient and sustained AhR activity. Biochem. Pharmacol. 77, 947-956.

Mommsen, T.P. 1986. Comparative gluconeogenesis in hepatocytes from salmonid fishes. Can. J. Zool. 64, 1110-1115.

Moon, T.W. 2004. Hormones and fish hepatocyte metabolism: "The good, the bad and the ugly!". Comp. Biochem. Physiol. 139B, 335-345.

Moyes, C.D., Schulte, P.M. 2006. Principles of Animal Physiology. Pearson Eduction Inc., San Francisco.

Nakata, K., Tanaka, Y., Nakano, T., Adachi, T. 2006. Nuclear receptor-mediated transcriptional regulation in phase I, II, and III xenobiotic metabolizing systems. Drug Metab. Pharmacokinet. 21, 437-457.

Navas, J.M., Segner, H. 2000. Antiestrogenicity of β-naphthoflavone and PAHs in cultured rainbow trout hepatocytes: Evidence for a role of the arylhydrocarbon receptor. Aquat. Toxicol. 51, 79-92.

Ney, J.J. 1993. Bioenergetics modeling today - growing pains on the cutting edge. Trans. Am. Fish. Soc. 122, 736-748.

Nielsen, J. 1998. Metabolic engineering: Techniques for analysis of targets for genetic manipulations. Biotechnol. Bioeng. 58, 125-132.

Nöh, K., Wiechert, W. 2011. The benefits of being transient: Isotope-based metabolic flux analysis at the short time scale. Appl. Microbiol. Biot., 1-19.

Nolan, R.P., Fenley, A.P., Lee, K. 2006. Identification of distributed metabolic objectives in the hypermetabolic liver by flux and energy balance analysis. Metab. Eng. 8, 30-45.

Oakhill, J.S., Steel, R., Chen, Z.P., Scott, J.W., Ling, N., Tam, S., Kemp, B.E. 2011. AMPK is a direct adenylate charge-regulated protein kinase. Science 332, 1433-1435.

Olivieri, C.E., Cooper, K.R. 1997. Toxicity of 2,3,7,8-tetrachlorodibenzo-p-dioxin (TCDD) in embryos and larvae of the fathead minnow (*Pimephales promelas*). Chemosphere 34, 1139-1150.

Orth, J.D., Thiele, I., Palsson, B.O. 2010. What is flux balance analysis? Nat. Biotechnol. 28, 245-248.

Pacheco, M., Santos, M.A. 2001. Tissue distribution and temperature-dependence of *Anguilla anguilla* L. EROD activity following exposure to model inducers and relationship with plasma cortisol, lactate and glucose levels. Environ. Int. 26, 149-155.

Pannevis, M.C., Houlihan, D.F. 1992. The energetic cost of protein synthesis in isolated hepatocytes of rainbow trout (*Oncorhynchus mykiss*). J. Comp. Physiol. B. 162, 393-400.

Pascussi, J.M., Gerbal-Chaloin, S., Duret, C., Daujat-Chavanieu, M., Vilarem, M.J., Maurel, P. 2008. The tangle of nuclear receptors that controls xenobiotic metabolism and transport: Crosstalk and consequences. Annu. Rev. Pharmacol. Toxicol. 48, 1-32.

Pesonen, M., Andersson, T.B. 1997. Fish primary hepatocyte culture; an important model for xenobiotic metabolism and toxicity studies. Aquat. Toxicol. 37, 253-267.

Pesonen, M., Goksøyr, A., Andersson, T. 1992. Expression of P4501A1 in a primary culture of rainbow trout hepatocytes exposed to β-naphthoflavone or 2,3,7,8-tetrachlorodibenzo-p-dioxin. Arch. Biochem. Biophys. 292, 228-233.

Pirozzi, I., Booth, M., Allan, G. 2010a. Protein and energy utilization and the requirements for maintenance in juvenile mulloway (*Argyrosomus japonicus*). Fish Physiol. Biochem. 36, 109-121.

Pirozzi, I., Booth, M.A., Allan, G.L. 2010b. A factorial approach to deriving dietary specifications and daily feed intake for mulloway, *argyrosomus japonicus*, based on the requirements for digestible protein and energy. Aquaculture 302, 235-242.

Plant, N. 2003. Molecular Toxicology. Garland Science, Oxford.

Polakof, S., Panserat, S., Craig, P.M., Martyres, D.J., Plagnes-Juan, E., Savari, S., Aris-Brosou, S., Moon, T.W. 2011. The metabolic consequences of hepatic AMP-kinase phosphorylation in rainbow trout. Plos One 6, e20228.

Prasada Rao, K.S., Ahammad Sahib, I.K., Ramana Rao, K.V. 1985. Methyl parathion (o-o-dimethyl o-4-nitrophenyl thiophosphate) effects on whole-body and tissue respiration in the teleost, *Tilapia mossambica* (Peters). Ecotoxicol. Environ. Saf. 9, 339-345.

Ramaiah, A., Atkinson, D.E., Hathaway, J.A. 1964. Adenylates as metabolic regulator - effect on yeast phosphofructokinase kinetics. J. Biol. Chem. 239, 3619-&.

Renaud, J.M., Moon, T.W. 1980. Characterization of gluconeogenesis in hepatocytes isolated from the American eel *Anguilla rostrata* Lesueur. J. Comp. Physiol. B. 135, 115-125.

Reynaud, S., Deschaux, P. 2006. The effects of polycyclic aromatic hydrocarbons on the immune system of fish: A review. Aquat. Toxicol. 77, 229-238.

Rissanen, E., Krumschnabel, G., Nikinmaa, M. 2003. Dehydroabietic acid, a major component of wood industry effluents, interferes with cellular energetics in rainbow trout hepatocytes. Aquat. Toxicol. 62, 45-53.

Rombough, P.J. 1994. Energy partitioning during fish development: Additive or compensatory allocation of energy to support growth? Funct. Ecol. 8, 178-186.

Safe, S., Bandiera, S., Sawyer, T., Robertson, L., Safe, L., Parkinson, A., Thomas, P.E., Ryan, D.E., Reik, L.M., Levin, W., Denomme, M.A., Fujita, T. 1985. PCBs - structure-function-relationships and mechanism of action. Environ. Health Perspect. 60, 47-56.

Sanden, M., Frøyland, L., Hemre, G.-I. 2003. Modulation of glucose-6-phosphate dehydrogenase, 6-phosphogluconate dehydrogenase and malic enzyme activity by glucose and alanine in Atlantic salmon, *Salmo salar* L. hepatocytes. Aquaculture 221, 469-480.

Sandvik, M., Horsberg, T.E., Skaare, J.U., Ingebrigtsen, K. 1998. Comparison of dietary and waterborne exposure to benzo(a)pyrene: Bioavailability, tissue disposition and CYP1A1 induction in rainbow trout (*Oncorhynchus mykiss*). Biomarkers 3, 399-410.

Sarioglu, H., Brandner, S., Haberger, M., Jacobsen, C., Lichtmannegger, J., Wormke, M., Andrae, U. 2008. Analysis of 2,3,7,8-tetrachlorodibenzo-p-dioxin-induced proteome changes in 5L rat hepatoma cells reveals novel targets of dioxin action including the mitochondrial apoptosis regulator VDAC2. Mol. Cell. Proteomics 7, 394-410.

Schwarzenbach, R.P., Egli, T., Hofstetter, T.B., von Gunten, U., Wehrli, B. 2010. Global water pollution and human health. Annu. Rev. Environ. Resour. 35, 109-136.

Seefeld, M.D., Corbett, S.W., Keesey, R.E., Peterson, R.E. 1984. Characterization of the wasting syndrome in rats treated with 2,3,7,8-tetrachlorodibenzo-p-dioxin. Toxicol. Appl. Pharmacol. 73, 311-322.

Segner, H., Blair, J.B., Wirtz, G., Miller, M.R. 1994. Cultured trout liver-cells - utilization of substrates and response to hormones. In Vitro Cell. Dev-An. 30A, 306-311.

Segner, H., Dolle, A., Bohm, R. 1997. Ketone body metabolism in the carp *Cyprinus carpio*: Biochemical and ^{1}H NMR spectroscopical analysis. Comp. Biochem. Physiol. 116B, 257-262.

Selye, H. 1950. Stress and the general adaptation syndrome. Br. Med. J. 1, 1383-1392.

Shen, L.C., Fall, L., Walton, G.M., Atkinson, D.E. 1968. Interaction between energy charge and metabolite modulation in regulation of enzymes of amphibolic sequences. phosphofructokinase and pyruvate dehydrogenase. Biochemistry 7, 4041-4045.

Sherwood, G.D., Rasmussen, J.B., Rowan, D.J., Brodeur, J., Hontela, A. 2000. Bioenergetic costs of heavy metal exposure in yellow perch (*Perca flavescens*): In situ estimates with a radiotracer (^{137}Cs) technique. Can. J. Fish. Aquat. Sci. 57, 441-450.

Široká, Z., Drastichová, J. 2004. Biochemical markers of aquatic environment contamination - cytochrome P450 in fish. A review. Acta Veterinaria Brno 73, 123-132.

Smolders, R., De Boeck, G., Blust, R. 2003. Changes in cellular energy budget as a measure of whole effluent toxicity in zebrafish (*Danio rerio*). Environ. Toxicol. Chem. 22, 890-899.

Suarez, R.K., Mommsen, T.P. 1987. Gluconeogenesis in teleost fishes. Can. J. Zool. 65, 1869-1882.

Tintos, A., Gesto, M., Miguez, J.M., Soengas, J.L. 2008. β-naphthoflavone and benzo[a]pyrene treatment affect liver intermediary metabolism and plasma cortisol levels in rainbow trout *Oncorhynchus mykiss*. Ecotoxicol. Environ. Saf. 69, 180-186.

Uygun, K., Matthew, H.W.T., Huang, Y. 2007. Investigation of metabolic objectives in cultured hepatocytes. Biotechnol. Bioeng. 97, 622-637.

Vaillancourt, E., Haman, F., Weber, J.M. 2009. Fuel selection in wistar rats exposed to cold: Shivering thermogenesis diverts fatty acids from re-esterification to oxidation. J. Physiol.-London 587, 4349-4359.

Van der Oost, R., Beyer, J., Vermeulen, N.P.E. 2003. Fish bioaccumulation and biomarkers in environmental risk assessment: A review. Environ. Toxicol. Pharmacol. 13, 57-149.

Varma, A., Palsson, B.O. 1994. Metabolic flux balancing - basic concepts, scientific and practical use. BioTechnology 12, 994-998.

Verdouw, H., Vanechteld, C.J.A., Dekkers, E.M.J. 1978. Ammonia determination based on indophenol formtion with sodium salicylate. Water Res. 12, 399-402.

Vijayan, M.M., Aluru, N., Maule, A.G., Jorgensen, E.H. 2006. Fasting augments PCB impact on liver metabolism in anadromous Arctic char. Toxicol. Sci. 91, 431-439.

Vijayan, M.M., Moon, T.W. 1992. Acute handling stress alters hepatic glycogen-metabolism in food-deprived rainbow trout (*Oncorhynchus mykiss*). Can. J. Fish. Aquat. Sci. 49, 2260-2266.

Volkoff, H., Canosa, L.F., Unniappan, S., Cerda-Reverter, J.M., Bernier, N.J., Kelly, S.P., Peter, R.E. 2005. Neuropeptides and the control of food intake in fish. Gen. Comp. Endocrinol. 142, 3-19.

Voss, B., Jankowsky, H.D. 1986. Temperature-dependence of lipogenesis in isolated hepatocytes from rainbow-trout (*Salmo-gairdneri*). Comp. Biochem. Physiol. B 83, 13-22.

Weber, R., Watson, A., Forter, M., Oliaei, F. 2011. Persistent organic pollutants and landfills - a review of past experiences and future challenges. Waste Manage. Res. 29, 107-121.

White, P.A., Robitaille, S., Rasmussen, J.B. 1999. Heritable reproductive effects of benzo[a]pyrene on the fathead minnow (*Pimephales promelas*). Environ. Toxicol. Chem. 18, 1843-1847.

Widdows, J., Donkin, P. 1991. Role of physiological energetics in ecotoxicology. Comp. Biochem. Physiol., Part C: Toxicol. Pharmacol. 100, 69-75.

Wieser, W., Krumschnabel, G. 2001. Hierarchies of ATP-consuming processes: Direct compared with indirect measurements, and comparative aspects. Biochem. J. 355, 389-395.

Wills, L.P., Jung, D., Koehrn, K., Zhu, S.Q., Willett, K.L., Hinton, D.E., Di Giulio, R.T. 2010. Comparative chronic liver toxicity of benzo[a]pyrene in two populations of the Atlantic killifish (*Fundulus heteroclitus*) with different exposure histories. Environ. Health Perspect. 118, 1376-1381.

Winzer, K., Van Noorden, C.J.F., Kohler, A. 2002. Glucose-6-phosphate dehydrogenase: The key to sex-related xenobiotic toxicity in hepatocytes of European flounder (*Platichthys flesus* L.)? Aquat. Toxicol. 56, 275-288.

Wirgin, I., Roy, N.K., Loftus, M., Chambers, R.C., Franks, D.G., Hahn, M.E. 2011. Mechanistic basis of resistance to PCBs in Atlantic tomcod from the Hudson River. Science 331, 1322-1325.

Xu, C.J., Li, C.Y.T., Kong, A.N.T. 2005. Induction of phase I, II and III drug metabolism/ transport by xenobiotics. Arch. Pharm. Res. 28, 249-268.

Zhou, H.L., Wu, H.F., Liao, C.Y., Diao, X.P., Zhen, J.P., Chen, L.L., Xue, Q.Z. 2010. Toxicology mechanism of the persistent organic pollutants (POPs) in fish through AhR pathway. Toxicol. Mech. Method 20, 279-286.

.

Appendix A – Metabolic Flux Analysis

Table A.1. Reactions used in metabolic flux analysis model of Iyer et al. (2010). Letters a and b indicate glycolysis and glucogenesis or fatty acid oxidation and synthesis, respectively.

Flux (#)	Reaction
1	Glucose-6-phosphate + H_2O ↔ Glucose + Pi
2	Pyruvate + NADH + H^+ ↔ Lactate + NAD^+
3	Arginine + H_2O → Ornithine + Urea
4	NADH + Acetoacetate + H^+ ↔ β-hydroxybutyrate
5	Cholesterol-ester + H_2O ↔ Palmitate + Cholesterol
6	24 Arginine + 32 Asparagine + 6Alanine + 24 Serine + 35 Cysteine + 57 Glutamate + 17 Glycine + 2Tyrosine + 33 Threonine + 53 Lysine + 26 Phenylalanine + 25 Glutamine + 30 Proline + 15 Histidine + 6 Methionine + 20 Asparagine + Trp + 35 Valine + 13 Isoleucine + 56 Leucine + 2332 ATP → Albumin + 2332 ADP + 2332 Pi
7a	Glucose-6-phosphate → Fructose-6-phosphate
7b	Fructose-6-phosphate → Glucose-6-phosphate
8a	Fructose-6-phosphate + Pi → Fructose-1,6-bisphosphate + H_2O
8b	Fructose-1,6-bisphosphate + H_2O → Fructose-6-phosphate + Pi
9a	Fructose-1,6-bisphosphate + Pi → 2 Glucose-3-phosphate
9b	2 Glucose-3-phosphate → Fructose-1,6-bisphosphate
10a	Glucose-3-phosphate + Pi + NAD^+ + ADP → Phosphoenolpyruvate + NADH + H^+ + ATP + H_2O
10b	NADH + Phosphoenolpyruvate + H^+ + ATP + H_2O → Glucose-3-phosphate + Pi + NAD^+ + ADP
11a	Phosphoenolpyruvate + ADP → Pyruvate + ATP
11b	Oxaloacetate + GTP → Phosphoenolpyruvate + GDP + CO_2

12a Pyruvate + CoA + NAD^+ → Acetoacetyl-CoA + CO_2 + NADH

12b Pyruvate + CO_2 + ATP + H2O → Oxaloacetate + ADP + Pi + 2 H^+

13 Oxaloacetate + Acetoacetyl-CoA + H_2O → CoA + Citrate + H^+

14 Citrate + NAD^+ ↔ NADH + α-Ketoglutarate + CO_2

15 α-Ketoglutarate + CoA + NAD^+ → NADH + Succinyl-CoA + CO_2 + H^+

16 Succinyl-CoA + GDH + Pi + FAD ↔ CoA + $FADH_2$ + Fumarate + GTP

17 Fumarate + H_2O ↔ Malate

18 Malate + NAD^+ ↔ NADH + Oxaloacetate + H^+

19 Ornithine + NH_4 + CO_2 + 2ATP + H_2O ↔ Citrulline + 2ADP + 2Pi + $3H^+$

20 Asparagine + Citrate + ATP ↔ Arginine + Fumarate + AMP + Ppi

21 Pyruvate + NH_4 + 0.5 NADH + 0.5 NADPH + H^+ ↔ Alanine + 0.5 NAD^+ + 0.5 $NADP^+$ + H_20

22 Serine → Pyruvate + NH_4

23 Pyruvate + 0.5 NADH + 0.5 NADPH + NH_4 + thiosulfate + H^+ ↔ Cysteine + 0.5 NAD+ + 0.5 $NADP^+$ + H_2O + SO_3^{2-}

24 NADH + Glycine + Acetyl-CoA → Threonine + NAD^+

25 Glycine + Methylene THF + H_2O ↔ THF + Serine

26 Succinyl-CoA + AMP + PPi ↔ Propionyl-CoA + ATP + CO_2

27 2 NH_4 + 5 H^+ + 5 NADH + 2 $C0_2$ + $FADH_2$ + Acetoacetyl-CoA ↔ Lysine + 3 H_20 + 3 O_2 + CoA

28 Phenylalanine + O_2 + H_4biopterin → Tyrosine + H_2O + H_2biopterin

29 Tyrosine + α-Ketoglutarate + 2 O_2 + $2H_2O$ → Glutamate + Acetoacetate + Fumarate + CO_2 + $2H^+$

30 Glutamate + H_2O ↔ 0.5 NADH + α-Ketoglutarate + NH_4 + 0.5 NADPH + H^+

31 Glutamine + H_2O → Glutamate + NH_4

32	Ornithine + H_2O → Glutamate + NADH + NH_4 + NADPH + H^+
33	Glutamate + 0.5 NADH + 0.5 NADPH + H^+ ↔ Proline + 0.5 O_2
34	Histidine + H_4folate + 2 H_2O → Glutamate + NH_4 + N_5formimoH_4folate
35	Serine + ATP + Methionine + CoA → PPi + Pi + Adenosine + Cysteine + Propionyl-CoA + CO_2 + NADH + NH_4
36	Asparagine + H2O ↔ Oxaloacetate + NH_4 + 0.5 NADH + 0.5 NADPH + H^+
37	Asparagine + H_2O → Asparagine + NH_4
38a	8 Acetyl-CoA + 14 NADPH + 7 ATP + 14 H^+ → Palmitate + 8 CoA + 6 H_2O + 7 ADP + 7 Pi + 14 $NADP^+$
38b	Palmitate + ATP +FAD + 7 NAD^+ → 8 Acetyl-CoA + 7 $FADH_2$ + 7 NADH + AMP + PP
39	2 Acetyl-CoA ↔ CoA + Acetoacetyl-CoA
40	Acetoacetyl-CoA + H_2O → Acetoacetate + CoA
41	NADH + 0.5 O_2 + H^+ + 3 ADP → 3 ATP + H_2O + NAD^+
42	$FADH_2$ + 0.5 O_2 + 2 ADP → 2 ATP + H_2O + FAD
43	12 NADPH + 6 CO_2 + 12 H^+ + Pi ↔ Glucose-6-phosphate + 12 NADP+ 7 H_2O
44	NH_4 + 0.5 NADPH + 3.5 NADH + $FADH_2$ + 2 CO_2 + 3 H^+ + Propionyl-CoA ↔ Valine + CoA + 2 H_2O
45	NH_4 + 0.5 NADPH + 2.5 NADH + $FADH_2$ + CO_2 + 3 H^+ + Acetoacetyl-CoA + Propionyl-CoA ↔ Isoleucine + 2 CoA + 2 H_2O
46	NH_4 + 0.5 NADPH + 1.5 NADH + $FADH_2$ + ADP + Pi + 2 H^+ + Acetoacetate + Acetoacetyl-CoA ↔ Leucine + CoA+ H_2O + ATP
47	Triglyceride + 3 H_2O → Glycerol + 3 Palmitate + 3 H^+
48	Glycogen + 2 Pi+ UDP ↔ Glucose-6-phosphate + UTP + H_2O
49	Glycerol + NAD^+ ↔ NADH + Glucose-3-phosphate + H^+
50	Malate + $NADP^+$ → Pyruvate + NADPH + H^+

Table A.2. Metabolite uptake or production constraints used for metabolic flux analysis (see text section 2.10).

Metabolite	0 - 24 h exposure (nmol h^{-1} mg^{-1} protein)						24 - 48 h exposure (nmol h^{-1} mg^{-1} protein)					
	Control		β-NF low CYP1A		β-NF high CYP1A		Control		β-NF low CYP1A		β-NF high CYP1A	
	Vmax	Vmin	Vmax	Vmin	Vmax	Vmin	Vmax	Vmin	Vmax	Vmin	Vmax	Vmin
Glucose	58.2	16.3	49.1	16	49.1	16	8	-4.4	2.2	-11.6	2.2	-11.6
Lactate	38	1.9	34.5	1.8	34.5	1.8	28.8	0.5	22.2	0.32	22.2	0.32
Urea	5	-5	5	-5	5	-5	5	-5	5	-5	5	-5
Aspartate	10	-10	10	-10	10	-10	10	-10	10	-10	10	-10
Serine	10	-10	10	-10	10	-10	10	-10	10	-10	10	-10
Glutamate	0.6	-1	0.7	-0.8	0.7	-0.8	0.6	-0.4	0.8	-0.8	0.8	-0.8
Glycine	10	-10	10	-10	10	-10	10	-10	10	-10	10	-10
Ammonia	5	-5	5	-5	5	-5	5	-5	5	-5	5	-5
Arginine	10	-10	10	-10	10	-10	10	-10	10	-10	10	-10
Threonine	10	-10	10	-10	10	-10	10	-10	10	-10	10	-10
Alanine	10	-10	10	-10	10	-10	10	-10	10	-10	10	-10
Proline	10	-10	10	-10	10	-10	10	-10	10	-10	10	-10
Cysteine	10	-10	10	-10	10	-10	10	-10	10	-10	10	-10
Tyrosine	10	-10	10	-10	10	-10	10	-10	10	-10	10	-10
Valine	10	-10	10	-10	10	-10	10	-10	10	-10	10	-10
Methionine	10	-10	10	-10	10	-10	10	-10	10	-10	10	-10
Ornithine	10	-10	10	-10	10	-10	10	-10	10	-10	10	-10
Lysine	10	-10	10	-10	10	-10	10	-10	10	-10	10	-10
Isoleucine	10	-10	10	-10	10	-10	10	-10	10	-10	10	-10
Leucine	10	-10	10	-10	10	-10	10	-10	10	-10	10	-10
Phenylalanine	10	-10	10	-10	10	-10	10	-10	10	-10	10	-10
Glutamine	1.8	-0.4	0.7	-0.6	0.7	-0.6	0.4	-1.8	0.4	-1.4	0.4	-1.4
Histidine	10	-10	10	-10	10	-10	10	-10	10	-10	10	-10
Asparagine	10	-10	10	-10	10	-10	10	-10	10	-10	10	-10
Tryptophan	10	-10	10	-10	10	-10	10	-10	10	-10	10	-10

Acetoacetate	0	0	0	0	0	0	0	0	0	0	0	0
β-Hydroxybutyrate	0	0	0	0	0	0	0	0	0	0	0	0
Glycerol	5	-5	5	-5	5	-5	5	-5	5	-5	5	-5
Free Fatty Acids	54.7	-8.5	38.1	-8.7	38.1	-8.7	15	-50	-6.4	-29.5	-6.4	-29.5
Cholesterol	5	-5	5	-5	5	-5	5	-5	5	-5	5	-5
Triglycerides	5	-5	5	-5	5	-5	5	-5	5	-5	5	-5
Glycogen	10	-10	10	-10	10	-10	10	-10	10	-10	10	-10
Oxygen	10	-10	10	-10	10	-10	10	-10	10	-10	10	-10
Albumin	10	-10	10	-10	10	-10	10	-10	10	-10	10	-10
EROD	0	1	4	5	399	400	0	1	4	5	499	500

Table A.3. Metabolic flux constraints for metabolic flux analysis (see text section 2.10)

Flux #	Constraints (nmol h^{-1} mg^{-1} protein)	
	Vmax	Vmin
1	50	-50
2	50	-50
3	50	-50
4	50	-50
5	50	-50
6	50	-50
7	50	0
8	50	0
9	50	0
10	50	0
11	50	0
12	50	0
13	50	-50
14	50	-50
15	50	0
16	50	-50
17	50	-50
18	50	-50
19	50	-50
20	50	0
21	50	-50
22	50	0
23	50	-50
24	50	0
25	50	-50
26	50	-50
27	50	-50

28	50	0
29	50	0
30	50	-50
31	50	0
32	50	0
33	50	-50
34	50	0
35	50	0
36	50	-50
37	50	0
38a	50	0
38b	50	0
39	50	-50
40	50	0
41	50	0
42	50	0
43	50	-50
44	50	-50
45	50	-50
46	50	-50
47	50	0
48	50	-50
49	50	-50
50	50	0

Table A.4. Metabolic flux analysis results determined as described in the text (section 2.10)

Flux #	0 - 24 h exposure (nmol h^{-1} mg^{-1} protein)						24 - 48 h exposure (nmol h^{-1} mg^{-1} protein)					
	Control		β-NF low CYP1A		β-NF high CYP1A		Control		β-NF low CYP1A		β-NF high CYP1A	
	Vmax	Vmin	Vmax	Vmin	Vmax	Vmin	Vmax	Vmin	Vmax	Vmin	Vmax	Vmin
1	50	16.3	49.1	16	49.1	16	8	-4.4	2.2	-11.6	2.2	-11.6
2	38	1.9	34.5	1.8	34.5	1.8	28.8	0.5	22.2	0.32	22.2	0.32
3	5	0	5	0	5	0	5	0	5	0	5	0
4	0	0	0	0	0	0	0	0	0	0	0	0
5	10	-10	10	-10	10	-10	10	-10	-5.1	-10	-5.1	-10
6	0	0	0	0	0	0	0	0	0	0	0	0
7	35	0	35	0	35	32.9	15.6	0	10	0	30.8	13.5
8	35	0	35	0	35	32.9	15.6	0	10	0	30.8	13.5
9	35	0	35	0	35	32.9	15.6	0	10	0	30.8	13.5
10	50	0	50	0	50	45.7	37.3	0	28.7	0	50	15.3
11	50	0	50	0	50	45.7	37.3	0	28.7	0	50	15.3
12	50	0	50	0	50	45.7	37.3	0	28.7	0	50	15.3
13	28.2	-35.7	28.2	-35.4	0.9	-22.6	28.7	-33.2	28.8	-32.3	24.1	-34.4
14	28.2	-35.7	28.2	-35.4	0.9	-22.6	28.7	-33.2	28.8	-32.3	24.1	-34.4
15	43.3	0	42.8	0	17.2	0	42.8	0	41	0	40.4	0
16	44.3	-10.6	44.2	-10.6	38.4	11.4	44.2	-10.8	43.9	-10.8	43.8	-8
17	50	-7.4	50	-6.8	50	31.2	50	-7	50	-7	50	4.5
18	50	-50	50	-50	24.1	-14.3	50	-50	50	-49.5	50	-39.3
19	15	0	15	0	15	8.5	15	0	15	0	15	0
20	15	0	15	0	15	8.5	15	0	15	0	15	0
21	14.4	-20.9	11.7	-20.9	11.7	-15.5	11	-20.9	11	-20.9	11	20.9
22	27.32	0	27.3	0	23.3	0	27.3	0	27.3	0	27.3	0
23	12.5	-26.5	11	-26.6	11	-23.1	10.6	-26.5	10.6	-26.2	10.6	-26.7
24	12.4	0	10.9	0	10.9	0	10.5	0	10.5	0	10.5	0
25	13	-13.2	13	-13.2	11.6	-12.3	13	-13.2	13	-13.2	13	-13.2

26	22.1	-35.1	21.3	-35.1	-7.4	-34.9	20.8	-35.1	20.8	-34.8	18.8	-35.1
27	13.8	-16.4	11.5	-16.5	11.1	-1	10.8	-17.1	10.7	-17	10.8	-12.6
28	12.5	0	12.5	0	12.5	0	12.5	0	12.5	0	12.5	0
29	14	0	11.6	0	11.6	0	10.9	0	10.9	0	10.9	0
30	45.8	-16.9	45	-13.1	33.2	1	43.5	-12	43.2	-12.2	43.9	-12.2
31	6.26	0	5.2	0	2.9	0	4.9	0	4.9	0	4.9	0
32	15	0	15	0	5.3	0	15	0	15	0	15	0
33	12.2	-15.4	10.8	-15.4	3.1	-12.8	10.5	-15.4	10.5	-15.4	10.5	-15.4
34	12.7	0	12.7	0	10.6	0	12.7	0	12.7	0	12.5	0
35	11.1	0	11.1	0	10.5	0	11.1	0	11.1	0	11.1	0
36	21.9	-27.3	22	-25.9	6.9	-25.9	22	-25.5	21.3	-25.5	16.3	-25.5
37	13.6	0	13.6	0	10.5	0	13.6	0	13.6	0	13.24	0
38a	7.44	0	7.4	0	1.4	0	7.5	0	4.9	0	4.5	0
38b	1.5	0	1.4	0	1.4	0	1.3	0	1.3	0	1.3	0
39	16.8	-16.1	16.7	-16.1	13.3	0.9	13	-16.7	11.6	-16.7	16.2	-11.7
40	14	0	11.6	0	7.2	0	10.9	0	10.9	0	10.9	0
41	50	0	50	0	45.7	0	50	0	50	0	50	0
42	50	0	50	0	50	11.2	50	0	50	0	50	0
43	6.5	-7.8	6.2	-8	-26.9	-29	6.5	-8	2.2	-7.9	-35.1	-47
44	12.5	-16.3	11	-16.3	5.1	-13.3	10.6	-16.3	10.6	-16.3	10.6	16.3
45	10.9	-12.3	10.3	-12.3	0	-11.2	10.2	-12.3	10.2	0	10.2	-12.3
46	14	0	11.6	0	11.6	0	10.9	0	10.9	0	10.9	0
47	10	0	10	0	10	7.9	10	0	10	0	10	0
48	20	-10	20	-10	20	15.8	18.8	-10	11.6	-10	11.6	-10
49	50	-42	50	-42.1	50	23.5	50	-43.3	50	-42.7	50	-42.3
50	10	0	10	0	10	5.8	8.8	0	1.6	0	1.6	0